University of Alberta

Examination of Immunoregulatory Receptors in the Channel Catfish (*Ictalurus punctatus*)

by

Herman Dario Cortes

A thesis submitted to the Faculty of Graduate Studies and Research in partial fulfillment of the requirements for the degree of

Master of Science
in
Physiology, Cell, and Developmental Biology

Department of Biological Sciences

Fall 2013
Edmonton, Alberta

ABSTRACT

In response to pathogens, immune cells induce protective effector functions, such as degranulation, phagocytosis and cytokine secretion, which are initiated by stimulatory or inhibitory immunoregulatory receptors expressed on leukocytes. Using a fish immunological model system, the focus of my thesis work was to examine immunoregulatory receptors in vertebrates by further characterizing members of the teleost Leukocyte Immune-type Receptor (LITR) family. IpLITRs share structural and phylogenetic features with certain mammalian receptors involved in activating and abrogating immune cell functions. As stimulatory IpLITR2.6b associates with signaling adaptor molecule IpFcRγ-L, I expressed a chimeric construct of IpLITR2.6b with IpFcRγ-L in mammalian immune cells to examine its functional abilities. Engagement of this receptor-adaptor induced intracellular signaling and activation of degranulation and phagocytosis. I also expressed IpLITR1.1b, a receptor previously reported to inhibit natural killer cell cytotoxicity to examine its functions further. This inhibitory receptor surprisingly facilitated phagocytosis. This represents dual functionality among select IpLITR-types, which, to our knowledge, has not been reported before in fish. Taken together, these results highlight conserved aspects of immunoregulatory receptor signaling and function while revealing new insights that may contribute to our overall understanding of immunity.

ACKNOWLEDGEMENTS

There are many people whom I would like to thank: were it not for their support, guidance, prayers and encouragement, I would not have successfully completed my Graduate Studies.

First and foremost, in accordance with my faith, I thank the Lord for the incredible blessing that has been the last three years of my life. So I am eternally grateful for this gift and for placing the following people in my life.

An incredible thank-you to Dr. James Stafford, my graduate supervisor, for his dependable and consistent help throughout my studies. His wealth of scientific knowledge and approachability have been extremely beneficial to my studies, so I also thank him for his endless patience. I thank him for granting me opportunities to present my research at conferences throughout Canada, U.S.A. and Japan. It has been both an honour and a treat being a student in his lab and I am fortunate that he chose me to be a graduate student in his lab.

Thank you to my Supervisory Committee, Dr. Kathy Magor and Dr. Bart Hazes, for their analysis and feedback of my research. Thank you to Dr. Keith Tierney for his role on my examining committee.

Thank you to Dr. Deborah Burshtyn and her students for their comments, suggestions and the sharing of ideas during weekly lab meetings.

Thank you to the current and former graduate students in the Stafford lab – Dustin Lillico, Myron Zwozdesky, Jackie Mewes, Karlijn Verheijen, Loes Wiersma and especially Benjamin Montgomery – for their wisdom and assistance with my project, as well as making the lab environment more enjoyable.

A gracious and genuine thank you to graduate students in the Goss, Chang, Ali, Belosevic and K. Magor and Barreda labs: James, Josh, Jordan, Van, Aga, Mariel, Laura, Alysson. I will truly cherish the friendships we had during our time as students, because, frankly, you guys made grad school kick ass.

Finally, a heartfelt and immeasurable thank you to my family – mami, papi y Juan – for their love, support, prayers and wisdom. *Los quiero con todo mi corazón.*

TABLE OF CONTENTS

LIST OF TABLES

LIST OF FIGURES

LIST OF ABBREVIATIONS

ADCC	Antibody-dependent cellular cytotoxicity
ASB	Antibody staining buffer
BSA	Bovine serum albumin
CD	Cluster of differentiation
CD3ζ	CD3 zeta subunit
CEACAM	Carcinoembryonic antigen-related cell adhesion molecule
CHIR	Chicken immunoglobulin-like receptor
ConA	Concanavalin A
Csk	C Src kinase
CYT	Cytoplasmic tail
DAP10	DNAX-binding protein of 10 kDa
DAP12	DNAX-binding protein of 12 kDa
DAPI	4',6-diamidino-2-phenylindole
ΔCYT	truncated cytoplasmic tail
DMEM	Dulbecco's modified Eagle medium
DMSO	Dimethyl sulfoxide
DNP	Dinitrophenyl
D-PBS	Dulbecco's phosphate-buffered saline
EBSS	Earle's balanced salt solution
ECM	Extracellular matrix
EDTA	Ethylenediaminetetraacetic acid
Endo	Endogenous
ERK	Extracellular signal-regulated kinase
EST	Expressed sequence tag
FBS	Fetal bovine serum
Fc	Fragment crystallizable
FcR	Fc Receptor
FcεRI	High-affinity IgE receptor
FCRL	Fc receptor-like
FITC	Fluorescein isothiocyanate
FL	Fluorescence
Fwd	Forward primer
g	Gravity
Gab2	Grb2-associated binder 2
GEF	Guanine nucleotide exchange factor
GM1	Monosialotetrahexosylganglioside
Grb2	Growth factor receptor-bound protein 2
HA	Hemagglutinin
HEK	Human embryonic kidney cell
H+L	Heavy and light chain
HRP	Horseradish peroxidase
HSA	Human serum albumin
IFN	Interferon

Ig	Immunoglobulin
IgG3	Immunoglobulin isotype G3
IgSF	Immunoglobulin superfamily
IL	Interleukin
ILLR	Immune-related, lectin-like receptor
IP	Immunoprecipitation
IpFcRI	Channel catfish Fc receptor I
IpFcRγ	Channel catfish Fc receptor γ subunit
IpFcRγ-L	Channel catfish Fc receptor γ subunit-like
IpLITR	Channel catfish leukocyte immune-type receptor
IREM	Immune receptor expressed on myeloid cells
ITAM	Immunoreceptor tyrosine-based activating motif
ITIM	Immunoreceptor tyrosine-based inhibiting motif
ITSM	Immunoreceptor tyrosine-based switch motif
JNK	c-Jun N-terminal kinase
kDa	Kilodalton
KIR	Killer cell immunoglobulin-like receptor
LAIR	Leukocyte-associated immunoglobulin-like
LB	Luria-Bertani
LILR	Leukocyte immunoglobulin-like receptor
LITR	Leukocyte immune-type receptor
LMIR	Leukocyte mono-immunoglobulin-like receptor
LPS	Lipopolysaccharide
LRC	Leukocyte receptor complex
mAb	Monoclonal antibody
MAF	Macrophage activating factor
MAPK	Mitogen-activated protein kinase
MEM	Minimum essential media
MHC	Major histocompatibility complex
MLC	Mixed lymphocyte culture
NCR	Natural cytotoxicity receptor
NILT	Novel immunoglobulin-like transcript
NITR	Novel immune-type receptor
NK	Natural killer cell
NO	Nitric oxide
OE	Overlap-extension
pAb	Polyclonal antibody
PAGE	Polyacrylamide gel electrophoresis
PAMP	Pathogen-associated molecular pattern
PBL	Peripheral blood lymphocyte
PCR	Polymerase chain reaction
PE	Phycoerythrin
PECAM	Platelet endothelial cell adhesion molecule
PFA	Paraformaldehyde
phospho	Phosphorylated
pIgR	Polymeric immunoglobulin receptor

PIR	Paired immunoglobulin-like receptor
PKC	Protein kinase C
PMA	Phorbol myristate acetate
PTK	Protein tyrosine kinase
RBL	Rat basophil leukemia
RFU	Relative fluorescence unit
Rvs	Reverse primer
SDS	Sodium dodecyl sulfate
SEM	Standard error of the mean
SH2	Src homology 2
SHP	Src homology 2-containing protein tyrosine phosphatase
SHIP	Src homology 2-containing inositol 5'-phosphatase
SITR	Soluble immune-type receptor
Sos	Son of sevenless
SRBC	Sheep red blood cell
SFK	Src family kinase
Syk	Spleen tyrosine kinase
TBS	Tris-buffered saline
TBS-T	Tris-buffered saline supplemented with Tween-20
TCR	T-cell receptor
TLR	Toll-like receptor
TM	Transmembrane domain
TNF-α	Tumour necrosis factor alpha
TREM	Triggering receptor expressed on myeloid cell
v/v	Volume to volume
WB	Western blot
XFL	*Xenopus* Fc receptor-like

CHAPTER 1

Introduction

1.1 Introduction

Cells of the innate immune system provide essential defensive roles, protecting the host organism from infection. They do so by inducing effector responses such as degranulation (the release of inflammatory molecules from intracellular compartments); phagocytosis (the internalization of large pathogenic molecules or organisms); cellular cytotoxicity (the killing of allogeneic, malignant or virally-infected cells); and cytokine secretion (soluble molecules involved in communication between immune cells). A balance of stimulatory and inhibitory signals controls these immune effector responses, transmitted by proteins termed immunoregulatory receptors, expressed on immune cell surfaces. These receptors are typically involved in the binding and recognition of host- or pathogen-derived molecules and relaying this information to the immune cell via complex intracellular signaling pathways. Many of these receptors are part of the Immunoglobulin (Ig) Superfamily (IgSF), characterized by protein folding into one or more Ig domains on the extracellular-side of these proteins. IgSF receptors are ubiquitously expressed on the surface of immune cells that comprise both the innate and adaptive arms of the immune system, which speaks to their central importance in regulating immune responses.

The majority of research into characterizing immunoregulatory receptors has been conducted in mammals. However, this paradigm of using surface-expressed proteins to promote protective responses is common across vertebrates, as recent discoveries have been made of immunoregulatory receptors in non-mammalian vertebrates, including avians (birds), amphibians and teleost (bony fish).

The *Ictalurus punctatus* Leukocyte Immune-type Receptor (IpLITR) is one such family recently described in the channel catfish [1]. This is a very large family of proteins expressed on many catfish immune cell lines, and includes both putative stimulatory and inhibitory types, based on structural similarities to mammalian immune receptors. As with other fish immunoregulatory receptors identified in the last twenty years, the ligand(s) to these receptors remain unknown. While we do have a limited understanding of the signaling and functional potential of these receptors [2–4], their endogenous functional significance in regulating catfish immune cells remains to be determined.

1.2 Objectives of this thesis

The main objective of my research was to characterize the signaling and functional responses of stimulatory and inhibitory IpLITR-types. The specific aims of my thesis are as follows:

(1) Generate and express a chimeric construct of a stimulatory IpLITR-type and its associated signaling adaptor in mammalian immune cells
(2) Characterize the signaling and functional responses induced by this stimulatory receptor-adaptor
(3) Characterize the signaling and functional responses of an inhibitory IpLITR-type in mammalian immune cells
(4) Determine the mechanisms behind IpLITR1.1b's unexpected stimulatory signaling and functional responses

1.3 Outline of this thesis

In the second chapter of my thesis, I will review innate immunoregulatory receptors expressed in mammals. I will then discuss the advantages to using teleost (bony fish) as model organisms to conduct immunological research; their

immune cell effector responses; and recently identified teleost immunoregulatory receptor families, as well as known functions. Chapter 3 contains a detailed description of the materials and methods used throughout this thesis. Chapter 4 will discuss my research into examining the signaling and functional potential of a stimulatory receptor-type, IpLITR2.6b and its associated adaptor molecule, IpFcRγ-L [4], when expressed in a mammalian immune cell line. Cross-linking this receptor-adaptor induced the phosphorylation of ERK1/2 as well as cellular degranulation. This receptor-adaptor also induced the phagocytosis of opsonized microbeads. These responses were all ITAM-dependent, providing strong support that this receptor indeed functions as a stimulatory immunoregulatory receptor. In Chapter 5, I further examine IpLITR2.6b/IpFcRγ-L-induced signaling and functions as well as express an inhibitory receptor-type, IpLITR1.1b, as comparison, since it is has been previously characterized to be inhibitory. While no signaling molecules appeared to be activated by cross-linking IpLITR1.1b after 10 mins using a signaling profiler array, transient ERK1/2 and Akt phosphorylation was observed prior to 10 mins. A comparison of cytokine secretion by cross-linking either receptor-type showed that only IpLITR2.6b/IpFcRγ-L, not IpLITR1.1b, was capable of inducing secretion of the cytokines IL-3,-4,-6 and TNF-α. Most surprisingly, when transfected RBL-2H3 cells were incubated with opsonized-beads, IpLITR1.1b significantly induced phagocytosis, despite its previously reported inhibitory role [2,3]. I determined that IpLITR1.1b's phagocytic ability is not due to an association with endogenous FcεRI γ subunit but likely due to tyrosines within its cytoplasmic tail (CYT), as truncating this region blocked its ability to phagocytose. IpLITR1.2a, a receptor encoding a CYT similar to the CYT membrane-distal region of IpLITR1.1b, was also able to significantly induce phagocytosis. Taken together, the inhibitory and stimulatory functions of IpLITR1.1b suggest a functional duality shared among select mammalian immunoregulatory receptors that are also capable of activating and suppressing immune responses. Finally, in Chapter 6 I will provide an overview of my results, discuss plausible mechanisms explaining the stimulatory

signaling and functions of IpLITR1.1b, and suggest future experiments to this effect. Chapter 7 lists the references for the work cited in this thesis.

CHAPTER 2

Literature Review[1]

2.1 Overview

The innate immune system provides the first line of defense against pathogens. Cells of the innate immune system include macrophages, granulocytes, dendritic cells, and natural killer (NK) cells, which mediate protective effector functions such as phagocytosis, degranulation, antigen presentation, and cellular cytotoxicity. The activation and suppression of these immune responses depend in part on a series of stimulatory and inhibitory signals, mediated by proteins expressed on immune cell surfaces, termed immunoregulatory receptors [5–9]. Many of these receptors belong to the IgSF, characterized by a specific protein-folding pattern into one or more Ig domains on the extracellular-surface of these receptors, as well as the C-type lectin family. The latter have been reviewed extensively elsewhere [10–14]. Studies into IgSF receptor expression and function have revealed their central importance in regulating critical immune cell responses. Immunoregulatory receptor-types belonging to the IgSF have also been discovered in other vertebrates, including aves, amphibians and teleost (bony fish) [15–17]. While there is a limited understanding in terms of their precise roles in regulating innate immune functions, their discovery will provide new insights in regulation of immune defense in non-mammals, and perhaps shed light on the conserved nature of immune strategies across all vertebrates.

In this chapter, I will focus on aspects of innate immunity by reviewing immunoregulatory receptors and their signaling mechanisms in mammals. I will also highlight innate immune receptor-types described in non-mammalian

[1] Portions of this chapter have been previously published. Montgomery, *et al.* 2011. Dev Comp Immunol. 35: 1223-37.

vertebrates. As my thesis research was focused on teleost, I will discuss the advantages of using fish as models for conducting immunological studies, as well as describe the effector responses of fish immune cells, focusing on phagocytosis, degranulation, cytokine secretion and cellular cytotoxicity. I will also review IgSF families recently discovered in fish, with a particular focus on the IpLITR family. Finally, I will review the current research focused on the functional characterization of select fish immunoregulatory receptors, in particular the members of the IpFcR, NITR, and LITR families.

2.2 Innate immunity in mammals

2.2.1 Immunoregulatory receptors and immune cell effector responses

In mammals, the IgSF family represents a vast array of proteins, many of which are expressed on the surface of immune cells, involved in the control and coordination of immune responses. Effector responses of innate immune cells are tightly regulated by a balance of counteracting signals initiated by these co-expressed receptors, which are coupled with distinct intracellular signaling events [5–9]. This has unveiled some of the central mechanisms that control our first line of immune defense.

In humans, a very large subset of IgSF genes are clustered on chromosome 19, in a region known as the Leukocyte Receptor Complex (LRC) [6]. Although the extracellular Ig domains of these receptors are related, they bind an incredible number of ligands. Innate immune cells express these LRC-encoded receptors (discussed shortly) and other IgSF receptors to translate environmental cues into effector responses. These immunoregulatory receptors are often co-expressed as stimulatory and inhibitory types. This paired receptor expression acts to control and coordinate these responses, inducing or abrogating cellular events leading to immune responses, respectively. Examples of receptor families in mammals that

are encoded within the LRC include killer cell Ig-like receptors (KIRs) [18–20] leukocyte Ig-like receptors (LILRs) [21–23], natural cytotoxicity receptors (NCRs) such as NKp46, NKp30 and NKp44 [6,24–27], and sialic acid-binding Ig-like lectins (Siglecs) [6,8,28].

Innate immune cells recognize a variety of host- or pathogen-derived molecules via distinct receptor-types, the recognition of which often engages intracellular signaling cascades that act to activate or abrogate immune effector responses. For example, binding of monomeric or antigen-aggregated antibodies is mediated by Fc receptors [29–31]. Macrophages and mast cells utilize these Fc receptor-antibody complexes to initiate phagocytosis and degranulation, respectively, and NK cells use Fc receptors to kill opsonized target cells, through a process known as antibody-dependent cellular cytotoxicity (ADCC) [30,32,33]. Major histocompatibility complex (MHC) class I (MHC I) proteins, as well as structural relatives to MHC I, including viral MHC homologs are recognized by KIRs [34,35], LIRs [36,37] and NCRs, such as NKp30, NKp44 and NKp46 [38]. Paired Ig-like receptors (PIRs) expressed in mice are homologs to human LIRs and are also involved in mouse MHC I recognition [39]. The expression of KIRs, LIRs, NCRs and FcRs on NK cells, in particular, act to regulate cellular cytotoxic responses and cytokine secretion [40,41,39]. These and other IgSF members exhibit key immunoregulatory roles, reinforcing the complexity of receptor networks participating in mammalian immune defense.

2.2.2 Stimulatory and inhibitory immunoregulatory receptor-types

Immunoregulatory receptors are typically classified as stimulatory or inhibitory, based on their ability to activate or suppress cellular effector functions, respectively. In general, stimulatory immunoregulatory receptor-types encode short cytoplasmic tails (CYT) devoid of any known signaling motifs, but contain a positively charged amino acid, lysine (K) or arginine (R), in their transmembrane (TM) segments that allows them to pair with signaling adaptor molecules with an

oppositely charged TM region, a requirement for stimulatory receptor surface expression [42] and function. Examples of stimulatory receptor-adaptor associations include the IgE-binding α subunit with β and γγ subunits, forming the FcεRI complex [43]; KIR2DS with its adaptor, DNAX-activating protein of 12 kDa (DAP12) in NK cells [44]; and LILR7 (LILRA2/ILT1) has been reported to associate with FcεRI γ subunit [45].

These signaling adaptors in turn have long CYT with tyrosines encoded within immunoreceptor tyrosine-based activating motifs (ITAMs). Upon receptor-ligand interaction, phosphorylation of these ITAM tyrosines by Src-family kinases (SFKs) enables the recruitment of spleen tyrosine kinase (Syk/ZAP70), which then serves to initiate a stimulatory signaling cascade leading to the overall activation of the immune cell and induction of effector responses [46,47]. It was also recently shown that activation of Syk and induction of effector responses can also occur independently of ITAM-bearing adaptors, against the paradigm that these receptors need an adaptor to signal. The α subunit of FcγRIIIA encodes a short CYT with an RSSST motif which becomes phosphorylated by PKC and initiates downstream signaling and effector responses [48]. Taken together, engagement of stimulatory receptor-types initiates downstream phosphorylation events that lead to the activation of an immune cell.

In contrast, inhibitory immunoregulatory receptors usually have uncharged transmembrane segments and long cytoplasmic tails (CYTs) encoding tyrosines found within one or more immunoreceptor tyrosine-based inhibitory motifs (ITIMs) [49,50]. Upon receptor-ligand interaction, these ITIM tyrosines become phosphorylated by SFKs, which enables the recruitment of src homology 2 (SH2)-domain-containing protein tyrosine phosphatases (SHP)-1, -2 and SH2 domain-containing inositol 5'-phosphatase (SHIP), which act to dephosphorylate ITAM-activated stimulatory signaling molecules, abrogating the induction of effector responses [49,50]. Together, co-expressed inhibitory and stimulatory receptors act to

coordinate cellular responses, initiating or suppressing protective functions in the presence or absence of infection, respectively.

2.3 Examples of immunoregulatory receptors in birds and frogs

The above-mentioned IgSF members, associated signaling pathways and effector responses have been very-well characterized in mammals; however, IgSF members have also been discovered in non-mammalian vertebrates, including birds [51–53] and frogs [54–56], which have been identified and categorized based on their predicted structures and phylogenetic relationships with mammalian IgSF members, however little information is available regarding their functional capacities.

Xenopus frogs encode proteins distantly related to mammalian FcRs, termed *Xenopus* FcR-Like (XFLs) [56]. Thirteen XFLs were originally described; however an estimated >75 XFL genes exist [56]. Of these, XFLs were largely divided into two groups: those encoding a charged TM and short CYT, predicted to be stimulatory; and those with uncharged TM and a long CYT encoding ITIMs, predicted to be inhibitory [56]. In addition to these receptors, *Xenopus* homologs of the signaling adaptors FcRγ and CD3ζ have also been found [55]. Surface expression of stimulatory XFL-2 in HEK 293T cells, was only able to occur when co-expressed with *Xenopus* FcRγ [56], so there is potential for this receptor and adaptor to activate immune effector responses.

Chicken Ig-like receptors (CHIRs), avian homologs to mouse paired Ig-like receptors (PIRs) [57], encode two receptor-types: CHIR-B, encoding an uncharged TM and a CYT containing two ITIMs; and CHIR-A, which has a positively charged TM and short cytoplasmic tail [57] and was reported to associate with the chicken homolog to FcεRI γ subunit, a requirement for surface expression in transfected cells [52]. In addition to these two molecules, the CHIR family encodes

>100 receptor types within the chicken Leukocyte Receptor Complex (LRC) [52]. CHIR-AB1, a receptor containing a single Ig domain, a positively charged TM and ITIMs within its CYT, was found to strongly bind the Fc region of IgY, an antibody isotype specific to birds, reptiles and amphibians, identifying this CHIR-type to be an FcR [58]. This is consistent with the initial identification of mouse PIRs as homologs to FcαRI (CD89), a member of the human LRC . Other CHIR-types have also been identified as variable-affinity IgY-binding receptors [59]. Functional characterization of different CHIR-AB-types as avian Fc receptors for IgY rather than MHC-binding molecules is one example of the difficulties in accurately predicting functional homologs to non-mammalian immunoregulatory receptors, based on sequence alone. Thus, this is an important consideration when examining additional vertebrate immunoregulatory receptor-types that have not had a ligand identified.

Taken together, that there are non-mammalian multigene IgSF families and ITAM-bearing signaling adaptors speaks not only to the complexity of immunoregulatory receptor networks but also to the potential conservation of signaling pathways, even among lower vertebrates, such as teleost fish.

2.3.1 Mechanisms of immunoregulatory receptor diversification

As demonstrated above, vertebrate IgSF immunoregulatory receptors exist as large, germline-encoded multi-gene families, consisting of closely related but unique members. Families of immunoregulatory receptors that bind similar ligands are commonly encoded as clusters of genes on different chromosomes. For example, there are 13 LILR, 17 KIR and 13 Siglec genes on the human LRC located on chromosome 19 [6]. On chromosome 1, up to 25 FcR and FCRL genes are encoded, as well as a single gene for FcαRI (CD89) found within the LRC [33]. Multigene immunoregulatory receptor families are not limited to humans, as the CHIR locus in chickens on microchromosome 31, equivalent to the human LRC, encodes over >100 possible CHIR genes[15,58,59]. Additionally, the *Xenopus* genome

encodes an estimated >75 XFL genes [56]. Mechanisms enabling this diversity include mutations, gene duplication, exon shuffling, gene splicing, gene conversion and non-homologous recombination [60–63].

The polymorphic and polygenic nature of these receptor families suggest that this diversity is likely due to positive selection pressures to match rapidly evolving ligands, to perhaps enable direct receptor interactions with a diverse range of pathogen products [18,62,64]. Human cytomegalovirus (HCMV) encodes UL18, an MHC class I homologue which binds inhibitory LILRB1 (LIR-1) as a potential immune evasion strategy [65,66]. LILRs may have then expanded, generating stimulatory LILRB-types to recognize UL18, induce an effector response and eliminate an infected cell. KIRs are another multigene family of immunoregulatory receptors encoded within the human LRC, that have diversified in primates by the gain of new KIR genes and loss of existing genes [61]. New KIR genes are then produced by gene duplication, domain shuffling and recombination between existing genes [67], resulting in receptors with 2 or 3 extracellular Ig domains and long or short CYT [61]. Additional studies into KIR origins suggest activating KIR-types evolved from inhibitory KIR-types, which was in turn favoured by natural selection [67]. Siglecs are another family of receptors, rapidly evolving by many processes, such as gene duplication, exon shuffling and gene conversion [63,68]. Siglecs bind sialic acid (*N*-acetylneuraminic acid; Neu5Ac) residue-containing proteins and the majority of Neu5Ac-expressing bacteria are pathogenic to humans, and so Siglecs specific for Neu5Ac may have emerged to keep pace with changing pathogenic sialylation [63]. Among human FcRs for IgG, FcγRs, there are three high-affinity FcγRs (FcγRIA-C) and five low-affinity FcγRs (FcγRIIA-C and FcγRIIIA-B) [33]. The preferential and competitive interaction of various mammalian FcRs with different Ig-types may set a threshold of activation and may enable the activation or inhibition of specific immune responses. Binding of Ig-isotypes with variable affinity has also been reported in the avian CHIR family: CHIR-AB1 binds IgY with high affinity[58], whereas six additional CHIR-AB1-like receptor-types were also identified to bind

IgY with high, intermediate and non-binding affinities [59]. Differential expression of individual CHIR-AB-types on immune cell may also affect cell activation, and the affinity differences between receptor-types may reflect a pathogen-driven selection process, influencing immune responses [59]. Taken together, the presence of complex multigenic immunoregulatory receptor families is no accident. The diversity of these germline-encoded receptor families has arisen out of a need to equip the immune cells with a large repertoire of receptors able to recognize and provide protective responses against rapidly-evolving pathogenic ligands and maintain the health of an organism.

2.4 Teleosts as model organisms for studying immunity

2.4.1 Overview

Teleost represent the largest group of vertebrates (~28, 000 species), and along with other fishes (including jaw-less and cartilaginous fish) represent about 43% of extant vertebrates [69]. This diverse group of animals is found in many different environments (salt vs. fresh water; arctic vs. tropical temperatures) and they have adapted to the different selective pressures present within these varied habitats. As well, due to their aquatic environment, fish are constantly 'bathed' in pathogens, coming in intimate contact with their skin, gills and other mucosal tissues. As such, fish have developed elaborate immune systems, comprised of sophisticated immune receptor-mediated regulatory systems. It is likely that these factors have allowed fish to elicit robust immune responses against a diverse array of pathogens and thrive in these different environments.

Immunological studies in teleost have focused on immune cells derived from a handful of fish species, including zebrafish (*Danio rerio*) rainbow trout (*Oncorhynchus mykiss*), goldfish (*Carrasius auratus*) and channel catfish (*Ictalurus punctatus*). Comparative immunologists have developed procedures for

the isolation, separation and *in vitro* cultivation of fish leukocytes, which has significantly contributed to our understanding of cellular immunity in fish. Channel catfish (*Ictalurus punctatus*) is particularly advantageous for conducting immunological studies. It is one of the few species from which functionally distinct, clonal, long-term leukocyte lines can be developed from peripheral blood lymphocytes (PBLs), without requiring cellular transformation [70]. Additionally, due to their physical size, it is possible to collect leukocytes in large quantities as well as the serum proteins necessary to culture them. Examples of catfish cell lines include 3B11 and 1G8: these are two B-cell lines generated from stimulating peripheral blood lymphocytes (PBLs) with lipopolysaccharide (LPS) [71,72]. Cytotoxic T cell lines TS32.15 and TS32.17 were established from mixed leukocyte culture cells (MLCs) of a fish immunized with irradiated allogeneic 3B11 cells [73,74]. A macrophage-like cell line, 42TA cells, was generated from PBLs treated with phorbol ester and calcium ionophore [75,72,74]. Finally, cytotoxic NK-like cells are derived from PBLs stimulated with allogeneic irradiated 3B11 cells [76,77]. The availability of culturing long-term, clonal immune cell lines has been a very valuable tool in sustainable characterization of immune cell functions. Using catfish cultured cells as well as primary cells from other fish species, it has been possible to functional studies, characterizing the protective immune responses utilized by fish leukocytes, discussed below.

2.4.2 Teleost immune cell effector responses

Prototypical immune cell effector functions carried out by innate immune cells include phagocytosis, degranulation, cytokine secretion and cellular cytotoxicity. These protective responses and the immune cell types that commonly induce them are very-well characterized in mammals, especially humans [78–82]. However, teleost immune cells also utilize these same inflammatory processes to provide immune protection against invading pathogens. Herein I will review immune effector responses carried out by cultured fish cell lines as well as primary leukocyte populations. While the immunoregulatory receptors responsible for

inducing these immune responses are not yet defined, a review of innate immune receptors expressed in fish that likely moderate these cellular responses follows in Section 2.5.

Phagocytosis, the internalization and destruction of large particulate antigens by phagocytes, has been extensively examined in many teleost species. Sea bass (*Dicentrarchus labrax*) peritoneal macrophages showed a strong phagocytic response of the bacteria *Escherchia coli* and *Salmonella typhimurium* [83]. Kidney-derived macrophages from Atlantic salmon (*Salmo salar*) were reported to phagocytose opsonized yeast glucan particles as well as sheep red blood cells (SRBCs) [84]. The phagocytic capacity of goldfish macrophages was also observed during incubations with SRBCs and *Leishmania major* promastigotes and amastigotes [85] as well as *Aeromonas salmonicida*, a bacteria pathogenic to fish [86]. In the rainbow trout macrophage cell line, RTS11, derived from the stromal layer of trout spleen [87], phagocytosis was observed by these cells when incubated with opsonized polystyrene beads [88]. Rainbow trout B lymphocytes were also reported to phagocytose opsonized beads as well as opsonized *A. hydrophila,* leading to their destruction in phagolysosomes [89]. As mammalian B cells do not internalize large particles by phagocytosis, the observation that a teleost B cell can suggests B cells in higher vertebrates may have developed into their highly specialized role in adaptive immunity from a phagocytic predecessor involved in innate responses [89]. Studying phagocytosis in teleosts reveals, as expected, the conserved role of macrophages in conducting this immune function, but also the unexpected phagocytic role of B-cells. These results demonstrate the value of conducting immunological research in teleost, as unexpected observations such as these can provide valuable insights into the origins of the vertebrate immune system.

The release of intracellular granules containing inflammatory mediators into the extracellular milieu by granulocytes, such as mast cells, basophils and neutrophils, has been reported in bream (*Abramis brama*) mast cells in gills infected with *Ergasilus sieboldi* parasites and in brown trout (*Salmo trutta*) mast cells in

intestines infected the parasite *Echinorhynchus truttae* [90]. Degranulation was also observed in neutrophils-like cells isolated from goldfish kidneys stimulated with the mitogen zymosan as well as upon exposure to *A. salmonicida* [91]. Neutrophil degranulation was also reported upon stimulation with calcium ionophore in fathead minnows (*Pimephales promelas*) [92] and carp (*Cyrprinus carpio carpio*) [93]. Taken together, the isolation and functional characterization of fish granulocytes, such as mast cells and neutrophils, has provided novel insights in innate immune responses against fish pathogens.

Another effector response induced in teleost fish is the production of soluble molecules involved in immune intercellular communication, termed cytokines. Fish do express a number of cytokines homologous to their mammalian counterparts, including interleukin (IL)-2, -6, -12 and interferons (IFN) [94,95]. Gene expression of IL-1β1, -1β2, -8, -11 and tumour necrosis factor (TNF)-α2 was up-regulated in rainbow trout macrophage cell line RTS11 upon infection with *Saprolegnia parasitica*, a fish fungal parasite [96]. It is important to consider that while cytokine messages can be detected, there is limited characterization of fish cytokines at the protein level. Having said that, goldfish kidney leukocytes, stimulated with concanavalin A (Con A) secrete Macrophage Activating Factors (MAFs), presumed to contain secreted cytokines, that can induce nitric oxide (NO) production of goldfish macrophages [97]. Cleavage products of transferrin were identified among these MAFs and reported to activate goldfish macrophages into producing NO [98], providing the first observation of a teleost iron-binding protein capable of facilitating proinflammatory responses.

Cellular cytotoxicity of allogeneic target cells has also been reported in teleost leukocytes, particularly in channel catfish. Nonspecific cytotoxic cells were reported to induce apoptosis of allogeneic B-cells [99]. NK-like cells, derived from PBLs of an alloantigen-immunized catfish [73], were also reported to induce apoptosis in allogeneic B cells, in a calcium-dependent mechanism [100]. Finally, PBLs and kidney lymphocytes of alloantigen-immunized ginbuna crucian carp

(*Carassius auratus langsdofii*) were cytotoxic against allogeneic erythrocytes [101]. Further studies are still required to confirm if the mechanisms behind cytotoxicity are similar as in mammals, i.e. the release of perforin and granzymes [102] or utilizing Fas ligand to induce apoptosis [103]. Nonetheless, these studies have broadened our understanding of additional host responses in teleost.

Taken together, teleost innate immune cells carry out a variety of protective responses against pathogens reminiscent of responses elicited by mammalian immune cells. While this speaks to the conserved nature of these protective responses against pathogens across vertebrates, there is a general lack of understanding regarding the regulatory mechanisms controlling and coordinating these cellular events in fish, presumably by cell-surface expressed immunoregulatory receptors, discussed below.

2.5 Teleost immunoregulatory receptors

2.5.1 Overview

Despite significant contributions of the studies above in fish immune cell effector functions to our understanding of teleost immunology, questions still remain regarding the immunoregulation of these and other effector functions in fish innate immune cells. For instance, what is the repertoire of immunoregulatory receptor expression on fish immune cell subtypes, such as macrophages, mast cells and NK-like cells? Which receptors do these cells utilize to bind and recognize targets and induce responses? And what are the mammalian counterparts to these receptors in fish? To that end, a number of innate immunoregulatory receptor families have recently been discovered in teleost, the majority of which belonging to the IgSF and C-type lectin family which has underscored the complexity of immune system regulation and provides valuable insights into the origins of vertebrate innate immune receptor networks. These teleost receptor families include Fc receptors (FcRs), novel immune-type

receptors (NITRs) and leukocyte immune-type receptors (LITRs), as well as polymeric immunoglobulin receptors (pIgRs) novel Ig-like transcripts (NILTs), immune-related lectin-like receptors (ILLRs), and soluble immune-type receptors (SITRs). For the sake of brevity, I will survey well-characterized teleost innate immune receptors, FcRs, NITRs and LITRs; however the reader is invited to read the following publications and reviews on pIgRs [17], NILTs [17], ILLRs [104] and SITRs [105].

Many of these receptor families exist as polygenic and polymorphic gene clusters found on different chromosomes. Through cloning and molecular characterization, these receptor families, reviewed below, have been identified and categorized based on their predicted structures and phylogenetic relationships with mammalian IgSF members. As such, the variety and complexity of fish immunoregulatory receptors speaks to the complexity of the vertebrate immune system and provides insights into the origins of vertebrate immunoregulatory receptor networks.

2.5.2 Teleost Fc receptors

The strongest evidence for FcR homologs in teleost came from studies using channel catfish NK-like cells. These cells stained positive for catfish IgM, [76]; when replacing the surface bound, pre-armed IgM (presumably from serum) with catfish anti-trinitrol-phenol (TNP) IgM antibodies, these specifically armed NK cells were able to kill TNP-haptenated target IM9 cells by antibody-dependent cellular cytotoxicity. As these processes were predicted to be mediated by a specific IgM-binding FcR expressed on NK-cells, searching catfish EST databases for homologs to mammalian FcRs resulted in the identification of IpFcRI [106]. IpFcRI encodes three Ig domains; the D1 and D2 domains were found to be highly homologous to FcRs and FCRLs expressed in *Xenopus*, rat and humans [106]. IpFcRI messages were not found in the above-mentioned catfish clonal cell lines; however, they were found in freshly isolated PBLs as well as

head-kidney and spleen tissues [106]. IpFcRI represents the first and, to date, only *bona fide* FcR homolog in teleost; while its role in Ig binding will be discussed below, its role in mediating cellular responses, such as the above-mentioned ADCC in catfish NK-like cells, has yet to be examined.

2.5.3 NITRs

NITRs were first described in Southern pufferfish (*Spheroides nephelus*) while attempting to discover T-cell receptor (TCR) homologs [107]. Since then NITRs have been identified in several teleost species, including zebrafish, rainbow trout, channel catfish, Japanese flounder (*Paralichthys olivaceus*), medaka (*Oryzias latipes*), and pufferfish (*Takifugu rubripes* and *Tetraodon nigroviridis*). [108–116] and NITR gene clusters have been fully annotated for zebrafish and medaka [113,115]. NITRs are proposed to be orthologs to human NCRs and KIRs, which, as mentioned above, function to regulate NK cell functions such as cellular cytotoxicity and cytokine secretion [117,118]. Structurally, NITRs encode one or two extracellular domains that are structurally related to T-cell receptor (TCR) Ig domains [118]. The majority of zebrafish and medaka NITRs encode uncharged TM and long CYT with ITIMs, and as such are predicted to be inhibitory; whereas other NITR types encode a charged TM with a short CYT and thus are predicted to be stimulatory [118]. While the expression pattern of NITRs on zebrafish immune cells is unclear [118], multiple NITRs were detected using catfish clonal NK-like cells, T-cells and macrophages, and a single NITR-type was detected in catfish B cells [108,109]. Altogether these extensive genomic studies of NITRs have represented a major contribution to our understanding of IgSF members expressed in teleost. Despite this, functional studies in NITRs remain limited, which will be described in a later section.

2.5.4 IpLITRs

The *Ictalurus punctatus* Leukocyte Immune-type Receptor (IpLITR) family, the most functionally characterized IgSF receptor family in fish to date, is another multi-gene family that was initially discovered from an EST library generated from alloantigen-stimulated cytotoxic lymphocytes [1]. The repertoire of IpLITRs is predicted to be polymorphic and polygenic, based on Southern blot analysis of sibling catfish showing a large number of IpLITR-bands [1]. IpLITRs are type 1 TM proteins with each encoding two to six extracellular Ig-like domains. Out of the three original prototypes discovered IpLITR1 has four Ig domains, an uncharged transmembranes and long CYT with two ITIMs and an overlapping ITSM, and is predicted to be inhibitory [1]. While IpLITR2 has three Ig domains and IpLITR3 has six, both encode a charged TM with short CYT, devoid of signaling motifs, suggesting they are stimulatory receptor-types requiring an association with an ITAM-bearing signaling adaptor [1,42]. Genomic analysis revealed multiple IpLITR loci within the catfish genome, but it is not known if these loci represent functionally redundant or distinct gene clusters [1]. IpLITR-like clusters are also found in the zebrafish genome [1] and are predicted to be ubiquitous among teleost species with LITR-like sequences identified in Atlantic salmon, halibut (*Paralichthys olivaceus*), green pufferfish (*Tetradon nigrovidis*) and tiger pufferfish (*Takifugu rubripes*) [17]. Database searches to identify potential IpLITR homologues were conducted using the extracellular Ig domains of IpLITR1 and IpLITR2 [1]. This revealed similarities to immunoregulatory receptors in higher vertebrate species, such as human FcRs, FcRLs and members of the human LRC, such as Siglecs, CEACAMs, KIRs and LILRs [1,119]. Similarities to amphibian XFLs and avian CHIRs were also observed [17]. Interestingly, IpLITRs were not closely related to teleost IgSF members such as NITRs, NILTs and IpFcRI [17].

IpLITR messages are found among different catfish immune cells, including macrophages, B-cells, T-cells and NK-like cells. These cells in turn co-expressed

multiple IpLITR-types with varying Ig domain number and CYT length [1]. Expression of stimulatory and inhibitory IpLITR-types was examined in activated catfish PBLs and cytotoxic T lymphocytes: Concanavalin A and lipopolysaccharide did not induce expression of IpLITRs [119]; however, co-expression of both IpLITR-types was observed upon stimulation with alloantigen in both PBLs and cytotoxic T-cells [119]. Furthermore, cloning of these expressed transcripts revealed a large repertoire of inhibitory and stimulatory IpLITR-types [119]. The variety of IpLITR-types expressed by catfish immune cells and their upregulation by alloantigen stimulation suggest clear roles in regulating effector responses in catfish immune cells. Unfortunately, these genomic studies do not provide information as to the signaling or functional roles, so further studies are still required to fully characterize this complex receptor family.

2.6. Teleost immunoregulatory receptor signaling and function

2.6.1 Overview

Since the discoveries of immunoregulatory receptor families in fish, functional and signaling responses induced by these receptors have been limited to studies in a few individual members of three immunoregulatory receptor families in fish, IpFcR, NITRs and LITRs. Examination of the functional and signaling pathways initiated by these receptors, though limited, also sheds light on the conserved signaling pathways necessary for the initiation and termination of immune responses and reveals the diversity of receptor-types that have evolved to coordinate and control vertebrate immunity.

2.6.2 IpFcR binding of catfish IgM

An FcR homolog was identified in channel catfish, termed IpFcRI [106]. It encodes three Ig domains but no TM or CYT and may likely be soluble, as it was secreted

when expressed in insect Sf9 cells [106]. It was reported to directly bind to catfish IgM, confirming its role as an FcμR, the first described in teleost [106]. Examination of this interaction determined that IpFcRI encodes a putative docking site and binds a conserved epitope, FxCxVxHE, on the constant Cμ3 and Cμ4 domains of catfish IgM [120]. While these studies demonstrate the first interaction between an IgM and FcR in teleost, additional studies are required to examine the role of IpFcRI in potentially modulating immune cell responses, such as phagocytosis or ADCC.

2.6.3 Known NITR signaling and functions

NITRs have been extensively characterized at the genomic level and include putative stimulatory and inhibitory types. Of these, zebrafish NITR 3.1 contains two ITIMs in its CYT and was expressed in human NK92 cells [114]. Incubation of NK92 cells with Raji tumour cells (a human Burkitt's lymphoma B cell line) induced phosphorylation of the downstream signaling molecule MAPK. However, cross-linking NITR3.1 during incubation with Raji tumour cells inhibited MAPK phosphorylation, in an ITIM-dependent manner [114], indicating that this NITR-type may serve as a negative regulator in zebrafish immune cells.

Zebrafish NITR 9L encodes a positively charged amino acid in its transmembrane [115] and was reported to associate with the zebrafish ortholog of the ITAM-bearing adaptor DAP12 when co-expressed in human AD-293 cells (a derivative of HEK 293 cells) [121,122]. Crosslinking of the NITR 9L-DAP12 complex induced the phosphorylation of ERK and Akt. Mutating the negative residue in the DAP12 TM prevents receptor-adaptor association and subsequent signaling events. This parallels stimulatory receptor-adaptor signaling in mammalian immune cells [123].

NITR Ig domains encode a Highly Variable (HV) region, characterized by a high level sequence diversity across NITR-types [115]; this observation combined with their phylogenetic relationship to human NCRs and KIRs [117,118], suggest NITRs

may recognize a wide array of ligands, perhaps even MHC [118,115]. IpNITR11 [109] was expressed on catfish cytotoxic NK-like cells to examine the potential role of NITRs in allogeneic recognition [124]. The extracellular domains of NITR 11 were fused with the ITAM-containing CYT of mouse CD3ζ and expressed in the 43-1 T cell hybridoma cell line. Incubations with the catfish 1G8 B-cell line demonstrated strong binding of the transfected T-cells to the B-cells. This was not observed utilizing NITR10, which shares 93% identity in the Ig domain [124]. Soluble NITR 11 constructs also bound to 1G8 cells. While the ligand for NITR11, presumed expressed on 1G8 cells, was not determined, the authors suggest a likely role for this receptor-type in allogeneic recognition. Despite these findings and the phylogenetic relationships of NITRs to human LRC members based on sequence and genomic analyses, it is important to consider the difficulties in predicting functional homologs based on sequence analysis alone. Thus further studies are required to characterize true NITR ligand(s) and functions.

2.6.4 IpLITR signaling and control of immune cell effector functions

Our laboratory has focused on the functional characterization of IpLITR-types. IpLITR1.2a encodes four Ig domains, one ITIM and an immunoreceptor tyrosine-based switch motif (ITSM) whereas IpLITR1.1b also encodes four Ig domains, but two ITIMs, an ITSM, and three additional tyrosines [1]. Chimeric constructs of IpLITR1.1b or 1.2a CYT were fused with the extracellular domain and TM of human KIR2DL3 and expressed in HEK 293T cells. When co-expressed with zebrafish homologues to the inhibitory phosphatases SHP1 or 2, each receptor bound SHP1 and 2 in an ITIM-dependent manner [2]. When these inhibitory IpLITR constructs were expressed in mouse lymphokine-activated killers (a primary NK cell type), cellular cytotoxic responses were inhibited, during incubation with MHC-deficient B cells [3]. Inhibition was mediated by SHP-recruitment as well as activation of the inhibitory C-src kinase (Csk), recruited to one of the non-ITIM tyrosines in IpLITR1.1b [3].

Among stimulatory IpLITR-types is IpLITR2.6b [1]. This receptor encodes two extracellular Ig domains, a positively charged TM and short CYT devoid of signaling motifs. In early biochemical studies to understand the biochemical requirements for optimal receptor surface expression, it was co-expressed in HEK 293T cells along with the catfish homologues to various ITAM-bearing signaling adaptors IpDAP12, IpCD3ζ, IpFcRγ and IpFcRγ-L [4]. IpLITR2.6b was reported to associate best with (IpFcRγ) and IpFcRγ-L and this association was necessary for surface expression [4]. This demonstrates the conserved nature of stimulatory receptor-adaptor interactions among vertebrates; however it does not provide information as to the functional consequences of this receptor-adaptor association when expressed in an immune cell.

2.7 Conclusions

Our understanding of fish immunology has greatly improved in the past two decades, owing both to studies in effector responses conducted by fish immune cells as well as the discovery of various IgSF immunoregulatory receptor families in teleost. Unfortunately, there is a disconnect in our understanding of the regulation of these responses by these immunoregulatory receptors. As there is such a variety and complexity of fish receptor families, the complete characterization of these families and their individual receptor-types will further our understanding of the receptor-ligand interactions and subsequent signaling cascades regulating these cellular events. To date, characterization has focused on the LITR and NITR families; and among them, only a handful of receptors have been examined. Nonetheless the discovery of these receptor families and their subsequent functional examinations, though limited, have broadened our understanding of the origins and complexity of vertebrate innate immune defense strategies.

CHAPTER 3

MATERIALS & METHODS

3.1 Cell Lines

Human embryonic kidney (HEK) 293T cells are an adherent, epithelial cell line derived from HEK 293 cells transformed with T antigen of simian virus 40 (SV40) and were kindly provided by Dr. Burshtyn (Dept of Medical Microbiology and Immunology, University of Alberta).

Rat basophil leukemia (RBL)-2H3 cells (ATCC® #CRL-2256™) are an adherent, transformed mast cell line derived from basophilic tumours of Wistar rat (*Rattus norvegicus*) treated with the carcinogen 2-(α-chlor-β-isoproylamine) ethylnaphthalene [125] and were kindly provided by Dr. Dean Befus, Dept of Medicine, University of Alberta.

3.2 Cell culturing

HEK 293T cells were grown at 37°C and 5% CO_2 in Dulbecco's modified Eagle's medium (DMEM)/High Glucose (HyClone) supplemented with 2mM L-Glutamine (Gibco), 100 units/mL penicillin (Gibco), 100 µg/mL streptomycin (Gibco), 1 mM sodium pyruvate (Gibco), 1% MEM non-essential amino acid solution (Gibco) and 10% heat-inactivated fetal bovine serum (FBS; characterized; Hyclone). Prior to use, culture media (DMEM/FBS) was filter sterilized using 0.22 µm filter units (Corning). Once confluent in a 10 cm tissue culture plate (~10 x 10^6 cells; BD Falcon), cells were gently washed in 2 mL Dublecco's phosphate buffered saline (D-PBS), then aspirated, then incubated in 500 µL 0.25% trypsin-EDTA (Gibco) for 1 min at 37°C. After gentle agitation to loosen cells, cells were collected in 6 mL fresh DMEM/FBS. Six hundred µL of

this cell suspension (~5 x 10^5 cells) was added to a new 10 cm culture dish containing 10 mL fresh DMEM/FBS.

RBL-2H3 cells were grown at 37°C and 5% CO_2 in Minimum essential media (MEM)/Earl's Balanced Salts Solution (EBSS; Hy-Clone) supplemented with 2mM L-Glutamine, 100 units/mL penicillin, 100 μg/mL streptomycin and 10% heat-inactivated FBS. Prior to use, culture media (MEM/EBSS/FBS) was filter sterilized using 0.22 μm filter units. For transfected RBL-2H3 cells used in this thesis, media was supplemented with 400 μg/mL of G418 disulfate salt solution (Sigma). Once grown to confluence in 6-well tissue-culture plates (~2.5 x 10^6 cells; Costar), media was removed and RBL-2H3 cells were harvested by the addition of 500 μL harvest buffer (1.5 mM EDTA, 135 mM NaCl, 5 mM KCl, 20 mM HEPES, pH 7.4, filter-sterilized) pre-warmed to 37°C. After incubating cells in harvest buffer for 10 min at 37°C, cells were detached from the tissue culture plates by gentle pipetting. Thirty μL of this cell suspension (~1.5 x 10^5 cells) was used to seed a new 6-well plate containing 3 mL fresh MEM/EBSS/FBS.

3.3 Antibodies

Antibodies used throughout this thesis are as follows: mouse α-hemagglutinin (HA) monoclonal antibody (mAb) clone HA.C5 (Cedarlane Laboratories); mouse IgG3 UNLB (Clone B10) (Beckman Coulter); phycoerythrin (PE)-conjugated goat anti-mouse immunoglobulin (Ig) G (H+L) polyclonal antibody (pAb); Beckman Coulter); goat anti-mouse IgG3 UNLB pAb (Beckman Coulter); horseradish peroxidase (HRP)-conjugated anti-HA pAb (Genscript); goat anti-mouse IgG (H+L) HRP-conjugated pAb (Bio-Rad); goat anti-rabbit IgG (H+L) HRP-conjugated pAb (Bio-Rad); anti-DNP IgE mAb (clone SPE-7; Sigma-Aldrich); anti-FcεRI α subunit mouse mAb (Upstate Cell Signaling Solutions); anti-FcεRI α subunit rabbit pAb (Santa Cruz Biotechnology); anti-FcεRI γ-subunit rabbit pAb (Upstate Cell Signaling Solutions). Additionally, the following antibodies were purchased from Cell Signaling Technologies: anti-extracellular

signal-regulated kinase (ERK) 1/2 rabbit mAb; anti-phosphorylated (phospho)-ERK1/2 (Thr202/Tyr204) rabbit mAb; anti-Akt rabbit mAb; anti-phospho-Akt (Ser473) rabbit mAb.

3.4 Generation of IpLITR 2.6b/IpFcRγ-L chimeric protein

Amino acid (aa) residues 20-193 of IpLITR 2.6b (NCBI accession number DQ860171.1) corresponding to its extracellular Ig domains D1 and D2 were fused to aa residues 22-87 (i.e. the TM and CYT) of IpFcRγ-L (AF543420.1) by overlap extension (OE) polymerase chain reaction (PCR). To obtain the extracellular region of IpLITR 2.6b with a 3' overhang at nucleotide position 576 corresponding to the 5' region of IpFcRγ-L at position 96, a PCR reaction was performed using the primers described in Table 3.1. The template used was a pDISPLAY vector containing the full-length IpLITR 2.6b sequence that we previously generated [4]. To obtain the TM and CYT region of IpFcRγ-L with a 5' overhang at position 96 corresponding to the 3' region of the extracellular domain of IpLITR2.6b at position 576, a PCR reaction was performed using the primers described in Table 3.1. The template used was a pCMV-14 vector containing the full-length IpFcRγ-L sequence [4]. Reactions were performed using Phusion High-Fidelity DNA polymerase (Finnzymes) in 20 μL reactions and the cycling parameters were as follows; 40s at 98°C, 35 cycles of 98°C for 15s, 60°C for 15s, 72°C for 15s, with a final extension step for 5min at 72°C. Amplified products were visualized, excised and gel-purified using the QIAquick Gel Extraction kit (Qiagen) and 100 ng of each product (i.e. IpLITR 2.6b D1D2 and IpFcRγ-L TM CYT) were mixed together and PCR-amplified with the primers listed in Table 3.1 to generate the final IpLITR2.6/IpFcRγ-L fusion product, which was then cloned into pDISPLAY (Invitrogen), generating an N-terminal HA epitope tagged IpLITR2.6b/IpFcRγ-L chimera. The cycling parameters for this final PCR were as follows: 120s at 98°C, 35 cycles of 98°C for 60s, 55°C for 60 s, 72 °C for 90 s, with a final extension step for 7 min at 72°C.

3.5 Generation of epitope tagged inhibitory IpLITRs

Ten nanograms of the pCR4-TOPO vector containing the sequence for TS32.15 L1.1b (DQ858228.1; termed IpLITR1.1b in this thesis) or TS32.17 L1.2a (DQ858242.1; termed IpLITR1.2a in this thesis) [1] were amplified with pDISPLAY L1.1b/SmaI Fwd and pDISPLAY L1.1b/SalI Rvs primers (Table 3.1) using 0.4 U of Phusion High-Fidelity DNA polymerase (Fermentas) in 20 µL reactions according to manufacturer's recommended instructions. Cycling parameters were as follows: 30 s at 98°C, 30 cycles of 98°C for 10 s, 60°C for 20s, 72°C for 30s, and a final extension step for 5 min at 72°C. Reactions were then separated on a 1.0% TAE-agarose gel, and visualized by staining with ethidium bromide solution (50 mg/L), and the PCR products (1500bp) were excised, gel purified (Qiagen Gel Extraction Kit) and cloned into pJET1.2/blunt using the blunt-end protocol (Fermentas). Cloning reactions were then transformed into NEB 10-beta *E. coli* (New England BioLabs) and plated on Luria-Bertani (LB) agar plates supplemented with 100 µg/mL ampicillin.

Positive clones were identified by performing colony PCR with the pJET1.2 Fwd and Rvs sequencing primers (Table 3.1). Cycling parameters were as follows: 10 mins at 94°C, followed by 30 cycles of 94°C for 30 s, 55°C for 30s, 72°C for 3:30 min, and a final extension step for 5 min at 72°C. PCR products were separated on a 1.0% TAE-agarose gel and visualized as above. Six randomly selected colonies were grown overnight in 8 mL of LB supplemented with ampicillin (100 µg/mL) and the plasmids isolated using the QIAprep® Spin Miniprep Kit (Qiagen) according to manufacturer's instructions. Five hundred ng of the purified plasmid was double digested for 10 minutes at 37°C with 10 U of SmaI and SalI Fast Digest restriction enzymes (Fermentas). The inserts were isolated on an agarose gel, gel-purified (as above) then ligated into the HA epitope-containing pDISPLAY vector (Invitrogen) using T4 DNA ligase (Fermentas) and a 2.5 h incubation at 25°C followed by an overnight incubation alternating between 4°C and 16°C every 45 min. Positive pDISPLAY-IpLITR 1.1b and pDISPLAY-

IpLITR 1.2a clones were identified by SmaI/SalI restriction digestion followed by agarose gel separation and visualization (as above) and purified plasmids were sequenced to verify the cDNA sequence and to ensure that the construct was in-frame without any base pair changes using primers listed in Table 3.1. All sequencing was performed at the Molecular Biology Services Unit in the Department of Biological Sciences, University of Alberta, on an ABI 3730 DNA Sequencer.

3.6 Site-directed mutagenesis

The aspartic acid (D) residue within the TM region of the IpLITR2.6b/IpFcRγ-L chimeric construct at position 183, which corresponds to D30 of IpFcRγ-L was mutated to an alanine (A) using D→A mutagenesis primers (Table 3.1), the pDISPLAY-IpLITR2.6b/IpFcRγ-L plasmid as a template and the QuickChange Lightning Site-Directed Mutagenesis Kit (Stratagene) according to the manufacturer's instructions. Tyrosines 218 and 229 encoded within the ITAM motif of the CYT of IpLITR2.6b/IpFcRγ-L (termed 'YY') were also mutated after two rounds of mutagenesis reactions, using "Y^{218} to F^{218}" and "Y^{229} to F^{229}" mutagenesis primers (Table 3.1). This generated a protein with a non-functional ITAM, termed IpLITR2.6b/IpFcRγ-L 'FF'.

A truncated version of IpLITR1.1b, termed IpLITR 1.1b Δ CYT was also created by site-directed mutagenesis, which introduced a C→T mutation at nucleotide position 1195, rendering a premature stop codon at aa position 398, eliminating all of the cytoplasmic tyrosine residues within this receptor, leaving a CYT segment 11 aa long. ΔCYT mutagenesis primers are also listed in Table 3.1.

3.7 Transient transfection of HEK 293T cells

Twenty-four hrs prior to transfection, 4.0 x 10^5 cells were seeded in a 6-well plate containing 2 mL DMEM/FBS and incubated at 37°C. Four μg purified

pDISPLAY-IpLITR2.6b/IpFcRγ-L was diluted in 400 µL serum-free DMEM, then 6 µL Turbofect *in vitro* transfection reagent (Fermentas) was added. Samples were mixed and incubated 20 mins at room temperature. The plasmid-DMEM-Turbofect mixture was evenly added drop-wise onto cells and cells were incubated 48 hrs at 37°C to allow for protein production. Expression of IpLITR 2.6b/IpFcRγ-L was verified by Western blotting (see 3.8).

3.8 Expression of IpLITR2.6b/IpFcRγ-L in HEK 293T cells by Western blot

Forty-eight hrs post-transfection, HEK 293T cells were washed gently with 2 mL D-PBS and lysed 200 µL ice-cold lysis buffer (50 mM Tris–HCl, 150 mM NaCl, 1% Triton X- 100, supplemented with cOmplete mini EDTA-free protease inhibitor; Roche) for 30 min on ice. Following the removal of cellular debris by centrifugation at 16,000x g, 10 mins, lysates were diluted in 200 µL 2x reducing buffer (500 µL beta-mercaptoethanol in 9.5 mL Laemmli buffer; Bio-Rad) and boiled at 95°C for 10 mins. Lysates were frozen at -20°C prior to analysis.

Twenty-five µL of lysates (equivalent to ~0.5 x 10^6 lysed cells) were electrophoresed on 8% sodium dodecyl sulfate polyacrylamide gel electrophoresis (SDS-PAGE) gels, and then transferred to 0.2 µm nitrocellulose membranes (Bio-Rad), then stained with Ponceau S (Sigma-Aldrich) to confirm successful transfer and equivalent loading of samples. Blots were blocked in tris-buffered saline (TBS) supplemented with 0.1% Tween-20 (TBS-T) and 5% skim milk for 30 mins at room temp, rocking gently. Membranes were then incubated overnight (~16 hr) at 4°C with TBS-T plus skim milk containing anti-HA: HRP (1:1000 v/v). Membranes were then washed 3x in TBS-T followed by 3 washes in TBS, 20 mins per wash at room temperature. Immunoreactive protein bands were detected using the Pierce® Enhanced Chemiluminescent Western Blot Substrate Kit (Thermo Scientific).

3.9 Stable transfection and cell sorting of RBL-2H3 cells

To generate RBL-2H3 stably expressing the N-terminal HA epitope-tagged IpLITR2.6b/IpFcRγ-L chimeras, 1.1b, 1.1b ΔCYT or 1.2a, we performed transfections, selection, and cell sorting as follows:

The RBL-2H3 cells were grown to confluence in a 6-well tissue culture plate and harvested (as described in 3.2). The cell suspension in harvest buffer was diluted in 2 mL MEM/EBSS/FBS and cells were counted on a hemocytometer, using Trypan Blue staining. Twenty-four hrs prior to transfection, 1.25 x 10^5 cells were seeded into a 24-well plate (Costar) and incubated overnight (~16 hrs). The next day, media was aspirated and replaced with 250 µL Opti-MEM (HyClone). One µg of pDISPLAY plasmids (IpLITR2.6b/IpFcRγ-L 'YY', IpLITR2.6b/IpFcRγ-L 'FF', IpLITR 1.1b, IpLITR1.1b ΔCYT, IpLITR 1.2a) were prepared for transfection using the Xfect™ transfection reagent (Clontech) according to the manufacturer's instructions. RBL-2H3 cells were incubated in the presence of plasmid and transfection reagent for 4 h at 37 °C prior to the addition of 750 µL of MEM/EBSS/FBS and a further overnight incubation at 37 °C. Media containing the transfection solution was aspirated and cells were incubated with 1mL of MEM/EBSS/FBS supplemented with 800 µg/mL of the selection reagent G418 disulfate salt solution (Sigma–Aldrich) for an additional 4 days. Cellular debris and dead/dying cells (i.e. detached cells) were removed by gentle aspiration of the media and the remaining viable (i.e. attached) cells were supplemented with 1 mL of fresh G418 selection media. After 8–12 days of selection (with G418 media replacement every 4 days), transfected RBL-2H3 cells reached confluence and were prepared for cell surface expression analysis (see 3.10), cell sorting (see 3.11) and Western blotting (see 3.12)

3.10 Surface expression of IpLITRs in RBL-2H3 cells by flow cytometry

Transfected RBL-2H3 cells were then examined for HA-tagged IpLITR surface expression by flow cytometry. Cells were washed, harvested in 500 µL harvest buffer and passed into new 6-well plates and cultured (see 3.2). Forty µL of each cell suspension in harvest buffer was placed into two 1.5 mL Eppendorf tubes per cell type and washed in ice-cold antibody staining buffer (ASB) containing 1% NaN_3, 0.05% EDTA, 1% bovine serum albumin (BSA) in D-PBS. Cells were centrifuged at 400x g for 6 mins at 4°C and supernatant aspirated. After disruption of cell pellets, cells were stained in 20 µg/mL of anti-HA mAb or IgG3 isotype in ASB. Tubes were agitated and incubated on ice for 24 mins. One mL of ASB was then added to each tube to wash off un-bound antibody; tubes were then inverted 4-6 times and centrifuged as above. After aspiration of the supernatant and disruption of the pellet, cells were incubated in 10 µg/mL of PE-conjugated goat anti-mouse IgG (H+L) pAb in ASB. Cells were incubated on ice as before, in the dark, followed by washing, centrifugation and aspiration as before. Cells were re-suspended in 250 µL ASB, loaded onto a 96-well flat bottom plate (Costar), then analyzed for surface staining on the fluorescence (FL)-2 gate using a Cell Lab Quanta SC flow cytometer (Beckman Coulter). Surface IpLITR expression was repeated weekly.

3.11 Cell sorting

Following verification of HA-IpLITR surface expression by flow cytometry, the RBL-2H3 cultures were harvested and then re-suspended (2×10^6 cells/mL) in cell sorting buffer (0.05% EDTA, 1% BSA in D-PBS), and stained in 20 µg/mL anti-HA mAb or IgG3 isotype in sorting buffer. Cells were incubated, washed and centrifuged as described above, followed by incubation with 10 µg/mL PE-conjugated goat anti-mouse IgG (H+L) pAb in sorting buffer, then washing and centrifugation. Cells were re-suspended in 1 mL sorting buffer and transferred to FBS-coated 5 mL BD Falcon tubes (BD Biosciences). The HA-positive

population was then sorted from the HA-negative cells using a FACSAria flow cytometer (Becton Dickinson) at the Faculty of Medicine and Dentistry Flow Cytometer Facility (University of Alberta). Sorted cells were cultured further in 400 μg/mL G418 selection media and tested weekly for IpLITR surface expression by flow cytometry (see 3.10).

3.12 Examination of intracellular signaling by Western blot

Untransfected RBL-2H3 cells or RBL-2H3 cells stably expressing IpLITR 2.6b/IpFcRγ-L YY, FF, or IpLITR1.1b were gently washed with 3 mL D-PBS and were activated by one of the following schemes. Endogenous FcεRI was sensitized by incubating cells for 1 hr with 1 mL of anti-dinitrophenyl (DNP) IgE mAb (200 ng/mL in media) at 37°C, followed by aspiration of media, gently washing with 3 mL D-PBS, then addition of 1 mL of pre-warmed antigen, 0.1 ng/mL DNP (23)-human serum albumin (HSA; Biosearch Technologies, Inc) at 37°C for 2 or 8 mins. Alternatively, cells were incubated with 1 mL of ice-cold 0.625 μg/mL of anti-HA mAb or IgG3 isotype for 20 mins at 4°C, gently washed then incubated with 1 mL of pre-warmed 1.25 μg/mL of the crosslinking goat anti-mouse IgG3 pAb for 2, 4, 8, 16, or 32 mins at 37°C. As positive controls for stimulation, cells were treated with 500 μL D-PBS containing 10 mM H_2O_2 and 0.1 mM sodium pervanadate (Na_3VO_4) for 10 mins at 37°C. Note: the optimal concentrations of primary antibodies (0.625 μg/mL IgG3 and anti-HA), crosslinking goat anti-mouse IgG3 (1.25 μg/mL), anti-DNP IgE sensitization (200 ng/mL) and DNP–HSA triggering (0.1 ng/mL) used in this thesis were all empirically determined in preliminary experiments. A schematic of these stimulation strategies is depicted in Fig. 3.1.

Following activation, cells were gently washed with 3 mL D-PBS, aspirated, and then lysed in 300 μL ice-cold lysis buffer (see 3.8; supplemented with PhosSTOP inhibitor cocktail tablets; Roche) for 30 mins on ice. Following the removal of cellular debris by centrifugation at 16,000x g, 10 mins, lysates were diluted in 300

µL 2x reducing buffer and boiled at 95°C for 10 mins. Lysates were frozen at -20°C prior to analysis by Western blot (See Section 3.8). Following electrophoresis and protein transfer, membranes were blocked in TBS-T and 5% skim milk or 5% BSA for 30 mins at room temp, rocking gently. Membranes were then incubated overnight (~16 hr) at 4°C with any of the following antibodies in TBS-T plus skim milk or BSA according to the manufacturer's instructions: anti-HA: HRP (1:1000 v/v); anti-ERK1/2 (1:2000 v/v), anti-phospho ERK1/2 (1:2000 v/v), anti-Akt (1:1000 v/v); anti-phospho Akt (1:1000 v/v). Membranes were then washed in TBS-T and TBS (as described in Section 3.8). For primary antibodies requiring an HRP-conjugated secondary antibody, blots were further incubated for 2 hrs in TBS-T plus 5% skim milk containing HRP-conjugated goat anti-rabbit IgG (H+L) or anti-mouse IgG (H+L) for 2 hrs at room temperature, followed by TBS-T and TBS washes as above. Immunoreactive protein bands were detected and analysis of band intensity was performed using ImajeJ v1.44, which was downloaded from http://rsbweb.nih.gov/ij/download.html.

3.13 Degranulation assays

The degranulation response of RBL-2H3 as a marker of effector responses induced by IpLITR engagement was assessed using an Annexin-V binding assay [126,127] and the beta-hexosaminidase release assay [128], using RBL-2H3 cells stably expressing IpLITR 2.6b/IpFcRγ-L YY or FF.

For the Annexin-V binding assay, RBL-2H3 cells were harvested and counted as above (see 3.2 and 3.7) and 1.5 x 10^5 cells were added to 1.5 mL Eppendorf tubes and incubated in 300 µL MEM/EBSS/FBS alone or sensitized with media supplemented with 200 ng/mL anti-DNP IgE for 1 hr at 37°C. Control cells or cells that were activated by other means (described below) were not sensitized with IgE. Cells were then centrifuged (400x g, 6 mins, 4°C); media was aspirated and the pellets were disrupted. IgE-sensitized cells were then resuspended in 300

uL ice-cold Tyrode's buffer (25 mM HEPES, 140 mM NaCl, 1.8 mM $CaCl_2$, 5.6 mM D-glucose, 12 mM $NaHCO_3$, 0.37 mM NaH_2PO_4, 0.49 mM $MgCl_2$, 0.1% BSA, pH 7.4), whereas other cell samples were resuspended in Tyrode's buffer containing 0.625 µg/mL anti-HA mAb or IgG3 isotype for 20 mins at 4°C, followed by centrifugation and aspiration of supernatant. Cell pellets were disrupted and cells were resuspended in 50 µL of pre-warmed staining solution, containing 2.5 µL fluorescein isothiocyanate (FITC)-annexin V (BD Pharmingen), 10 µM cytochalasin B (Sigma-Aldrich) and 47.5 µL 1x Annexin V binding buffer (0.01 M HEPES, 0.14 M NaCl, and 2.5 mM $CaCl_2$, pH 7.4; BD Pharmingen) alone (control, non-sensitized cells) for 15 mins at 37°C. For other treatments, staining solution was supplemented with the following: 0.1 ng/mL DNP-HSA for cells sensitized with anti-DNP IgE; or 1.25 µg/mL goat anti-mouse IgG3 for cells treated with anti-HA mAb or IgG3 isotype. Additional, non-sensitized cells were incubated with staining solution supplemented with 0.625 µM calcium ionomycin from *Streptomyces conglobatus* (Sigma-Aldrich), as a positive control for stimulation. After 15 min incubation at 37°C with either of the above treatments, 1 mL ice-cold 1x Annexin V binding buffer was added to each tube, followed by centrifugation, aspiration and pellet disruption. Cells were then fixed by adding 300 µL ice-cold 1% paraformaldehyde (PFA; Sigma-Aldrich) in D-PBS for 10 mins at 4°C. Annexin V-FITC binding (as a measure of RBL-2H3 degranulation) was then analyzed by flow cytometry using the FL-1 gate. Alternatively, to directly visualize Annexin V-FITC binding, cell stimulations were performed as indicated, but after fixation, cells were pelleted and re-suspended in 10 µL Vectashield Hard Set™ mounting medium with 1.5 µg/mL DAPI (Vector Laboratories, Inc), mounted on glass slides, then visualized under a Zeiss Axiovert 2500M fluorescence microscope (Cross Cancer Institute Microscopy Facility, University of Alberta). NB: optimal concentration of ionomycin (0.625 µM) was determined empirically during preliminary experiments.

For the beta-hexosaminidase release assay, 5 x 10^4 cells were seeded in triplicate in a 96-well, flat bottom plate in 100 µL MEM/EBSS/FBS for 1 hr at 37°C to

allow cells to adhere. Some cells were sensitized with 200 ng/mL anti-DNP IgE for 1 hr at 37°C. Media from all wells was decanted from the plate and cells were washed in 300 µL ice-cold Tyrode's buffer or ice-cold Tyrode's buffer containing 0.625 µg/mL anti-HA mAb or IgG3 isotype for 20 mins at 4°C. Solutions were then decanted; cells washed with 300 µL Tyrode's buffer. Control (non-sensitized) cells were incubated with 100 µL pre-warmed Tyrode's buffer. Remaining cells were treated with 100 µL Tyrode's supplemented as follows: IgE-sensitized cells treated with 0.1 ng/mL DNP-HSA; anti-HA- or IgG3-treated cells 1.25 µg/mL goat anti-mouse IgG3; additional, non-sensitized cells with 0.625 µM ionomycin. After 1 hr incubation at 37°C, 25 µL cellular supernatants (containing secreted beta-hexosaminidase) were transferred in the same well-locations in a new, black 96-well flat bottom plates. One hundred uL beta-hexosaminidase substrate (2mM 4-methylumbelliferyl N-acetyl-β-D-glucosaminide [Sigma-Aldrich] in 0.1 M citrate, pH 4.5) was added. The reaction (cleavage of substrate into N-acetyl-glucosamine and fluorescent methylumbelliferrone) proceeded for 30 mins at 37°C followed by addition of 150 µL quenching buffer (0.2 M L-glycine, pH 10.7) to stop the reaction. Fluorescent reaction products (i.e. measure of RBL-2H3 degranulation) was measured on a Perkin-Elmer microplate reader using 360 nm excitation and 450 nm emission filters (Goss lab, Dept of Biological Sciences, University of Alberta) [128]. For some experiments, cells were pre-treated with pharmacological inhibitors or dimethylsulfoxide (DMSO, vector control) for 30 mins at 37°C, prior to and during beta-hexosaminidase release assays. Inhibitors, target molecules and concentrations used are listed on Table 4.1; all were purchased from EMD Biosciences. Relative fluorescence units (RFU) represent the relative release of beta-hexosaminidase and were normalized by setting IgE-DNP-stimulated cells to 100%. The relative release for all samples was then calculated using the following equation: [RFU of experimental treatment/RFU of IgE-DNP stimulated cells) x 100].

3.14 Phagocytosis assay

The protocol for the internalization of opsonized microspheres by RBL-2H3 was adapted from [129]. 250 µL of well-suspended Fluoresbrite™ Carboxy YG 4.5 µm microspheres (Polysciences) were washed 3x with 1 mL 0.1 M boric acid, pH 8.5, centrifuging at max spend, 3 mins, and carefully aspirating supernatants. After final wash, re-suspend in 500 µL boric acid and incubated with 200 µg of protein A (from *Staphylococcus aureus*; Sigma-Aldrich) overnight at room temperature, in the dark on a rotating mixer. The following day, these protein A-coated beads were centrifuged 10 mins, max speed and supernatants aspirated. Pelletted beads were washed 3x in 1 mL of 0.1M boric acid supplemented with 10 mg/mL BSA, and incubated 30 mins, room temperature, rotating, and centrifuged for 5 mins and max speed. After final wash, beads were re-suspended in 500 µL D-PBS supplemented with 10 mg/mL BSA (1×10^8 beads/mL). Ten µg of anti-HA mAb or IgG3 isotype (for 10 µg/mL) was added to beads and incubated for 2 hrs, 4°C, rotating. Opsonized beads were then washed 3x with 1 mL PBS/BSA, followed by centrifuging and aspirating. Finally, opsonized beads were re-suspended in 500 µL PBS/BSA to ensure consistent concentration of 1×10^8 beads/mL. Opsonized are stored at 4°C in the dark for a maximum of two weeks.

RBL-2H3 cells expressing IpLITR2.6b/IpFcRγ-L 'YY' or 'FF', IpLITR 1.1b, IpLITR 1.1b ΔCYT or IpLITR 1.2a are harvested and enumerated; 1×10^5 cells in 100 µL serum-free MEM/EBSS per 1.5 mL Eppendorf tube were incubated with 3 µL antibody-opsonized 4.5 µm beads for 30 mins, at 4°C or 37°C. The 4°C incubation was used to determine if phagocytosis is an active process rather than non-specific internalization. Cells were then pelleted at 5000x g for 1 min at 4°C and supernatants carefully aspirated. To remove non-internalized but attached beads, cells were resuspended in 100 µL of 0.05% trypsin (Hyclone)/1 mM EDTA in D-PBS for 15 mins on ice. Two hundred fifty µL ice-cold 2 mM EDTA/0.5% BSA in D-PBS was immediately added and cells were centrifuged and supernatants aspirated as above, followed by re-suspending pellets in 300 µL 1%

PFA in D-PBS. Increases in cell fluorescence (a measure of internalized fluorescent microspheres) were analyzed by flow cytometry using the FL-1 gate.

3.15 Examination of IpLITR-induced cytokine production using proteome profilers

To determine the identity and relative levels of secreted cytokines induced by IpLITR engagement, a proteome profiler kit was used, specifically the Rat Cytokine Array Panel A Array Kit (R&D Systems). As in Section 3.10, untransfected RBL-2H3 cells or cells expressing IpLITR 2.6b/IpFcRγ-L or IpLITR 1.1b, confluent in 6-well plates, were washed in D-PBS and sensitized with ASB containing 0.625 μg/mL anti-HA mAb or IgG3 isotype for 20 mins at 4°C or containing 200 ng/mL anti-DNP IgE for 1 hr at 37°C. Following sensitizations, cells were washed in D-PBS and crosslinked with 1.25 μg/mL goat anti-mouse IgG3 pAb (for anti-HA- or IgG3-treated cells) or 0.1 ng/mL DNP-HSA) for 24 hrs at 37°C. Additional, non-sensitized wells were stimulated with 50 ng/mL phorbol 12-myristate 13-acetate (PMA; Sigma-Aldrich) and 0.5 μM calcium ionophore A23187 (Sigma-Aldrich) for 24 hrs at 37°C, as a positive control for stimulation. The following day, culture media containing secreted cytokines were collected in 15-mL conical tubes (Costar) and centrifuged 10 mins, 16,000x g, 4°C to remove cellular debris.

Cleared media was assessed for relative cytokines using the manufacturer's instructions, as follows. Membranes with capture-antibodies against cytokines spotted in duplicate at specific locations on the membrane were blocked for 1 hr. One mL of cleared media (containing cytokines) was mixed with 500 μL Array Buffer 4 and15 μL Detection Antibody Cocktail (containing biotinylated antibodies against cytokines) for 1 hr, room temperature. Blocking buffer was aspirated and membranes incubated with Sample/Antibody Cocktail mixture overnight (~16 hr), at 4°C, rocking. The following day, membranes were washed with 1X Wash Buffer 3x for 10 mins, rocking, then incubated with Streptavidin-

HRP (in Array Buffer 6) for 30 mins, rocking at room temperature then washed as before. Immunoreactive duplicate spots, indicative of secreted cytokines, were detected as in Section 3.8. Analysis of duplicate spot intensity was performed using ImajeJ v1.44, which was downloaded from http://rsbweb.nih.gov/ij/download.html.

3.16 Examination of IpLITR-induced phospho-MAPK activation using proteome profilers

Akin to Section 3.15, to determine identity and extent of phosphorylation of signaling molecules induced by IpLITR engagement, the proteome profiler Phospho-Kinase Array Kit (R&D System) was used. Untransfected RBL-2H3 cells or cells expressing IpLITR 2.6b/IpFcRγ-L or IpLITR 1.1b were sensitized as in Section 3.15. However, crosslinking by goat anti-mouse IgG3 pAb occurred for only 10 mins at 37°C. This time was chosen as phosphorylation of ERK1/2 peaked between 8 and 16 mins post-crosslinking [130]. After crosslinking, ASB was removed and cells were washed with ice-cold D-PBS. After aspiration, cells were lysed in 400 µL ice-cold Array Lysis Buffer 6 for 30 mins on ice. Lysates were cleared of cellular debris (as in Section 3.8) and samples were processed per the manufacturer's instructions, as follows.

Membranes with capture-antibodies against phosphorylated kinases spotted in duplicate at specific locations on the membrane were blocked for 1 hr. After aspirating blocking buffer, 334 µL of lysates was mixed with 1666 µL Array Buffer 1 was added to membranes and overnight (~16 hr), at 4°C, rocking. The following day, membranes were washed with 1X Wash Buffer 3x for 10 mins, rocking. Membranes were incubated with 1x Array Buffer 2/3 containing Detection Antibody Cocktail (containing biotinylated antibodies against phosphorylated kinases) for 2 hrs, room temperature, rocking. Following removal of Antibody Cocktail, membranes were washed as above and incubated with diluted Streptavidin-HRP (in 1x Array Buffer 2/3) for 30 mins, rocking at room

temperature then washed as before. Immunoreactive duplicate spots, indicative of phosphorylated kinases, were detected as in Section 3.8. Analysis of duplicate spot intensity was performed using ImajeJ v1.44, which was downloaded from http://rsbweb.nih.gov/ij/download.html.

3.17 Co-immunoprecipitations

As in Section 3.10, one confluent well in a 6-well plate (~2.5 x 10^6 cells) of untransfected RBL-2H3 cells or cells expressing IpLITR 1.1b were gently washed in 3 mL D-PBS and then stimulated with 500 µL of 10 mM H_2O_2 and 0.1 mM Na_3VO_4 in D-PBS or D-PBS alone for 10 mins at 37°C, then lysed 200 µL ice-cold lysis buffer for 30 mins on ice, and debris removed by centrifugation. Fifty µl of the cell lysates were mixed with 50 µl of 2X reducing buffer and the remaining lysate was immunoprecipitated by the addition of either 2 µg anti-HA mAb or anti-FcεRI α subunit mouse mAb overnight (~16 hrs, 4°C on a rotary mixer). Thirty µL of pre-washed (with lysis buffer) protein G Agarose beads (Roche) were then added to the samples and incubated for a further 2 hrs at 4°C on a rotary mixer. Beads were washed three times with 1 mL of ice-cold lysis buffer followed by the addition of 100 µL of 2X reducing buffer and boiling. As in section 3.8, 25 µL (equivalent to ~0.5 x 10^6 lysed cells) were electrophoresed on 8% or 10% SDS-PAGE gels. Bands were detected using an anti-HA:HRP pAb, the anti-FcεRI γ subunit rabbit pAb, or an anti-FcεRI α subunit rabbit pAb. Primary and secondary body antibody dilutions, incubation times, and washes were performed as in Section 3.8.

3.18 Statistics

A Student's T-test (two tails) was performed when assessing potential differences between experimental groups. P-values <0.05 were designated as statistically significant.

Primer Name	Primer sequence 5'-3'
pDISPLAY IpLITR SmaI Fwd[a,c]	CCCGGGGTTCTGTCTGTGGAGCCG
O.E. IpLITR-IpFcRγ-L Rvs[a]	ATAACACAATCCACCCTCAGCTCTTCCATCTGACACA
O.E. IpLITR-IpFcRγ-L Fwd[b]	TCAGATGGAAGAGCTGAGGGTGGATTGTGTTAT
O.E. IpLITR-IpFcRγ-L SalI Rvs[b,c]	GTCGACTTATGCCAAAGGTTCCTTCTTCACATGGAG
IpFcRγ-L D^{30} to A^{30} Fwd[d]	GTGGATTGTGTTATATCCTTGCTGGGGTTTTGATTCTCTATGG
IpFcRγ-L D^{30} to A^{30} Rvs[d]	CCATAGAGAATCAAAACCCGACCAAGGATATAACACACTACAC
IpLITR2.6b/IpFcRγ-L Y^{218} to F^{218} Fwd[d]	TGAAGAGAATCCAGATGGCATCTTCCAGGGTTTGAA
IpLITR2.6b/IpFcRγ-L Y^{218} to F^{218} Rvs[d]	TTCAAACCCTGGAAGATGCCATCTGGATTCTCTTCA
IpLITR2.6b/IpFcRγ-L Y^{229} to F^{229} Fwd[d]	CATAAGAATCAGGACACCTTTGAGACACTCCATGTGA
IpLITR2.6b/IpFcRγ-L Y^{229} to F^{229} Rvs[d]	TCACATGGAGTGTCTCAAAGGTGTCCTGATTCTTATG
pJET1.2 Fwd sequencing[e]	CGACTCACTATAGGGAGAGCGGC
pJET1.2 Rvs sequencing[e]	AAGAACATCGATTTTCCATGGCAG
pDISPLAY IpLITR1.1b SmaI Fwd[f,g]	CCCGGGGTTCTGTCTGTGGAGCCG
pDISPLAY IpLITR1.1b SalI Rvs[f]	GTCGACCTATGTGTTCTGCTTCAGCTG
pDISPLAY IpLITR1.1b ΔCYT Fwd[d]	CAACAAAGGAAAGGACAGAGACATATAGCAGAACAGCAA
pDISPLAY IpLITR1.1b ΔCYT Rvs[d]	TTGCTGTTCTGCTATATGTCTCTGTCCTTTCCTTTGTTG
IpLITR1.2a 318/IpLITR1.1b 303 Fwd[g]	GCAGCCTGATGGACAGATATT
IpLITR1.2a 699/IpLITR1.1b 687 Fwd[g]	CACCGACACACTCCATGATAC
IpLITR1.2a 1058/IpLITR1.1b 1046 Fwd[g]	ATGCTGTTACGCTGACTGTATC

Table 3.1. Primers used in this thesis. [a]Primers used for the amplification of the ectodomain of IpLITR 2.6b containing an overhang on the 3' end corresponding to the 5' end of IpFcRγ-L. [b]Primers used for the amplification of the TM and ITAM containing CYT of IpFcRγ-L containing an overhang on the 5' end corresponding to the 3' end of IpLITR 2.6b. [c]Primers used to fuse the overlap extension (O.E.) products generated from reactions[a,b]. [d]Mutagenesis primers. [e]Colony PCR primer. [f]Primers used to generate pDISPLAY IpLITR1.1b and pDISPLAY IpLITR1.2a. [g]Primers used to sequence constructs. Number refers to nucleotide position. All primers were obtained from Integrated DNA Technologies (IDT).

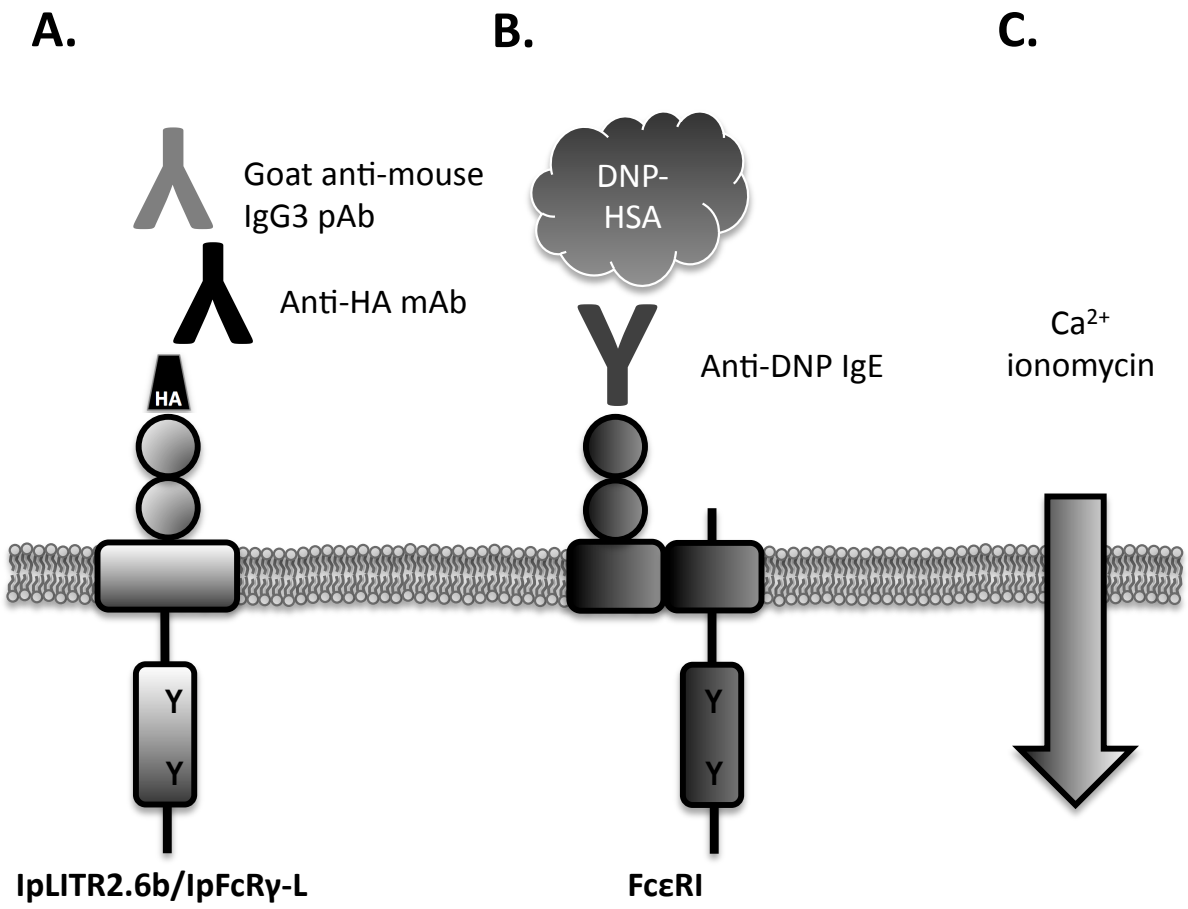

Figure 3.1. Simplified schematic of RBL-2H3 activation strategies used throughout this thesis. (A) N-terminal HA-epitope tagged IpLITR (shown here is IpLITR2/6b/IpFcRγ-L) is sensitized with anti-HA mAb followed by crosslinking with goat anti-mouse IgG3 pAb for varying lengths of time. (B) Endogenous FcεRI (only α subunit and a single γ subunit are depicted here) is sensitized with anti-DNP IgE, followed by triggering with DNP-HSA antigen, for varying lengths of time. (C) RBL-2H3 cells are incubated with calcium ionomycin salt for varying lengths of time.

CHAPTER 4

Examination of the signaling and functional potential of a stimulatory channel catfish leukocyte immune-type receptor and its associated adaptor molecule[2]

4.1 Introduction

Innate immune cell effector responses (e.g. degranulation, phagocytosis, and cytokine secretion) are initiated and regulated by surface-expressed receptors, including but not limited to members of the IgSF. Some examples of these receptor-types in mammals include Fc receptors (FcRs) [29,30,33,131], triggering receptors expressed on myeloid cells (TREMs) [132,133], leukocyte-associated Ig-like receptors (LAIR) [134] and carcinoembryonic antigen-related cell adhesion molecules (CEACAMs) [135]. Innate immune cell-types utilize these surface-expressed receptors to recognize host- or pathogen-derived molecules such as FcRs binding monomeric or aggregated Igs [29]; binding of extracellular matrix (ECM) collagens by LAIR-1 [136]; or binding of Opa protein expressed on *Neisseria gonnorhoeae* by CEACAM-3 [137]. These receptor-ligand interactions then initiate intracellular signaling cascades, inducing or inhibiting effector responses. As many of these receptors can be classified as stimulatory or inhibitory, the paired expression of stimulatory and inhibitory immunoregulatory receptor-types can coordinate the activation or suppression of immune responses [21,33].

Immunoregulatory receptor families have also been recently discovered in teleost, such as IpLITRs [1]. Structurally, this receptor family is related to mammalian immunoregulatory receptors and includes putative stimulatory and inhibitory types. Prototypical stimulatory IpLITRs contain a charged TM and a short CYT.

---

[2] A version of this chapter has been published. Cortes, *et al.* 2012. Dev Comp Immunol. 36: 62-73.

Previous studies of the putative stimulatory receptor IpLITR2.6b co-expressed with the channel catfish adaptor molecules IpFcRγ, IpFcRγ-L, IpCD3ζ-L or IpDAP12 in HEK 293T cells revealed that this receptor achieved highest surface expression when co-expressed with IpFcRγ-L or IpFcRγ [4]. Mutation of the lysine in the receptor TM to similarly charged arginine or neutral alanine did not greatly diminish surface expression of IpFcRγ-L, indicating that the charged residue of a stimulatory IpLITR-type may assist in receptor recruitment but is not required for it. However, neutralizing the negatively charged aspartic acid in the IpFcRγ-L TM greatly reduced its interaction with wild-type IpLITR2.6b, observed by surface staining and co-immunoprecipitation, suggesting a key role for this residue in receptor-adaptor interactions.

The observation that IpLITR2.6b pairs with the ITAM-bearing adaptor IpFcRγ-L for surface expression suggests that this association is a prerequisite for IpLITR2.6b-mediated signaling events. To this end, I hypothesized that engagement of this receptor-adaptor construct expressed in a mammalian immune cell line will successfully recruit stimulatory signaling molecules leading to the induction of effector functions (i.e. degranulation and phagocytosis) in an ITAM-dependent manner.

To address these hypotheses, I generated a chimeric construct containing the two extracellular Ig domains of IpLITR2.6b fused with the TM and CYT of IpFcRγ-L, with a aspartic acid (D) → alanine (A) mutation in the TM to prevent any potential associations with other endogenous surface receptors. I also generated a construct with the ITAM tyrosines mutated to phenylalanines to 'knock out' the ITAMs. I then transfected and stably expressed these receptor-adaptor chimeric constructs in the rat basophil leukemia (RBL)-2H3 cell line. In order to examine their activation of signaling molecules, I engaged these receptor constructs with epitope-specific mAb. Further, I also examined the induction of prototypical innate immune effector responses degranulation and phagocytosis, using soluble mAb or opsonized microspheres, respectively. I report that IpLITR2.6b/IpFcRγ-L

is capable of engaging ERK1/2 phosphorylation and inducing the effector responses degranulation and phagocytosis. Through the use of pharmacological inhibitors against signaling molecules, I observed the likely engagement of Src family kinases, PI3-K, MEK and Protein Kinase C during degranulation. Overall, these responses are dependent upon intact ITAMs with the CYT of IpLITR2.6b/IpFcRγ-L.

4.2 Results

4.2.1 Generation of IpLITR2.6b/IpFcRγ-L chimeric constructs and stable expression in RBL-2H3 cells

The fusion of the extracellular portion of IpLITR2.6b with the TM and CYT of IpFcRγ-L was generatd by overlap extension (OE) PCR (Fig. 4.1). The TM was neutralized with a D→A mutation, preventing potential associations with any endogenous RBL-2H3 expressed surface receptors, such as FcεRI. The chimera with intact tyrosines (Y) in the ITAM is designated IpLITR2.6b/IpFcRγ-L YY. These residues were both mutated to phenylalanines (F) in order to 'knock out' the ITAM in a construct designated as IpLITR/IpFcRγ-L FF. Both constructs were cloned into the pDISPLAY vector, in order to encode an N-terminal HA epitope tag (Fig. 4.2). Primers used are listed in Table 3.1. Both constructs were then transfected using a cationic polymer Turbofect into HEK 293T cells and the cellular lysates were examined by Western blot using the HRP-conjugated anti-HA pAb (Fig. 4.3), confirming that the chimeric constructs were expressed at the expected size of 25 kDa. RBL-2H3 cells were also transfected with the IpLITR2.6b/IpFcRγ-L YY and FF chimeric constructs and after 8–12 days of G418 selection, transfected RBL-2H3 cells were sorted by anti-HA staining (Fig. 4.4). Shown in Fig. 4.5 is a representative flow cytometric profile of HA-epitope tagged, chimeric construct-expressing RBL-2H3.

4.2.2 Examination of IpLITR2.6b/IpFcRγ-L-induced signaling

To examine if IpLITR2.6b/IpFcRγ-L engagement induced the activation of intracellular signaling, cross-linking of IpLITR2.6b/IpFcRγ-L YY with α-HA mAb resulted in the phosphorylation of ERK1/2 in RBL-2H3 cells, using phospho-specific antibodies (Fig. 4.6A). Comparatively, phosphorylation of ERK1/2 was not observed when the IpLITR2.6b/IpFcRγ-L FF chimera was cross-linked with α-HA (Fig. 4.6B), confirming that activation of intracellular signaling by this construct is ITAM-dependent. Further, this suggests that RBL-2H3 cells do not express an Fc receptor for the anti-HA mAb or cross-linking antibody. As a positive control, both IpLITR2.6b/IpFcRγ-L YY and FF expressing RBL-2H3 cells were stimulated through endogenous FcεRI using IgE-DNP or sodium pervanadate (Fig. 4.6), resulting in increased levels of phospho-ERK1/2. All increases in phospho-ERK1/2 were relative to untreated RBL-2H3 cells (Control; Fig. 4.6) and were normalized to the expression of endogenous ERK1/2 (Fig. 4.7).

4.2.3 Induction of degranulation by IpLITR2.6b/IpFcRγ-L

To examine the effect of IpLITR/IpFcRγ-L engagement on the activation of an degranulation, I used both the flow cytometric Annexin V binding assay [126] and the plate-based β-hexosaminidase release assay [128] as quantitative measures of RBL-2H3 cellular degranulation.

For the flow cytometric Annexin V binding assay, unstimulated RBL-2H3 cells stably expressing IpLITR2.6b/IpFcRγ-L YY or FF chimeras demonstrated 15% and 16.6% Annexin V-FITC staining (i.e. degranulation positive) in comparison to 62% and 55% staining when the cells were stimulated through FcεRI with IgE-DNP, respectively (Fig. 4.8). This increased staining was statistically significant (p <0.05) and was also observed when the transfected cells were stimulated by ionomycin (Fig. 4.8; 80.5% for YY; 55.3% for FF). When the cells were incubated with isotype control mouse IgG3 followed by the cross-linking goat

anti-mouse IgG3 pAb, the IpLITR2.6b/IpFcRγ-L YY- and the IpLITR2.6b/IpFcRy-L FF-expressing RBL-2H3 cells did not demonstrate a significant increase in Annexin V-FITC binding (i.e. 12.4% and 20% staining, respectively; Fig. 4.8). However, if the cells were incubated with α-HA mAb and then cross-linked with goat anti-mouse IgG3 pAb, only the RBL-2H3 cells expressing IpLITR2.6b/IpFcRγ-L YY, not FF, exhibited a significant increase (i.e. 44.1%) in their degranulation response indicating that this response is ITAM-dependent (Fig. 4.8). Pooled % Annexin V-FITC staining results (as a measure of degranulation) of RBL-2H3 cells expressing either IpLITR2.6b/IpFcRγ-L YY or FF after each treatment are also indicated (Fig. 4.9). Increased Annexin V-FITC staining was also visualized by fluorescence microscopy (Fig. 4.10). When the IpLITR2.6b/IpFcRγ-L-expressing cells were stimulated with IgE-DNP or anti-HA mAb, pronounced, punctate Annexin V-FITC staining was detected, which was not observed on cells incubated with the isotype control antibody IgG3.

An initial examination of the signaling mediators that may participate in IpLITR-induced degranulation was performed using the microplate-based degranulation assay, which measures β-hexosaminidase secretion [128]. To ensure this assay could detect IpLITR-mediated degranulation, IpLITR2.6b/IpFcRγ-L YY-expressing cells were stimulated to degranulate by IgE-DNP stimulation, (normalized to 100%), treating with calcium ionomycin (117.9%, compared to IgE-treatment), or cross-linking of the chimeric receptor with anti-HA mAb, 100% , Fig. 4.11A), consistent with the Annexin V-FITC staining assay. By comparison, unstimulated cells showed 12.7% degranulation (compared to IgE-DNP treatment, Fig. 4.11A). IpLITR2.6b/IpFcRγ-L FF-expressing cells also degranulated in response to IgE-DNP treatment (normalized to 100%) and calcium ionomycin (104.5%, compared to IgE-DNP treatment), and when unstimulated, showed 25.9% degranulation (Fig. 4.11B). As predicted, these cells did not release β-hexosaminidase in response to anti-HA mAb cross-linking (31.7%, Fig. 4.11B), relative to the unstimulated cells value.

In order to determine which kinases are likely involved in IpLITR2.6b/IpFcRγ-L-mediated signaling, transfected RBL-2H3 cells were pre-treated with pharmacological blockers against select intracellular signaling molecules. Upon anti-HA mAb cross-linking, the β-hexosaminidase release induced by IpLITR2.6b/IpFcRγ-L YY cross-linking was reduced significantly by pre-treating the cells with PP2 (Src kinase family inhibitor; 69.8% ± 4.3), LY294002 or Wortmannin (59.7% ± 4.5 and 50.3% ± 10.7, respectively; both PI3-K inhibitors), U0126 or PD 98059 (51.9% ± 5.6 and 41.9% ± 8.1 respectively; both MEK inhibitors), and BISII (42.2% ± 10.8; PKC inhibitor), relative to anti-HA mAb cross-linking without inhibitors (Fig. 4.11A). Comparatively, no significant inhibition of IpLITR2.6b/IpFcRy-L-induced β-hexosaminidase release was observed by pre-treatments with SP 600125 (14.1% ± 6.8; JNK inhibitor), SB 203580 (-19.9% ± 6.8; p38 MAPK inhibitor), or DMSO (9.7% ± 1.2; vehicle control). Since IpLITR2.6b/IpFcRγ-L FF expressing RBL-2H3 cells did not degranulate following anti-HA mAb cross-linking, the different pharmacological inhibitors had no effect (Fig. 4.11B). A summary of the inhibitors used, their target signal molecules, and their ability to block IpLITR2.6b/IpFcRγ-L YY-mediated RBL-2H3 degranulation is listed in Table 4.1.

4.2.4 Induction of phagocytosis by IpLITR2.6b/IpFcRγ-L-expressing RBL-2H3 cells

To determine if IpLITR2.6b/IpFcRγ-L engagement can induce phagocytosis, I used a flow cytometric fluorescent microsphere phagocytosis assay [129]. Following incubation with anti-HA mAb- or IgG3 isotype-opsonized 4.5 μm fluorescent microspheres, RBL-2H3 cells were measured for increases in fluorescence, indicative of phagocytosis, by flow cytometry. Cells expressing the YY chimeric construct internalized significantly more anti-HA mAb-coated beads (48.5%) than IgG3-coated beads (17.4%; Fig. 4.12A). This increase in phagocytosis was completely abrogated when the cells were incubated at 4°C (Fig. 4.12B) indicating that this is an active cell process. When RBL-2H3 expressing the FF

chimera were incubated with opsonized beads, no significant difference was observed between anti-HA mAb-coated beads (15.9%) and IgG3-coated beads (12.1%; Fig. 4.12A), confirming that this effector response is also ITAM-dependent. Pooled data from three independent phagocytosis experiments are also shown in a bar graph (Fig. 4.12B).

4.3 Discussion and conclusions

The recent discovery and characterization of several teleost immunoregulatory receptor including NITRs, novel Ig-like transcripts (NILTs), LITRs, immune-related, lectin-like receptors (ILLRs), and soluble immune-type receptors (SITRs) have uncovered a complex array of immune proteins, which likely play significant roles in teleost immunity [1,104–106,114–116,138,139]. Some of these receptors encode structural features akin to various mammalian immunoregulatory receptors (i.e. FcRs, Fc receptor-like proteins (FCRLs), KIRs, TREMs, Nkp44 and LIRs) (Reviewed in [17,140]. Despite these discoveries, a complete understanding of their role in teleost immunoregulation requires further functional examination.

Given the lack of monoclonal antibodies against fish immunoregulatory receptors and lack of transfection reagents/protocols for fish cells, alternative strategies have been useful to conduct preliminary functional studies of teleost immunoregulatory receptors. To that end, the strategy of generating recombinant receptor constructs and their expression in mammalian immune cells has been a valuable research tool to gain insights into receptor function, as observed with NITRs, SITRs and rainbow trout (*Oncorhynchus mykiss*) toll-like receptor (TLR)-5 [105,124,141]. The use of these alternative strategies is not without its drawbacks: heterologous protein over-expression, non-physiological temperatures and unnatural receptor construct design may not provide a complete picture of teleost receptor functions in their ‘native’ environments. However, in the absence of mAbs, known ligands or reliable fish immune cell transfection reagents/protocols,

these surrogate systems have been useful in the preliminary functional characterization of these immune proteins, including members of the IpLITR family.

In early biochemical studies into stimulatory IpLITR-types, co-transfection of epitope-tagged receptors and catfish adaptors in HEK 293T cells showed that the association between IpLITR2.6b with either IpFcRγ or IpFcRγ-L was required for surface receptor expression, assessed by flow cytometry and immunoprecipitation. This suggests that this receptor-adaptor association is likely a requirement for IpLITR2.6b-mediated signaling events in fish, setting the stage for the results reported in this chapter. Expanding on these biochemical studies, I performed functional studies by expressing a chimeric fusion of IpLITR2.6b with IpFcRγ-L in the myeloid cell line RBL-2H3. Using RBL-2H3 cells is advantageous because of its well-characterized FcεRI-mediated innate effector responses such as degranulation, cytokine secretion and phagocytosis, as well as the signaling mechanisms associated with these responses, allowing it to be used as a reporter assay system in high-throughput assays [43,128,142]. Using this system, the results provided in this chapter provide insights into the signaling and functional capacity of IpLITR2.6b and its associated adaptor molecular, IpFcRγ-L.

Crosslinking this receptor/adaptor chimera by epitope-specific soluble antibodies induced the phosphorylation of the downstream signaling molecule, ERK1/2. The chimera with mutated ITAMs was unable to induce phosphorylation. As a positive control, the cells were stimulated through endogenous processes, including IgE-DNP-mediated triggering of their endogenous FcεRI or calcium-dependent activation by ionomycin treatment. Many ITAM-driven signaling events converge onto the phosphorylation of ERK1/2, which is also associated with the induction of effector responses [32]. Thus ERK1/2 was a good candidate for exploring IpLITR2.6b-mediated signaling. The activation of this molecule in a mammalian cell by a teleost receptor speaks to the conserved nature of

intracellular ITAM-mediated signaling pathways among vertebrates, which may lead to the induction of effector responses.

With this in mind, the role of this receptor-adaptor association in the induction of degranulation, a characteristic effector response of RBL-2H3 cells [32,79], was studied. As expected, given the activation of signaling kinases, IpLITR2/6b/IpFcRγ-L induced a potent degranulatory response as measured by a flow cytometry-based Annexin V-FITC staining assay and a microplate-based β-hexosaminidase release assay. This effector response was also observed only with an intact adaptor ITAM. Degranulation induced by IgE-DNP triggering or ionomycin treatment also occurred and provided a basis for comparison. As many innate immune cells, such as mast cells and neutrophils degranulation as part of a host's first line of defense, the observation that IpLITR2.6b induces such a response provides insights into the potential role of IpLITRs in innate defense as they are also expressed on catfish myeloid cells [1].

Pre-treatment of cells with pharmacological inhibitors highlights the signaling molecules likely involved in IpLITR2.6b/IpFcRγ-L-dependent degranulation. Degranulation was most potently inhibited by PP2 treatment (70% inhibition), which blocks the activity of Src family protein tyrosine kinases (PTKs), including Lyn, found in RBL-2H3 cells [143]. Engagement of endogenous FcεRI in RBL-2H3 cells with IgE sensitization and antigen triggering (ex. DNP-HSA) induces activation of Src PTKs and subsequent phosphorylation of ITAM tyrosines encoded in the β and γγ subunits of the FcεRI complex [143–145]. This then recruits the phosphorylation and activation of spleen tyrosine kinase (Syk), which phosphorylates downstream targets leading to the overall activation of the cell and induction of effector responses, including degranulation [144,145]. Given that degranulation by IpLITR2.6b/IpFcRγ-L is sensitive to PP2 inhibitor treatment, Lyn and Syk are likely also key signaling mediators. Inhibition of phosphoinositide-3 kinase (PI3K), another molecule activated by FcεRI aggregation [144] by LY294002 and Wortmannin, also significantly reduced

IpLITR2.6b/IpFcRγ-L-induced degranulation. Mitogen-activated protein kinase kinase (MEK) and protein kinase C (PKC) are also involved in FcεRI-mediated signaling [145,146]. Similarly, treatment with inhibitors to these molecules, U0126 and PD98059 (MEK/ERK1/2 inhibitors) and BIS II (PKC inhibitor), resulted in inhibition of IpLITR2.6b/IpFcRγ-L induced degranulation, also indicating a potential role for these molecules. Interestingly, while c-Jun N-terminal kinases (JNKs) and p38 MAPK are recruited during FcεRI-mediated activation [147–149], inhibitors to these molecules, SP600125 and SB203580 did not significantly abrogate degranulation through the chimeric construct. Taken together, these findings provide new information regarding the stimulatory roles of an IpLITR and its recruited ITAM-encoding adaptor, IpFcRγ-L, regarding their ability to trigger effector responses in leukocytes (i.e. degranulation), as well as their ability to activate and utilize different intracellular signaling components (i.e. Lyn, Syk, ERK/MAPK/MEK1/2, PI3-K and PKC). A summary of the predicted IpLITR2.6b/IpFcRγ-L induced signaling events in RBL-2H3 cells is presented in Fig. 4.13.

Cell surface-expressed immunoregulatory IgSF members are also involved in the direct and indirect (i.e. via Ig) binding and internalization of pathogens. Phagocytosis can be of Ig-opsonized pathogens by FcRs [29,30,33,131] or by direct binding to pathogen-associated molecular patters (PAMPs) expressed on pathogens, as with TREM-2 [150–152] and CEACAM-3 [137]. As the ligands to IpLITRs are unknown, then there exists the possibility that they bind aggregated Ig, as an FcR, or PAMPs, like TREM-2 or CEACAM-3, to induce phagocytosis. To study this, 4.5 μm fluorescent beads were opsonized with anti-HA or isotype beads and incubated with RBL-2H3 cells, followed by analysis by flow cytometry. Incubation of RBL-2H3 cells expressing either YY or FF chimera with isotype-coated beads resulted in only 17.4% and 12.1% phagocytosis, respectively, measured by an increase in cell fluorescence. However, when cells expressing the YY construct were incubated with anti-HA-coated beads, phagocytosis significantly increased to 48.5%, compared to 15.9% phagocytosis by cells

expressing the FF construct. That the receptor IpLITR2.6b induces both degranulation and phagocytosis, two prototypical innate immune effector responses, provides support of this receptor family's potential role in mediating innate defensive functions in catfish immune cells. However, this needs to be explored further using fish immune cells and IpLITR-specific antibodies.

Taken together, the ability of the receptor IpLITR2.6b, when associated with its adaptor IpFcRγ-L, to induce signaling, degranulation and phagocytosis provides a first-look at the potential innate effector functions of this receptor. These responses were shown to be ITAM-dependent as the receptor-adaptor construct with mutated ITAMs did not yield any significant effects. Furthermore, the use of pharmacological inhibitors provided additional details into the potential signaling cascades occurring during degranulation. As these studies were conducted using chimeric constructs over-expressed in a mammalian immune cell line, further studies are still required to explore and confirm these results in channel catfish. Nonetheless, as the IpLITR family is polymorphic and polygenic, there remain many other receptor-types to be studied. As such, the ability to stably express functional IpLITR-adaptor chimeras in RBL-2H3 cells will be valuable in the further characterization of stimulatory IpLITR-types as well as functionally characterizing additional IpLITR-types, including ITIM-bearing (i.e. inhibitory) receptors, examined in the following chapter.

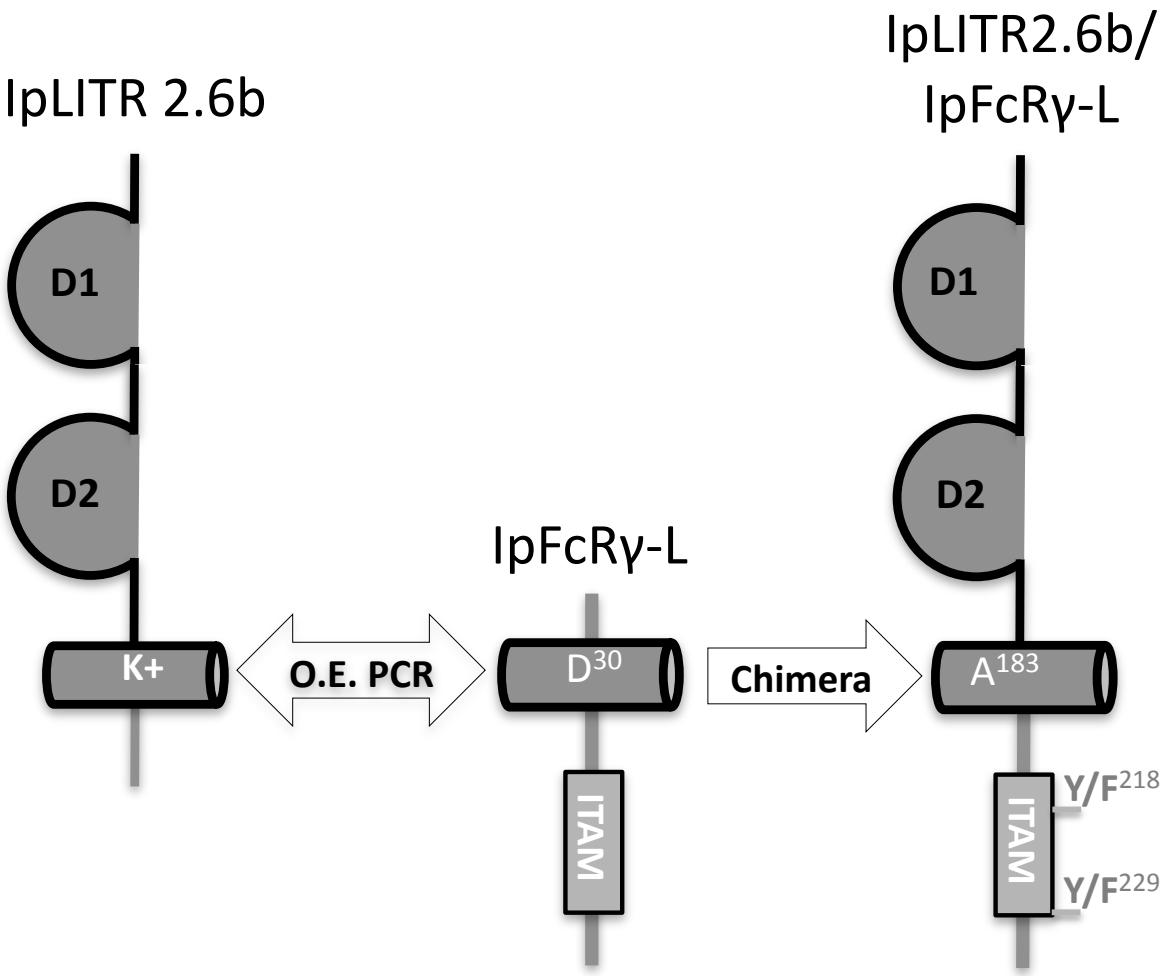

Figure 4.1. Generation of IpLITR2.6b/IpFcRγ-L fusion proteins. (A) Overlap-extension (OE) PCR was used to combine the extracellular domain of IpLITR 2.6b (DQ860171.1) with the TM and ITAM-encoding CYT of IpFcRγ-L (AF543420.1). The TM segment of the chimera was neutralized by a D^{183} to A^{183} mutation and the tyrosine residues (Y^{218} and Y^{229}) within the ITAM motif are indicated. The chimera with an intact ITAM was designated as IpLITR/ IpFcRγ-L YY and following Y^{218} to F^{218} and Y^{229} to F^{229} mutations the chimera with the mutated ITAM was designated as IpLITR/IpFcRγ-L FF.

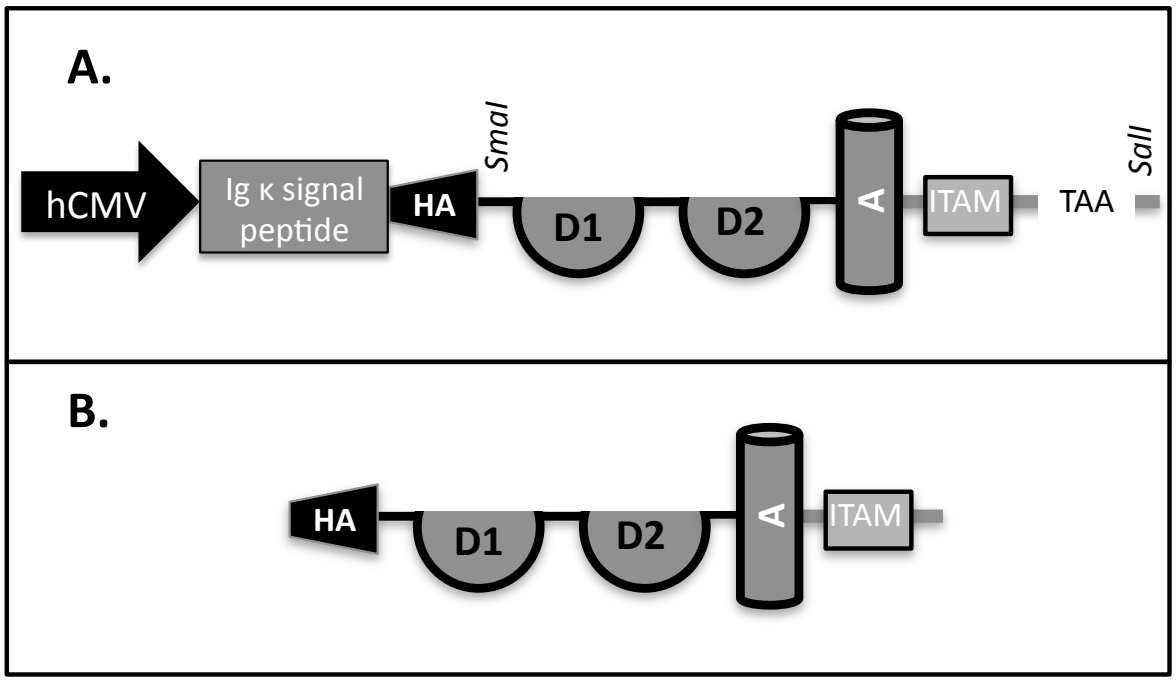

Figure 4.2. Chimeric constructs for transfection in RBL-2H3 cells.
(A) IpLITR2.6b/IpFcRγ-L 'YY' and 'FF' chimeric constructs were cloned into the pDISPLAY vector using SalI and SmaI restriction sites. The vector contains an hCMV promoter to drive expression of the cloned genes and the mammalian Ig κ leader signal. (B) The resulting construct has an N-terminal HA epitope tag for surface staining and receptor engagement by epitope-specific antibodies.

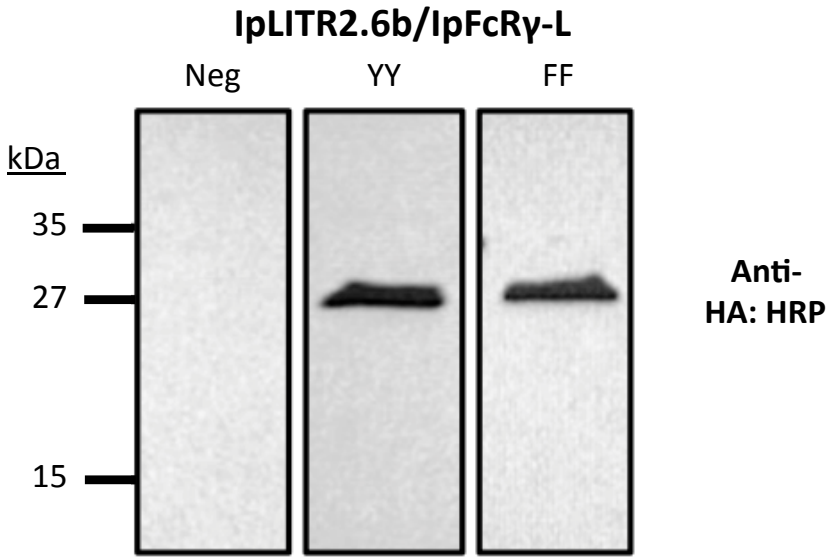

Figure 4.3. Detection of the HA epitope-tagged IpLITR2.6b/IpFcRγ-L fusion proteins in HEK-293T cells. A Western blot demonstrates that following cellular transfections in HEK 293T cells, both IpLITR2.6b/IpFcRγ-L YY and FF generated recombinant proteins of the expected size; ~25 kDa. Samples were separated on an 8% SDS-PAGE gel under reducing conditions, transferred to nitrocellulose and duplicate blots were probed with HRP-conjugated goat anti-HA pAb (1:1000 v/v). Neg refers to lysates prepared from control (i.e. non-transfected) HEK 293T cells.

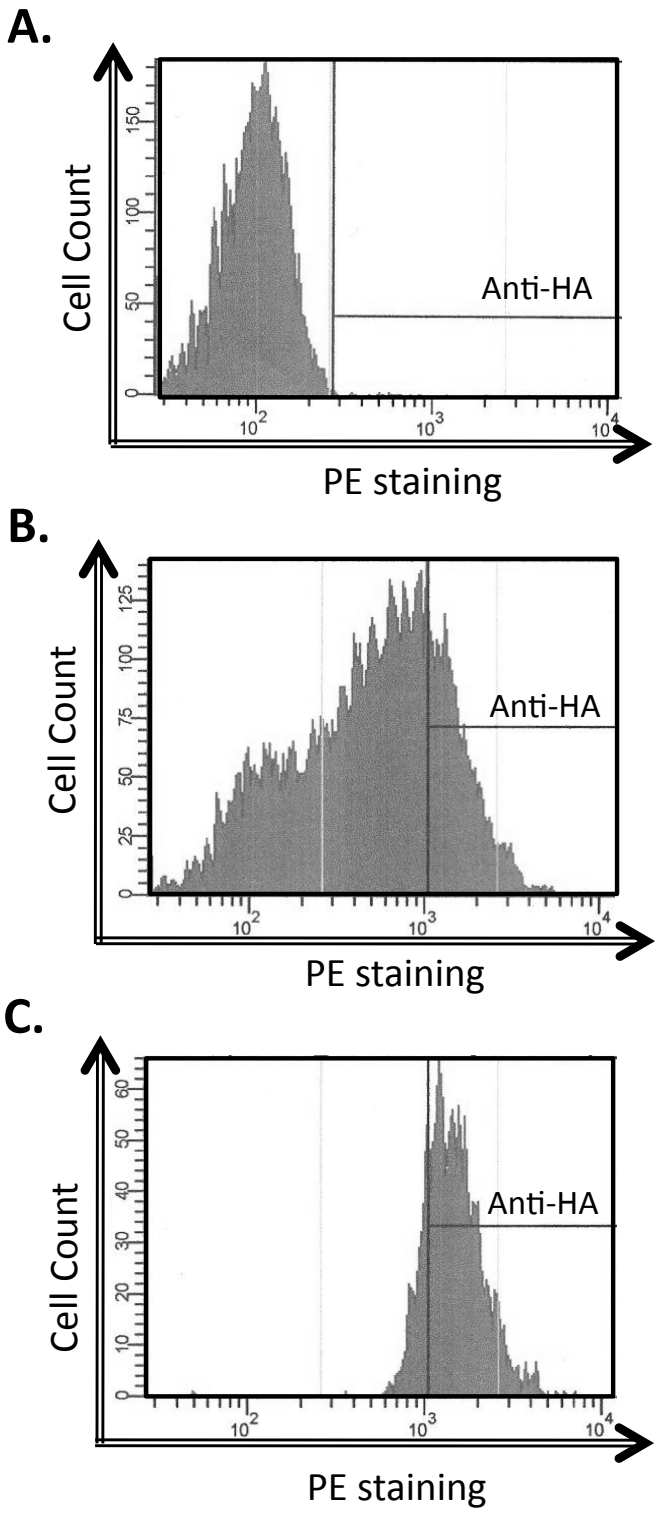

Figure 4.4. Sorting of IpLITR2.6b/IpFcRγ-L-transfected RBL-2H3 cells. Detection of the cell surface expression of IpLITR2.6b/IpFcRγ-L in RBL-2H3 after flow cytometric staining. RBL-2H3 cells were stained with 20 μg/mL IgG3 isotype (A) or 20 μg/mL anti-HA mAb (B) followed by staining with 10 μg/mL PE-conjugated goat anti-mouse IgG (H+L). Surface expression was then detected as an increase in fluorescence (i.e. PE staining, FL-2) in comparison with IgG3-stained cells. (C) HA-positive cell population was sorted from HA-negative cells and further cultured in G418 selection media.

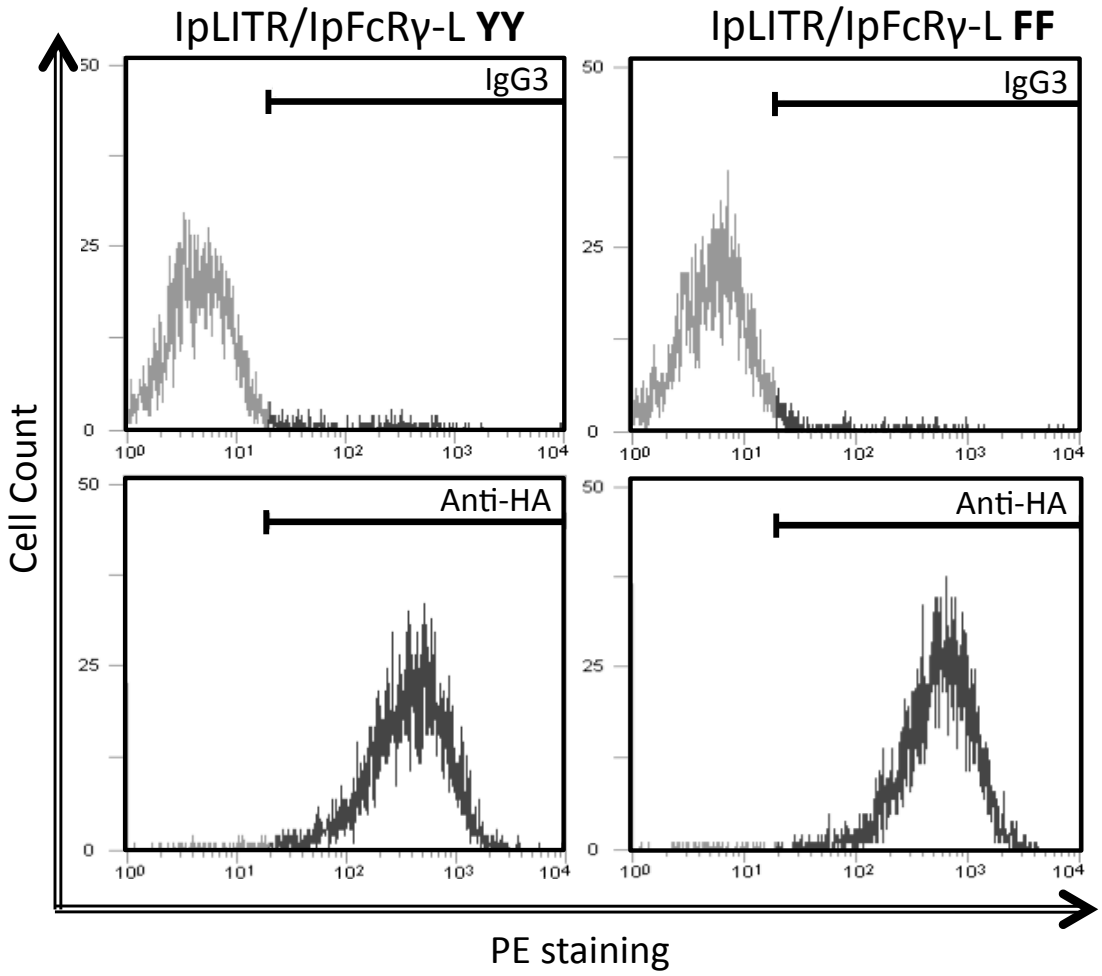

Figure 4.5. Surface expression of the HA epitope-tagged IpLITR2.6b/ IpFcRγ-L fusion proteins in RBL-2H3. Detection of the cell surface expression of IpLITR2.6b/IpFcRγ-L YY (left panels) and FF (right panels) in RBL-2H3 after flow cytometric staining. RBL-2H3 cells were stained with 20 μg/mL anti-HA mAb (lower panels) or IgG3 (isotype control; upper panels) followed by staining with 10 μg/mL PE-conjugated goat anti-mouse IgG (H +L). Surface expression was then detected as an increase in fluorescence (i.e. PE staining, FL-2) in comparison with IgG3-stained cells.

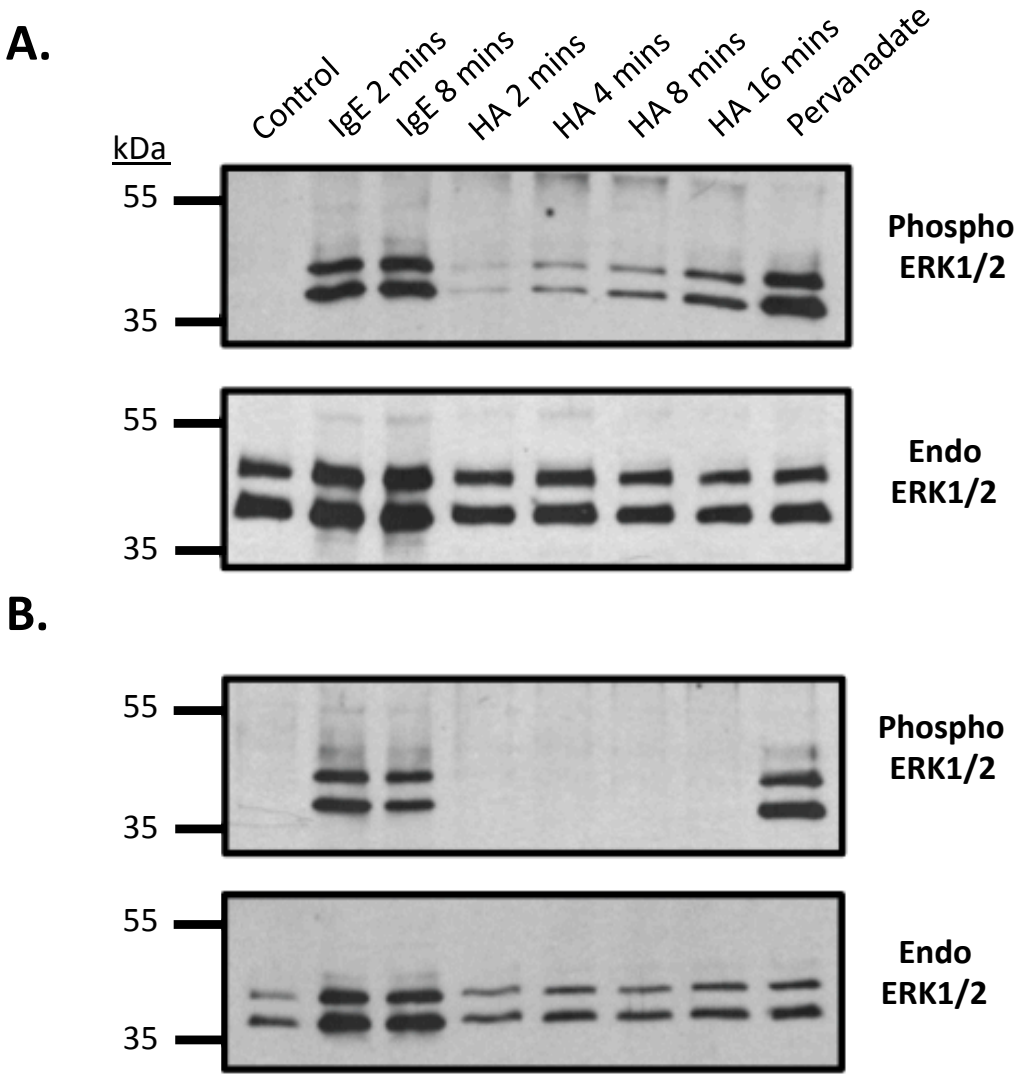

Figure 4.6. Cross-linking of IpLITR2.6b/IpFcRγ-L YY, but not FF, induces an ITAM-dependent activation of the ERK1/2 pathway in RBL-2H3 cells. RBL-2H3 cells (~5x10^6 cells) stably expressing IpLITR2.6b/IpFcRγ-L YY (A) or FF (B) were untreated (control) or incubated with: 0.625 μg/mL anti-HA mAb followed by cross-linking with 1.25 μg/mL goat anti-mouse IgG (H+L) for 2, 4, 8 and 16 mins; 200 ng/mL anti-DNP IgE followed by crosslinking with 0.1 ng/mL DNP-HSA for 2 and 8 min; or 0.1mM Na_3VO_4 (Pervanadate). Samples were separated on an 8% SDS-PAGE gel under reducing conditions, transferred to nitrocellulose and duplicate blots were probed with anti-phospho-ERK1/2 (1:2000 v/v) or anti-ERK1/2 ("endo") (1:2000 v/v), followed by HRP-conjugated goat anti-rabbit IgG (H+L) (1:5000 v/v).

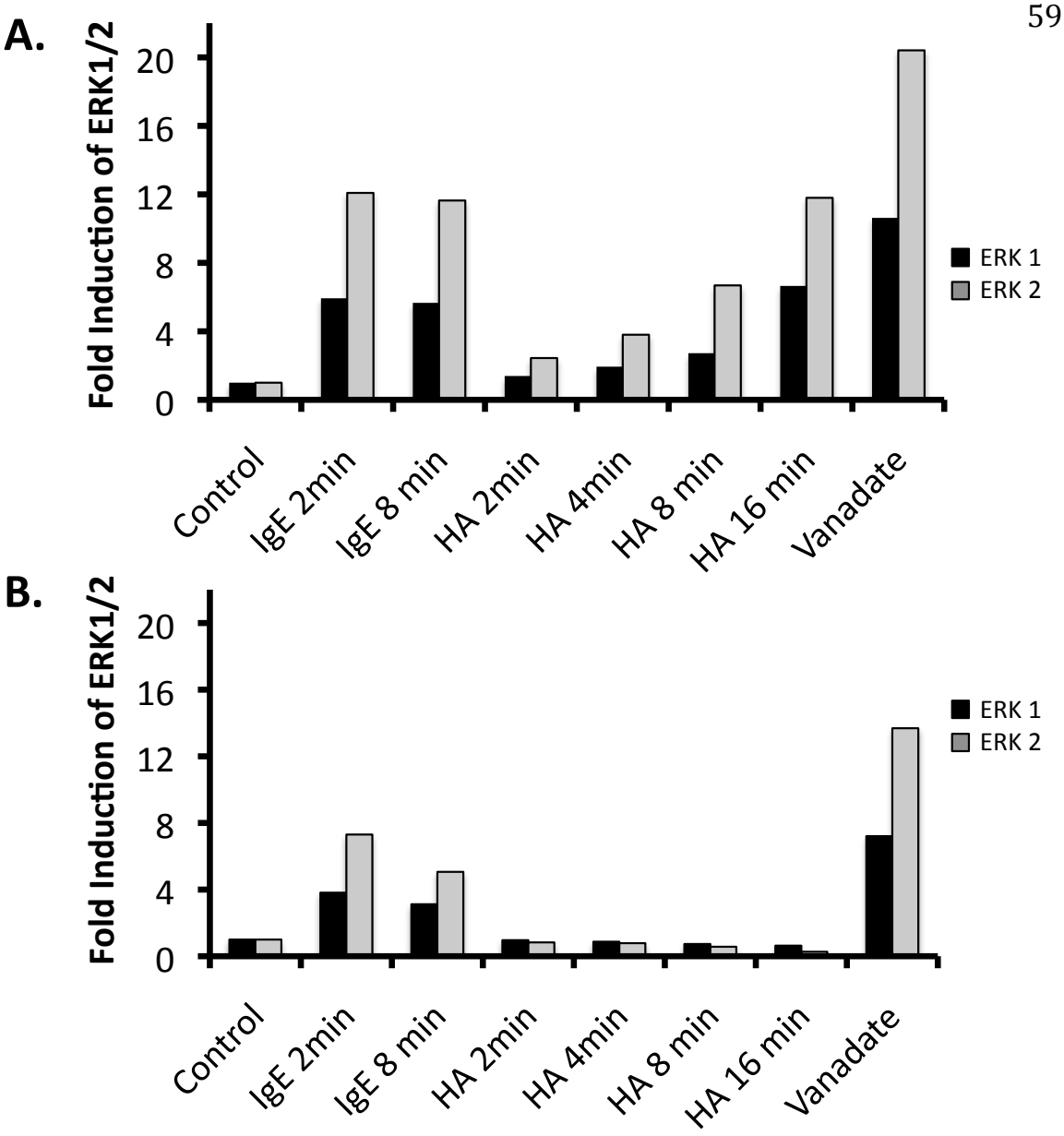

Figure 4.7. Fold-induction of ERK1/2 phosphorylation following cross-linking of IpLITR2.6b/IpFcRγ-L YY or FF in RBL-2H3 cells. All Changes in phospho-ERK1/2 levels upon IpLITR2.6b/IpFcRγ-L YY (A) or FF (B) engagement from Fig. 4.6 are reported here as a fold induction value relative to the untreated RBL-2H3 cells (control), which was normalized to a value of 1.0 using the equation below. All phospho ERK1/2 band intensity levels were corrected based on the endogenous expression levels of ERK1/2 (i.e. endo) as follows: [(phospho ERK1 densitometry value for # min/endo ERK1 value for # min) * 100]. This value was then divided by the calculated relative fold induction value of ERK1 expression obtained for untreated cells (control) and is shown as the black histogram bars. The grey histogram bars represent the relative fold induction values of phospho ERK2 expression in each lane calculated using the same equation but using the phospho and endo ERK2 values instead. Results presented are from a representative of two independent experiments that gave similar results.

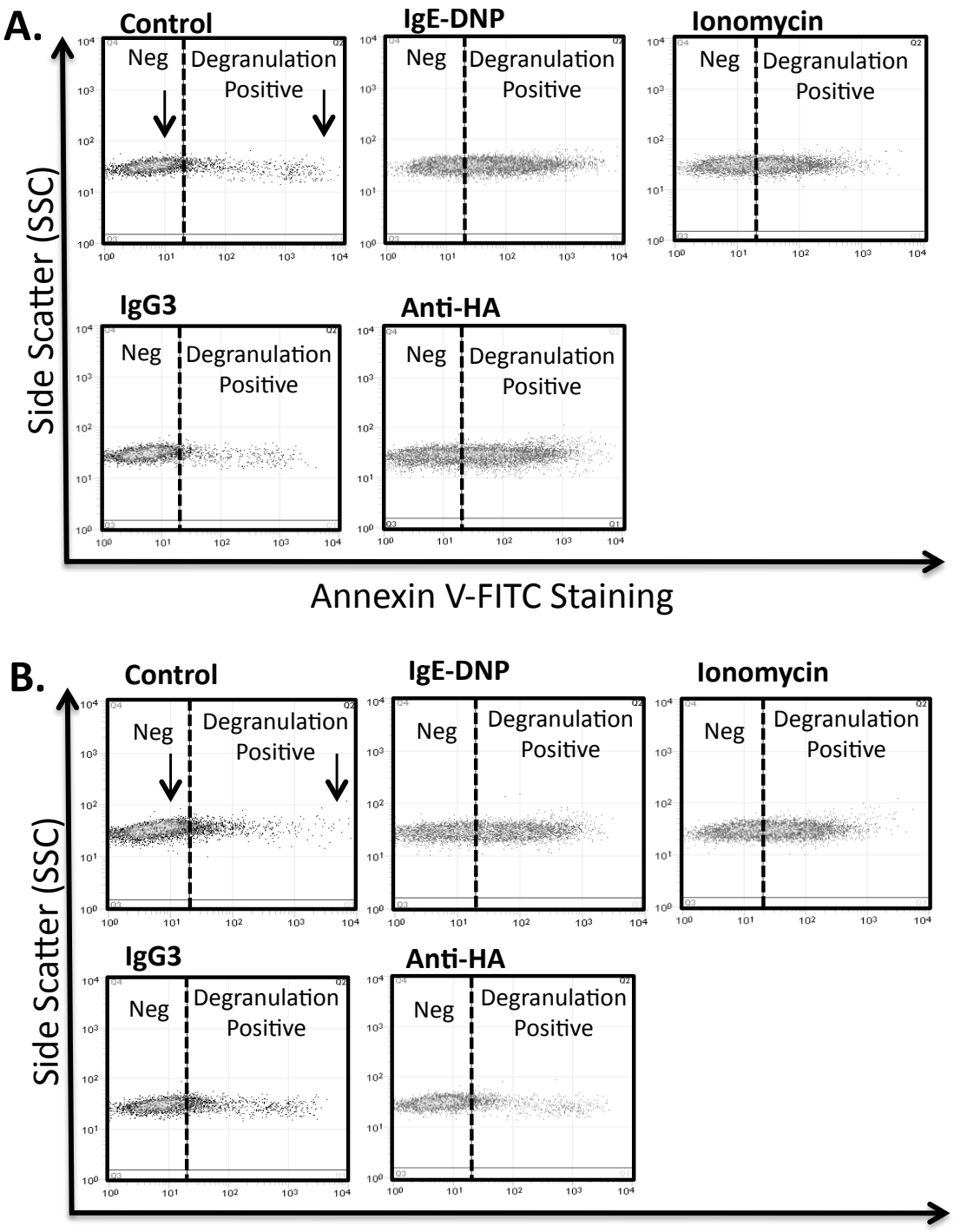

Figure 4.8. Flow cytometric detection of degranulation in RBL-2H3 cells upon cross-linking of IpLITR2.6b/IpFcRγ-L based on Annexin V-FITC staining. RBL-2H3 cells expressing IpLITR2.6b/IpFcRγ-L YY (A) of FF (B) were treated culture media (Control); sensitized with 200 ng/mL anti-DNP IgE and cross-linked with 0.1 ng/mL DNP-HSA; 0.625 µg/mL mouse IgG3 isotype or anti-HA mAb and cross-linked with1.25 µg/mL goat anti-mouse IgG (H+L); or 0.625 µM calcium ionomycin salt (Iono). Cells were then treated with 10 µM cytochalasin B, fixed and stained in 1 µg/mL Annexin V-FITC.

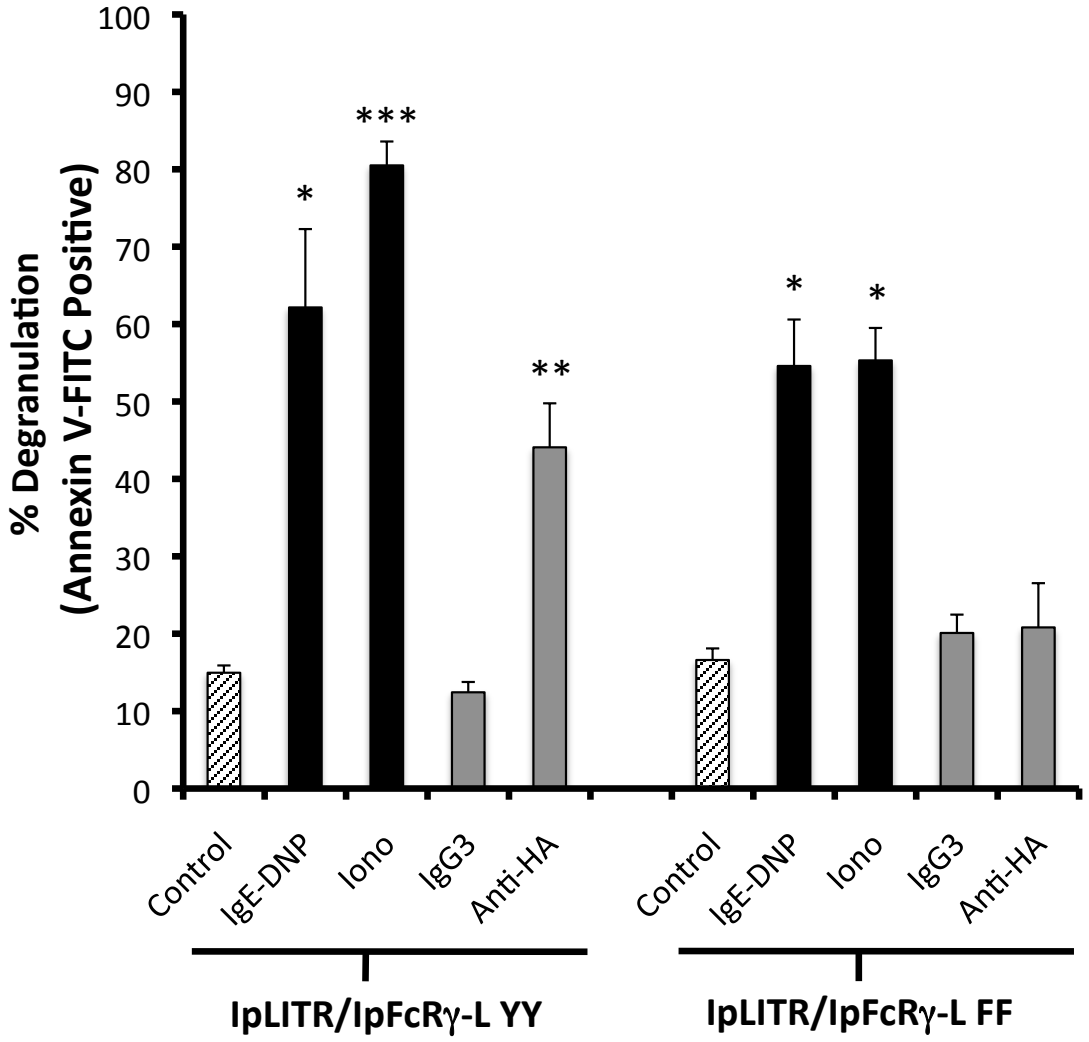

Figure 4.9. Histogram representation of IpLITR2.6b/IpFcRγ-L-induced degranulation in RBL-2H3 cells. RBL-2H3 cells expressing IpLITR2.6b/ IpFcRγ-L YY (A) of FF (B) were treated with culture media (Control); sensitized with 200 ng/mL anti-DNP IgE and cross-linked with 0.1 ng/mL DNP-HSA; 0.625 µg/mL mouse IgG3 isotype or anti-HA mAb and cross-linked with 1.25 µg/mL goat anti-mouse IgG (H+L); or 0.625 µM calcium ionomycin salt (Iono). Cells were then treated with 10 µM cytochalasin B, fixed and stained in 1 µg/mL Annexin V-FITC from Fig. 4.8. Each bar represents the mean +/- SEM of three independent experiments performed measuring the % increase in Annexin V-FITC positive cells after individual treatments (* $p<0.05$, ** $p<0.01$, *** $p<0.001$; when compared to control cells).

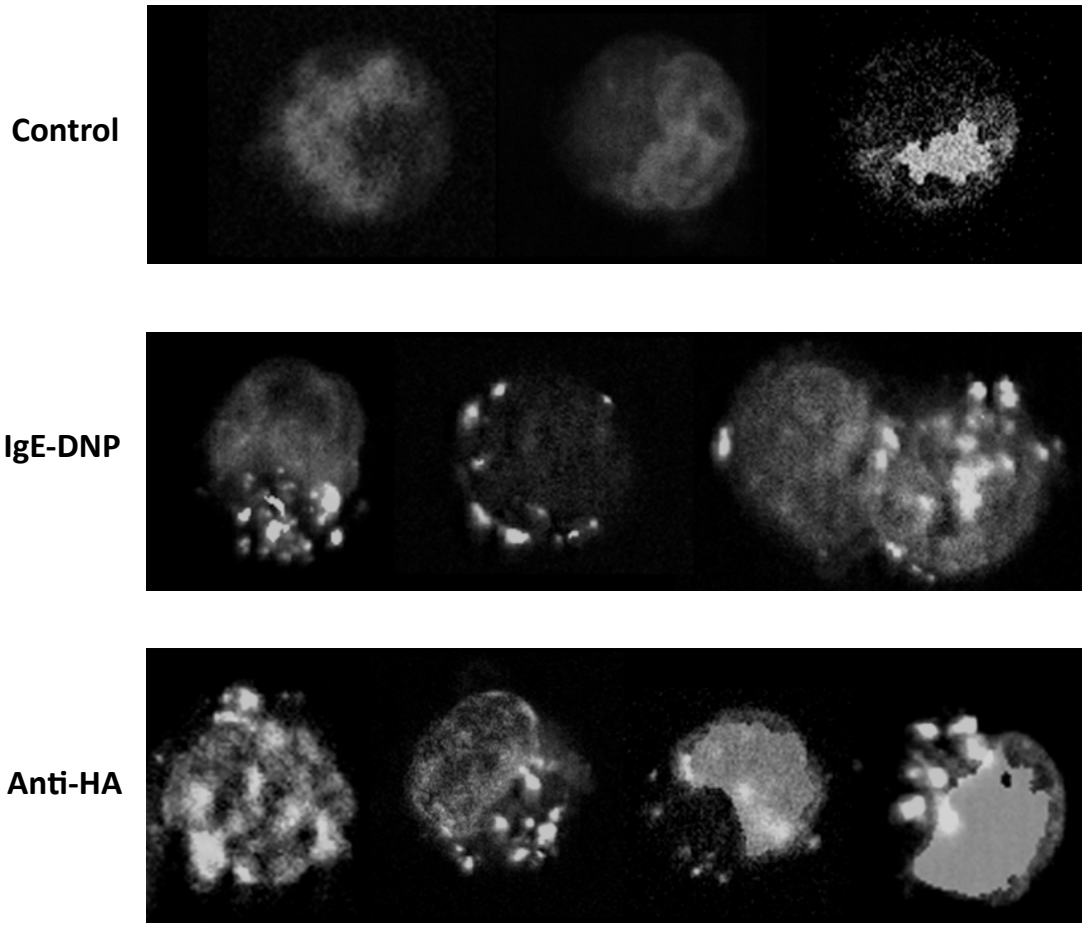

Figure 4.10. Fluorescence microscopic visualization of Annexin V-FITC staining of IpLITR2.6b/IpFcRγ-L YY-expressing RBL-2H3 cells during degranulation. RBL-2H3 cells expressing IpLITR2.6b/IpFcRγ-L YY were treated culture media (Control, top panel); sensitized with 200 ng/mL anti-DNP IgE and cross-linked with 0.1 ng/mL DNP-HSA (middle panel); 0.625 μg/mL anti-HA mAb and cross-linked with 1.25 μg/mL goat anti-mouse IgG (H+L) (bottom panel). Cells were then treated with 10 μM cytochalasin B, fixed and stained in 1 μg/mL Annexin V-FITC (white regions). Cell nuclei were counterstained with 1.5 μg/mL DAPI (grey regions).

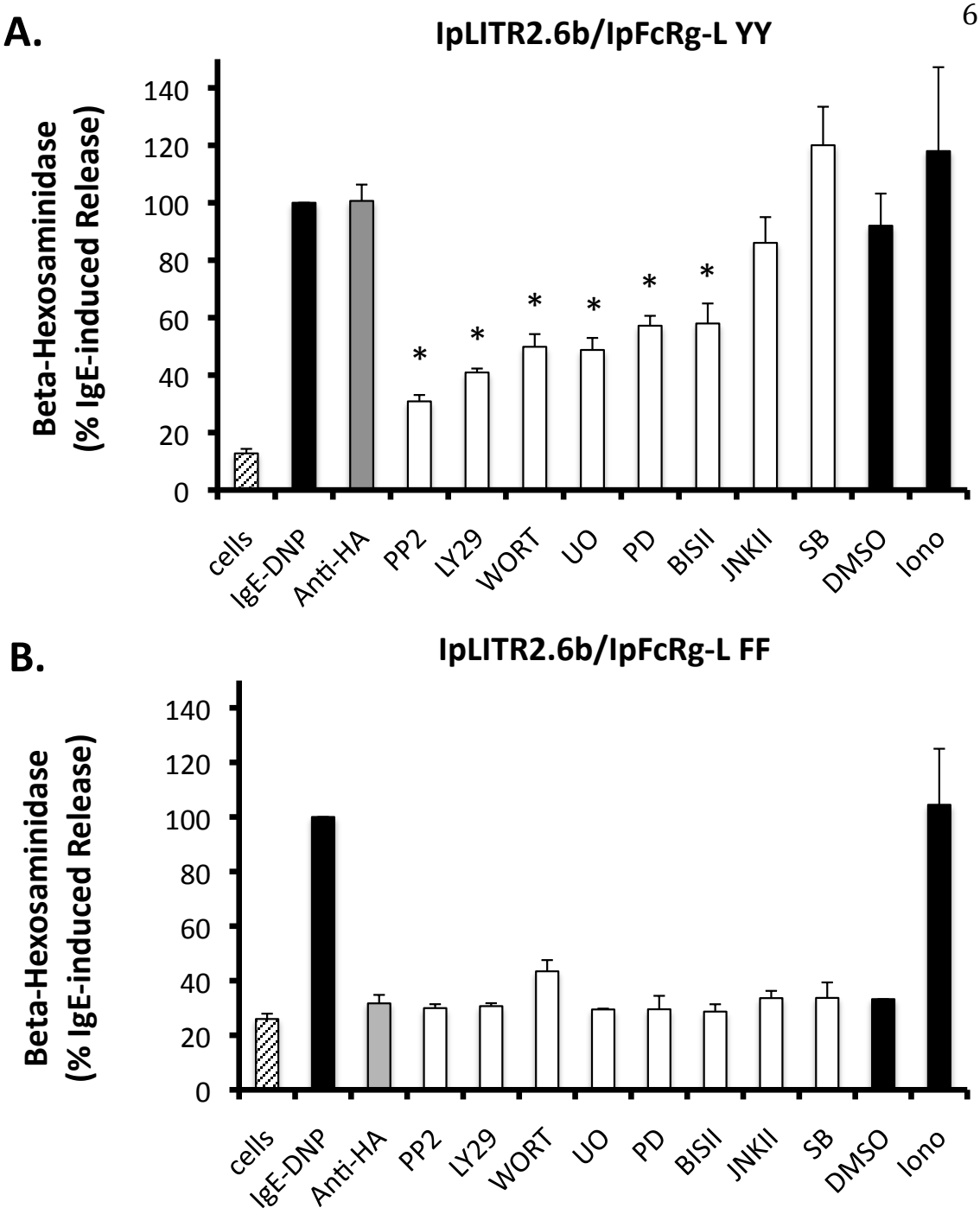

Figure 4.11. Pharmacological inhibition of IpLITR2.6b/IpFcRγ-L-induced β-hexosaminidase release in RBL-2H3 cells. IpLITR2.6b/IpFcRγ-L YY (A) or FF (B) expressing RBL-2H3 cells were treated with (white bars) or without pharmacological blockers prior to stimulation with 0.625 μg/mL anti-HA mAb and 1.25 μg/mL goat anti-mouse (H+L) pAb cross-linking. Cells were also treated with 200 ng/mL anti-DNP IgE and 0.1 ng/mL DNP-HSA cross-linking; or 0.625 μM calcium ionomycin salt (iono) stimulation. Each bar represents the mean +/- SEM of three independent experiments performed (* $p<0.001$; when compared to Anti-HA stimulated cells). Concentrations of inhibitors used and their targets are listed on Table 4.1.

Inhibitor	Target signal molecule	Concentration	% Inhibition ± SEM
PP2	Src family PTK	10 µM	69.8% ± 4.3
LY294002	PI3K	10 µM	59.7% ± 4.5
UO126	MEK 1/2	10 µM	51.9% ± 5.6
Wortmannin	PI3K	100 nM	50.3% ± 10.7
PD98059	MEK	25 µM	42.9% ± 8.1
BIS II	PKC	500 nM	42.2% ± 10.8
SP600125	JNK1,2,3	1 µM	14.1% ± 6.8
SB203580	p38 MAPK	10 µM	-19.9% ± 6.8
DMSO	Vehicle control	0.1% (v/v)	9.7% ± 1.2

Table 4.1. Pharmacological inhibition of IpLITR2.6b/IpFcRγ-L-induced degranulation. Results are calculated from data in Fig. 4.8 (A) and represent the % reduction of β-hexosaminidase release after anti-HA crosslinking, when compared to release after anti-HA crosslinking in absence of inhibitors, calculated using the following formula: [1- [inhibitor values for; (% HA degranulation - % IgG3 degranulation)] / [Control values for; (% HA degranulation - % IgG3 degranulation)]]*100. Note: a negative % inhibition value represents an increased level of β-hexosaminidase release when the cells were treated with SB203580. Bold values indicate statistically significant differences ($p < 0.05$). Vehicle control refers to the amount of DMSO added per well based on the volume of inhibitors (dissolved in DMSO) used.

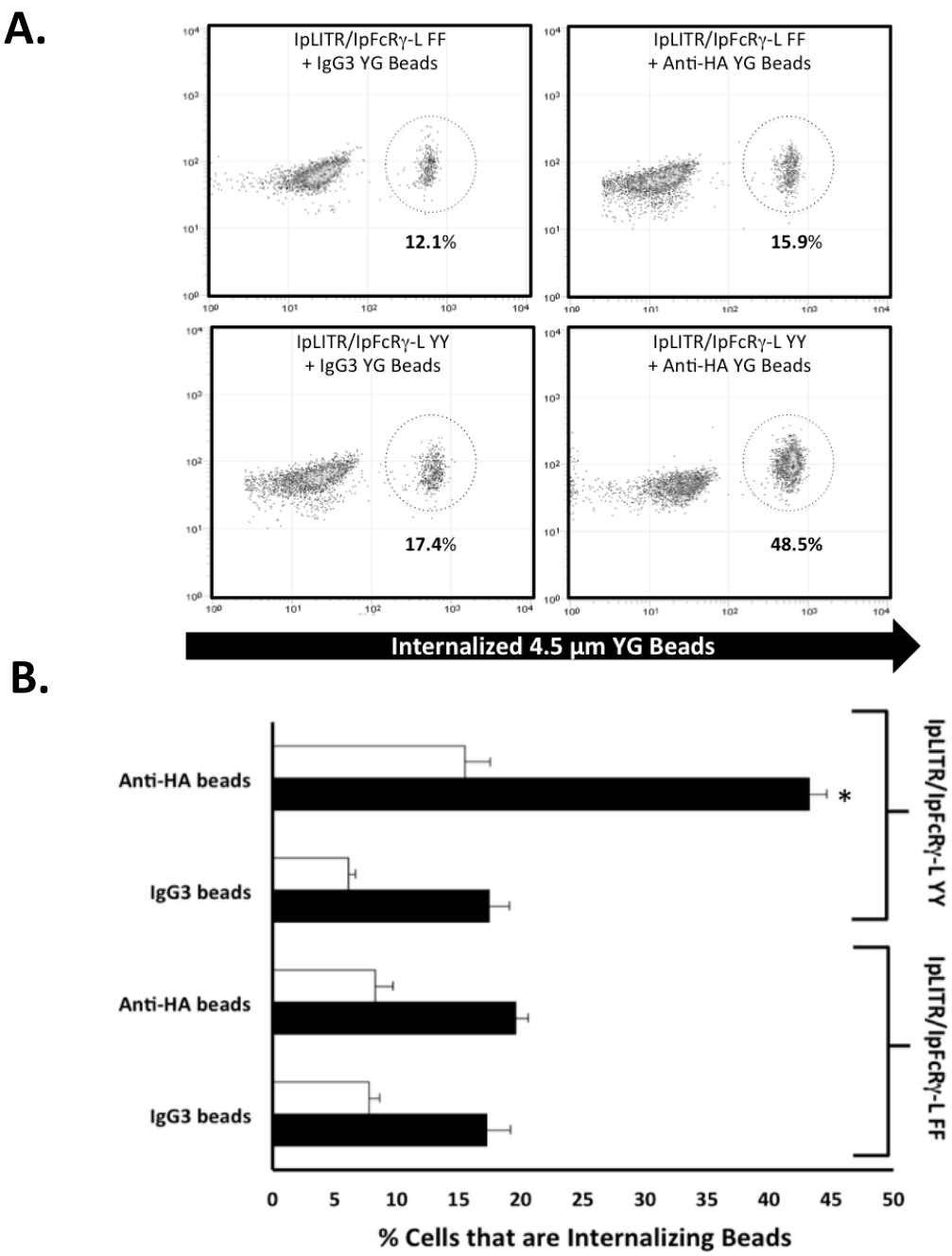

Figure 4.12. IpLITR2.6b/IpFcRγ-L-mediated phagocytosis of opsonized microspheres requires an intact ITAM. (A) A representative flow cytometric scatter plot is shown demonstrating the increase of internalized anti-HA mAb coated beads by RBL-2H3 cells expressing IpLITR2.6b/IpFcRγ-L YY (bottom right panel) at 37°C, as measured by a shift in FL-1 staining (hatched circle). RBL-2H3 cells expressing IpLITR2.6b/IpFcRγ-L FF (top right panel) and cells incubated with IgG3-coated beads (left panels) have a significantly lower amount of internalized beads. (B) Pooled results from three phagocytosis experiments is shown. Each bar represents the mean +/- SEM of three independent experiments performed measuring the % increase in internalized microspheres. * $p<0.001$; when compared to all other % phagocytosis at 37^{o}C (black bars) and 4^{o}C (white bars).

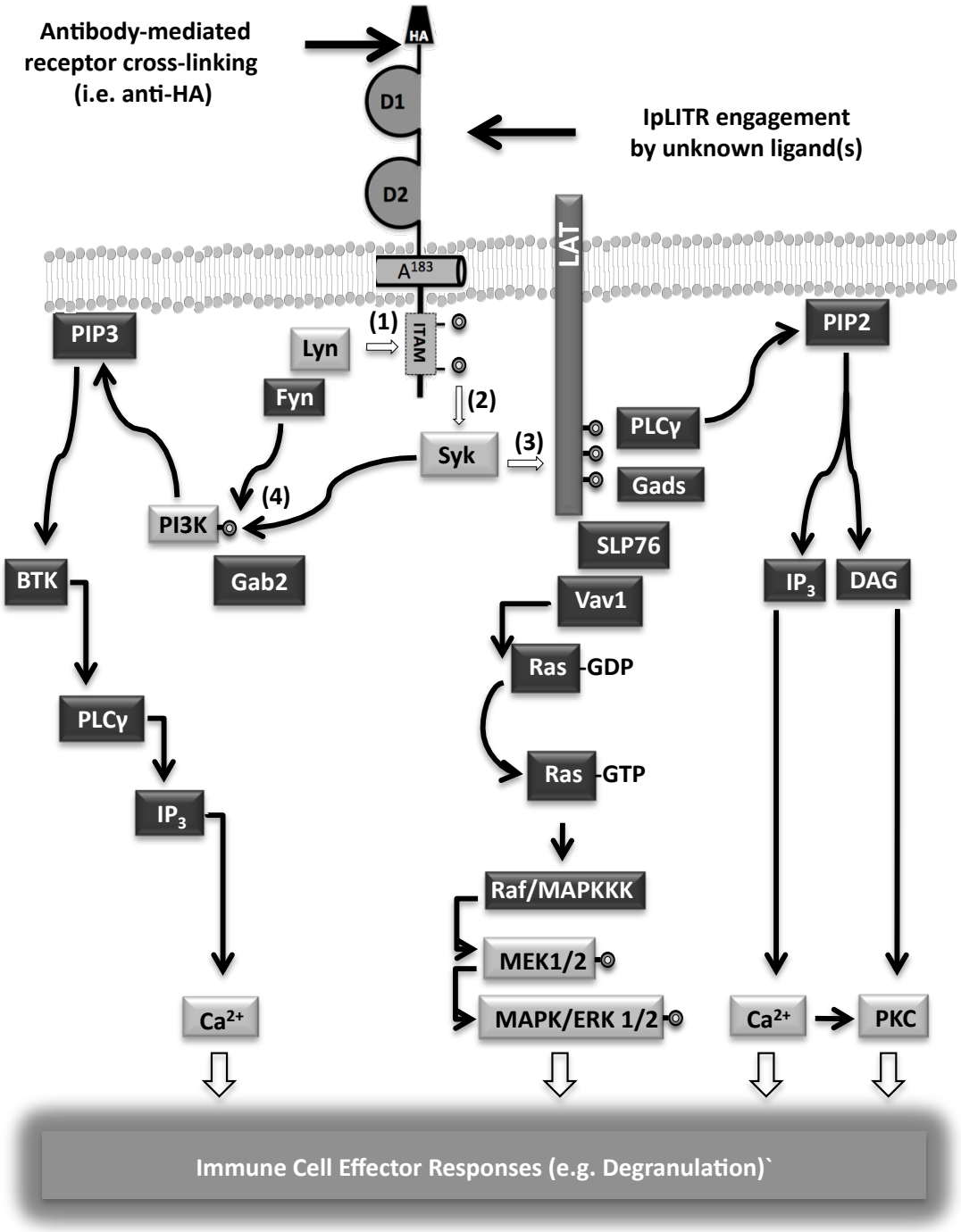

Figure 4.13. Predicted IpLITR2.6b/IpFcRγ-L-mediated intracellular signaling events in RBL-2H3 cells. A summarized schematic of the known 'classical' signaling events that occur in RBL-2H3 cells following antigen-induced aggregation of IgE- sensitized FcεRI [32, 135] is indicated by black boxes (white text) and is used as a guideline for the predicted signaling pathway(s) initiated by IpLITR2.6b/IpFcRγ-L activation of RBL-2H3 cells. From this thesis, predicted signaling events that occur following antibody cross-linked IpLITR2.6b/IpFcRγ-L are indicated by grey boxes (black text).

CHAPTER 5

Induction of intracellular signaling and phagocytosis by an inhibitory IpLITR-type: Evidence for functional duality in a teleost immunoregulatory receptor[1]

5.1 Introduction

Innate immune cells receive activating and suppressive signals from their environment using surface immunoregulatory receptors that are expressed as pairs of stimulatory and inhibitory-types. As stimulatory receptors promote effector responses and inhibitory receptors oppose them, then the balance of these two signals act to coordinate appropriate cellular responses to infection. Such paradigms of using immunoregulatory receptors to modulate immune effector responses are well characterized in mammals but immunomodulatory receptor-classes have also begun to be examined in lower vertebrates as well, including teleost [1,121,122]. IpLITRs represent one such receptor family expressed by channel catfish and encode putative inhibitory and stimulatory receptor-types. One putative inhibitory receptor is IpLITR1.1b, which contains four Ig-like domains, an uncharged TM segment, and CYT with six tyrosine residues [1]. Two of these residues are encoded in ITIMs: early biochemical studies revealed the association of this receptor with the inhibitory phosphatases SHP-1 and SHP-2, in an ITIM-dependent manner [2]. Subsequent expression of this receptor-type in mouse NK cells demonstrated their ability to abrogate NK-mediated cellular cytotoxicity mediated by SHP-dependent mechanisms, as well as by an additional tyrosine required for the recruitment of the inhibitory C-src kinase (Csk) [3]. Finally, IpLITR1.1b encodes a membrane-distal tyrosine within an immunoreceptor tyrosine-based switch motif (ITSM), as well as two additional TM proximal

[1] The manuscript of a version of this chapter has been submitted. Cortes, *et al.* 2013. J Innate Immunol. In submission.

tyrosine residues with unknown or no known functions. By comparison, stimulatory IpLITR-types, examined in Ch 4 of this thesis, can associate with the ITAM-bearing adaptor IpFcRγ-L, required for surface expression [4]. This receptor-adaptor association initiated signaling events leading to the induction of degranulation and phagocytosis in an ITAM-dependent fashion [130]. While these studies have been beneficial in understanding stimulatory IpLITR-mediated signaling and effector responses, further characterization is still required to provide a more complete picture of the signaling capacity of stimulatory IpLITRs as well as additional effector responses induced. The objective of this chapter was to further characterize IpLITR2.6b/IpFcRγ-L signaling and effector responses in RBL-2H3 cells. As well, while IpLITR1.1b was previously characterized as an inhibitory receptor in mouse NK cells [3], it encodes four tyrosines, in addition to its two ITIM-tyrosines, not found within canonical ITAM, so my other objective was to characterize the signaling and effector functions of this non-ITAM-containing IpLITR.

To explore the signaling capabilities of IpLITR2.6b/IpFcRγ-L and IpLITR1.1b in RBL-2H3 cells, I utilized a signaling array to identify additional mediators of IpLITR-induced signaling. As expected, multiple kinases were phosphorylated by IpLITR2.6b/IpFcRγ-L but very few by IpLITR1.1b. Unexpectedly, a time-course examination of ERK1/2 and Akt activation revealed early but transient phosphorylation of these molecules by IpLITR1.1b.

To examine IpLITR2.6b/IpFcRγ-L's ability to induce additional effector responses other than degranulation and phagocytosis [130] and to determine if IpLITR1.1b-mediated stimulatory signaling resulted in effector responses, I examined cytokine secretion using a cytokine array. IpLITR2.6b/IpFcRγ-L induced the secretion of interleukin (IL)-3, 4, 6 and tumour necrosis factor (TNF)-α; however, these cytokines were not secreted upon IpLITR1.1b activation.

Phagocytosis of opsonized beads by both receptor-types was also examined: surprisingly, IpLITR1.1b induced a strong phagocytic response, at higher levels than IpLITR2.6b/IpFcRγ-L. In light of initial evidence into the inhibitory capacities of this receptor [3], its ability to induce effector functions was highly unexpected, so further studies into the biochemical requirements for phagocytosis were undertaken. IpLITR1.1b did not associate with endogenous FcεRI γ subunit in RBL-2H3 cells and phagocytosis by this receptor required an intact CYT; however, the membrane-proximal region (containing the Csk-binding tyrosine and two uncharacterized tyrosines) was not required for phagocytosis. This suggests a potential role for the membrane-distal region of IpLITR1.1b in promoting effector responses in RBL-2H3 cells: while the tyrosine found within the ITSM is a likely candidate, the ITIM tyrosines may play a novel, stimulatory role. In a broader context, the ability of an ITIM-bearing receptor to inhibit and activate immune effector responses suggests a dual functionality among, at least some, immunoregulatory receptors that may be involved in the fine coordination of appropriate immune responses to infection.

5.2 Results

5.2.1 Stable expression of HA epitope-tagged IpLITR2.6b/IpFcRγ-L and IpLITR1.1b constructs in RBL-2H3 cells

RBL-2H3 cells were transfected with N-terminal HA epitope-tagged IpLITR2.6b/IpFcRγ-L 'YY' chimera or with IpLITR1.1b followed by selection and sorting as described in Ch 4 of this thesis. Shown in Fig. 5.1 is a representative flow cytometric profile of RBL-2H3 cells transfected with either IpLITR-type. Notably, IpLITR1.1b demonstrated increased surface expression, compared with IpLITR2.6b/IpFcRγ-L.

5.2.2 Phosphorylation status of select signaling kinases engaged by IpLITR2.6b/IpFcRγ-L or IpLITR1.1b

Phospho-signaling profiles were obtained of IpLITR-activated RBL-2H3 cells using the Phospho-MAPK Array Kit (R&D Systems). Activation of IpLITR2.6b/IpFcRγ-L by anti-HA cross-linking for 10 mins at 37°C increased the phosphorylation several signaling molecules, including ERK1/2, GSK-3α/β, GSK-3β, RSK1, CREB, JNK pan, MEK6, MSK2, p38δ, and Akt2 (Fig. 5.2 B). This effect was not observed when cells were incubated with IgG3 isotype (Fig. 5.2 A). Conversely, activating cells expressing IpLITR1.1b with IgG3-isotype or anti-HA did not result in significant phosphorylation of these signaling molecules (Fig. 5.3 B). Representative proteome profiler array results are shown for IgG3 isotype-treated or anti-HA-stimulated IpLITR2.6b/IpFcRγ-L- (Fig. 5.2) or IpLITR1.1b- (Fig 5.3) expressing cells. Also indicated are the duplicate spots used to calculate the relative phosphorylation levels of select signaling molecules (Fig. 5.2 C and Fig. 5.3 C). The complete set of RBL-2H3 phospho-MAPK array data and profiler array coordinates are also provided in the Appendix.

5.2.3 Temporal phosphorylation of ERK1/2 and Akt in RBL-2H3 cells by IpLITR2.6b/IpFcRγ-L or IpLITR1.1b engagement

RBL-2H3 cells expressing either IpLITR-type were cross-linked with anti-HA mAb and the time-course induction of ERK1/2 and Akt phosphorylation was measured by Western blot using phospho-specific primary antibodies. Cross-linking of IpLITR2.6b/IpFcRγ-L with anti-HA mAb induced phosphorylation of ERK1/2 (shown as two bands at ~44 and ~42 kDa, respectively) at 2 mins, peaking at 4 mins and then gradually declined after 8, 16 and 32 mins (Fig. 5.4 A, upper panel). This correlated with the Phospho-MAPK array data, which demonstrated a relative increase ERK1/2 phosphorylation after 10 mins of anti-HA cross-linking (Fig. 5.2). RBL-2H3 cells expressing IpLITR1.1b were also cross-linked under the same conditions and showed unexpected differences in the

temporal pattern of ERK1/2 phosphorylation. Early phosphorylation was observed at 2 mins then declined at 4 mins and was no longer observed at 8, 16 and 32 mins (Fig. 5.4 B, upper panel). This time-course of ERK1/2 activation was consistent with that observed using the Phospho-MAPK Array Kit, in which no ERK1/2 phosphorylation was detected after 10 mins cross-linking (Fig. 5.3). Endogenous ERK1/2 was blotted for (lower panels in Fig. 5.4 A and B) and used to calculate fold-induction of ERK1 or 2 phosphorylation at each time point (Fig. 5.5)

Activation of Akt was also examined. Cross-linking RBL-2H3 cells expressing IpLITR2.6b/IpFcRγ-L with anti-HA mAb induced rapid phosphorylation of Akt after 2 mins and maintained up to 32 mins (Fig. 5.6 A, upper panel). Phosphorylated Akt levels were similar to those induced by FcεRI cross-linking (Fig. 5.6 A, upper panel). For IpLITR1.1b there was also a rapid increase in the phosphorylated levels of Akt following anti-HA cross-linking (Fig. 5.6 B, upper panel). However, unlike the sustained Akt activation observed by IpLITR2.6b/IpFcRγ-L, phosphorylated Akt levels diminished after 4, 8, 16 and 32 mins. Engagement of FcεRI in IpLITR1.1b-expressing RBL-2H3 also increased phosphorylated Akt levels (Fig. 5.6 B, upper panel). In these experiments, IgE served as a positive control for Akt activation. Endogenous Akt was blotted for (Fig. 5.6) and were used to calculate % change Akt phosphorylation (% ΔpAkt) (Fig. 5.7).

5.2.4 Cytokine production by IpLITR2.6b/IpFcRγ-L- and IpLITR1.1b-expressing RBL-2H3 cells

Using the Rat Cytokine Array Panel (R&D Systems), neither IpLITR 2.6b/IpFcRγ-L- nor IpLITR1.1b-expressing RBL-2H3 cells produced interleukin (IL)-3, IL-4, IL-6, or tumor necrosis factor-α (TNF-α) when treated with IgG3 isotype control IgG3 (Fig. 5.8, 5.9). However, PMA and A23187-stimulated IpLITR 2.6b/IpFcRγ-L-expressing cells produced significantly higher levels of IL-3, IL-4, IL-6, and TNF-α when compared to the untreated control (Fig. 5.8).

Also, when activated via the FcεRI, a significant induction of IL-3 and IL-4 was also detected in the supernatants of IpLITR 2.6b/IpFcRγ-L-expressing cells (Fig. 5.8). Cells expressing IpLITR 1.1b were responsive to PMA and A23187 (Fig. 5.9), and following activation via the FcεRI these cells also produced IL-3 and IL-4 (Fig. 5.9) indicating that IpLITR-transfected RBL-2H3 cells are responsive to cytokine-inducing stimuli and that the profiler can effectively detect these responses. When cross-linked using anti-HA mAb, cells expressing IpLITR 2.6b/IpFcRγ-L produced cytokine levels comparable to PMA/A23187 or IgE treatments (Fig. 5.8). However, IpLITR 1.1b-activated cells failed to produce cytokine levels significantly higher than the amounts obtained using the IgG3 isotype antibody (Fig. 5.9). Duplicate spots of the select cytokines of interest are indicated on the profilers (Fig. 5.8, 5.9). The spots located at positions A7, C1, D2, and D5 represent the cytokines sICAM-1, IL-13, CXCL7, and VEGF, respectively. These cytokines were constitutively produced by cultured RBL-2H3 cells under all conditions tested and were also detected in the supernatants of non-transfected cells. The complete set of RBL-2H3 cytokine array data and profiler array coordinates/legend are provided in the Appendix.

5.2.5 IpLITR2.6b/IpFcRγ-L- and IpLITR1.1b-induced phagocytosis

Untransfected or transfected RBL-2H3 cells were incubated with anti-HA- or IgG3 isotype-opsonized, fluorescent, 4.5 μm beads, for 30 mins at 37°C, as described in Ch 4 of this thesis. Untransfected cells showed <10% phagocytosis of either anti-HA- or IgG3-opsonized beads (Fig. 5.10). Cells expressing IpLITR2.6b/IpFcRγ-L also phagocytosed <10% of IgG3-coated beads (Fig. 5.10); however, this responses increased to ~35% when anti-HA mAb-opsonized beads were used. IpLITR1.1b-expressing cells also phagocytosed <10% isotype-coated beads, but these cells surprisingly phagocytosed ~50% anti-HA-coated beads (Fig 5.10).

IpLITR-mediated phagocytosis of opsonized beads was also observed by confocal microscopy. Prior to incubation with beads, cells were stained with FITC-conjugated cholera toxin B subunit, which binds a marker of lipid rafts, monosialotetrahexosylganglioside (GM1). Confocal transverse sectioning (Z-stack analysis) was used to observe IpLITR2.6b/IpFcRγ-L or IpLITR1.1b-mediated phagocytosis of anti-HA-opsonized, 4.5 μm beads, visualizing the interface between the surface of a phagocytosed bead and the cell membrane of a single cell (Fig. 5.11). From the top image to the bottom image (i.e. consecutive transverse sections [Z-stack] of the same cell), the FITC-staining gradually changes from a bright ring surrounding the bead to a more diffuse pattern, where the 'cap' of the bead and the cell membrane are in contact (areas highlighted with a dashed circle, Fig. 5.11).

5.2.6 IpLITR1.1b-mediated phagocytosis is not due to an association with the RBL-2H3 FcεRI γ chain

To determine if IpLITR1.1b-mediated phagocytosis could be due to an association with the ITAM-bearing FcεRI γ chain, endogenously expressed in RBL-2H3 cells, I performed co-immunoprecipitation experiments. FcεRI α subunit, a component of the FcεRI tetrameric complex [43], was immunoprecipitated in untransfected and IpLITR1.1b-transfected RBL-2H3 cells, and associated with FcεRI γ subunit (Fig. 5.12 A). This association was observed in unstimulated cells and cells stimulated with sodium pervanadate (Na_3VO_4), a global phosphatase inhibitor. Immunoprecipitating cells with anti-HA mAb and blotting with anti-HA:HRP, a 70 kDa protein, corresponding to the expected size of IpLITR1.1b, only present in transfected cells (Fig. 5.12 B, upper panel). When probed for FcεRI γ subunit, no bands were detected in unstimulated or pervanadate-treated cells (Fig. 5.12 C, upper panel), despite the presence of FcεRI γ subunit in cell lysates (Fig. 5.12 C, lower panel).

5.2.7 IpLITR1.1b-mediated phagocytosis is dependent upon its cytoplasmic region

As IpLITR1.1b contains six tyrosines in its CYT, a truncated version of IpLITR1.1b, lacking its CYT (IpLITR1.1b ΔCYT) was generated and expressed in RBL-2H3 (Fig. 5.13). A representative flow cytometric staining profile of IpLITR1.1b ΔCYT is shown (Fig. 5.14 A). Lysates of RBL-2H3 cells expressing either IpLITR1.1b or ΔCYT, probed with anti-HA, is shown, revealing a ~70 kDa band (i.e. IpLITR1.1b) or a band at ~45 kDa, the expected size of IpLITR1.1b ΔCYT (Fig. 5.14 B). Phagocytosis assays were performed with untransfected RBL-2H3 and cells expressing IpLITR1.1b (as above) as well as IpLITR1.1b ΔCYT. Consistent with previous experiments, untransfected cells, or cells expressing IpLITR1.1b 'wildtype' or ΔCYT internalized <10% isotype-coated beads (Fig. 5.14 C). For anti-HA-opsonized beads, RBL-2H3 cells also phagocytosed <10% beads, but IpLITR1.1b-expressing cells phagocytosed 59.9% beads (Fig. 5.14 C). Interestingly, IpLITR1.1b ΔCYT-expressing cells only internalized 14.3% beads (Fig. 5.14 C), implying that the intact CYT is required for phagocytosis.

5.2.8 IpLITR1.1b-mediated phagocytosis does not depend upon the membrane-proximal region of its CYT

The membrane-distal region of IpLITR1.1b contains two tyrosines at positions 477 and 499, found in ITIMs as well as tyrosine-503 encoded in an immunoreceptor tyrosine-based switch motif (ITSM) (Fig. 5.13). To determine if this region of CYT is required for phagocytosis, as opposed to the membrane proximal region of this receptor, containing a tyrosine at position 453, implicated in the recruitment of Csk [3] and two tyrosines at positions 433 and 463 which are not part of obvious signaling motifs, I cloned an additional IpLITR-type, IpLITR1.2a. This receptor shares 88% sequence identity with IpLITR1.1b (Fig. 5.15). The CYT of this receptor does not include IpLITR1.1b's membrane-

proximal region but it does closely resemble the membrane-distal region of IpLITR1.1b: IpLITR1.2a encodes an ITIM at tyrosine-407 and an ITSM at tyrosine-433, but encodes a serine at position 429, instead of a tyrosine as in IpLITR1.1b's ITIM tyrosine-499 (Figs. 5.13 and 5.15).

IpLITR1.2a was expressed in RBL-2H3 cells and a representative flow cytometric profile is shown in Fig. 5.16 A. Lysates of RBL-2H3 cells expressing either IpLITR-type were electrophoresed on a 4-20% gradient SDS-PAGE gel and blotted with anti-HA (Fig. 5.16 B) in an attempt to resolve the ~3 kDa size difference between both receptors. However, as anti-HA-reactive bands were both observed at ~72 kDa, then it is likely that there is no size difference between both receptors when expressed in RBL-2H3. Phagocytosis assays were performed with untransfected RBL-2H3 and cells expressing IpLITR1.1b (as above) as well as IpLITR1.2a. Untransfected cells, and cells expressing IpLITR1.1b or IpLITR1.2a internalized <10% isotype-coated beads (Fig. 5.16 C). For anti-HA-opsonized beads, RBL-2H3 cells also phagocytosed <10% beads, but IpLITR1.1b-expressing cells phagocytosed 58.9% beads (Fig. 5.16 C). No statistically significant difference was observed with IpLITR1.2a-mediated phagocytosis, as it induced the internalization of 56.4% of beads (Fig. 5.16 C).

5.3 Discussion and conclusions

My research focuses on understanding IpLITR-mediated signaling events responsible for the control of effector cell responses including degranulation, phagocytosis, and cytokine secretion. My findings represent the first demonstration of functional duality for an ITIM-containing teleost immunoregulatory receptor. IpLITR 1.1b, a previously defined inhibitory receptor, unexpectedly induced the activation of ERK1/2 and Akt as well as activated the phagocytic response in transfected RBL-2H3 cells. However, engagement of IpLITR 1.1b failed to induce the secretion of cytokines and displayed temporal

differences in the phosphorylation of ERK1/2 and Akt, when compared with IpLITR 2.6b. IpLITR 1.1b-mediated phagocytosis was not facilitated by an association with the ITAM-containing adaptor protein FcεRI γ chain but required an intact CYT region containing tyrosines within an ITIM and ITSM.

Immunoregulatory receptor-mediated control of effector responses is often predictable based on characteristic features encoded within the different receptor types (i.e. ITIM-mediated inhibition or ITAM-mediated induction of effector functions). Several immunoregulatory receptor families comprise of both stimulatory receptor types that associate with ITAM-bearing adaptors, as well as inhibitory, ITIM-bearing receptor-types. The KIR family of receptors encodes 14 receptors that either stimulate (KIR2DS1-5 and 3DS13D) or inhibit (KIR2DL1-3, 2DL53, DL1-3) NK cell function, or both (KIR2DL4) [153]. Another family includes the Leukocyte Ig-like receptors (LIRs), that contain stimulatory receptor-types that typically associate with FcεRI γ subunit (LIR 6, 7, 9 as well as ILT7 and 8) as well as ITIM-encoding inhibitory types (LIR1-3, 5, 8) [21]. Finally, the paired Ig-like receptor (PIR) family, the mouse homolog of LIRs, also encodes paired-expressed receptor-types: the inhibitory ITIM-bearing PIR-B as well as PIR-A which associates with FcR common γ subunit [39]. Taken together, immunoregulatory receptors are can be classified as stimulatory or inhibitory by the presence of canonical motifs, ITAMs or ITIMs, respectively. The paired expression of both these receptor-types on an immune cell allows them to receive both activating and immunosuppressive signals, which acts to finely coordinate the appropriate cellular response [154].

Members of the teleost IpLITR family are also co-expressed as stimulatory and inhibitory types and share signaling motifs with mammalian immunoregulatory receptors [1]. The ITIM-bearing receptor IpLITR1.1b was shown to recruit the inhibitory phosphatases SHP-1 and SHP-2 and abrogate NK cell-mediated cellular cytotoxicity in SHP-dependent and -independent mechanisms [2,3]. Additionally, the positively-charged TM of IpLITR2.6b allows it to associate with the ITAM-

bearing adaptor IpFcRγ-L, leading to the activation of ERK1/2 signaling and induction of several ITAM-dependent effector responses including degranulation and phagocytosis, when expressed in RBL-2H3 cells [4,130]. My objectives were to further characterize signaling events and effector responses activated by IpLITR2.6b/IpFcRγ-L in RBL-2H3 cells, as well as using the inhibitory IpLITR1.1b in RBL-2H3 cells as a comparison.

After 10 mins cross-linking with anti-HA mAb, IpLITR2.6b/IpFcRγ-L induced the activation of several intracellular signaling molecules. In contrast, activation of these same kinases was not observed following IpLITR1.1b cross-linking for 10 mins. This may be due to the lack of ITAMs in this receptor's CYT, or perhaps its potential signaling partners were not detected by this particular signaling array. Nonetheless, based on the results of this array, more detailed phosphorylation studies of select kinases were conducted, such as ERK1/2 and Akt, two molecules involved in many immunoregulatory signaling pathways. A time course examination of ERK1/2 activation by IpLITR2.6b/IpFcRγ-L demonstrated peak phosphorylation at 4 mins, followed by sustained phosphorylation after 32 mins. In addition, phosphorylation of Akt was detected in unstimulated cells but was also up-regulated upon IpLITR2.6b/IpFcRγ-L cross-linking and consistently sustained for at least 32 mins. These results are expected as ITAM-driven signaling initiated by IpLITR2.6b/IpFcRγ-L may be similar to mammalian stimulatory immune-type receptors and has in part been previously observed [130]. By comparison, IpLITR1.1b induced early but transient activation of ERK1/2, peaking at 2 mins, but dissipating partially at 4 mins, then completely after 8 mins. Akt was also transiently activated, peaking at 4 mins but diminishing steadily afterwards. While this explains the absence of ERK1/2 and Akt activation after 10 mins using the Profiler Array, these results were unexpected given this receptor's previously-reported inhibitory functions. [2,3]. Nonetheless the differences in the temporal regulation of signaling molecules unique to each receptor type warrant further study.

In order to determine if IpLITR1.1b-mediated signaling results in the activation of immune cells, as well as to further characterize IpLITR2.6b/IpFcRγ-L-induced effector responses, I examined cytokine secretion in RBL-2H3. Cytokine secretion was observed in untransfected RBL-2H3 cells or cells expressing either IpLITR-type when stimulated through endogenous FcεRI or with PMA/A23187 calcium ionophore. IpLITR2.6b/IpFcRγ-L activation alone induced the secretion of IL-3,-4,-6 and TNF-α; however these cytokines failed to secrete upon IpLITR1.1b cross-linking. Taken together, IpLITR2.6b/IpFcRγ-L continues to function as a classical stimulatory receptor, yet IpLITR1.1b, despite its ability to activate ERK1/2 and Akt signaling molecules is unable to induce the release of cytokines.

Another effector response examined was the internalization of opsonized beads, measured by flow cytometry. Consistent with previous observations [130], IpLITR2.6b/IpFcRγ-L-expressing cells internalized anti-HA-coated beads significantly more than isotype-coated beads. In addition to this, an unexpected phagocytic response was observed in IpLITR1.1b-expressing cells. An apparent ~15% increase in IpLITR1.1b-mediated phagocytosis over IpLITR2.6b/IpFcRγ-L was observed, which may be in part due to increased surface expression of IpLITR1.1b (Fig. 5.1). Phagocytosis by cells expressing either IpLITR-type was visualized by confocal microscopy, showing the intimate association of internalized beads with lipid-raft containing membranes. Lipid rafts are involved in the activation of lymphocytes and the induction of effector responses, including phagocytosis [155,156]. Further, lipid rafts can localize at the site of phagocytosis in teleost macrophages [157]. Thus, IpLITR-mediated phagocytosis likely involves receptor aggregation at lipid rafts in RBL-2H3 cells, and potentially even catfish immune cells.

There are several possibilities that may explain IpLITR1.1b's unpredicted stimulatory functions in RBL-2H3 cells. Perhaps this receptor associates with an endogenous ITAM-bearing signaling adaptor to indirectly induce stimulatory

signaling. Conversely, perhaps IpLITR1.1b directly initiates signaling using one (or more) of its six cytoplasmic tyrosines. As one of the membrane-proximal tyrosines recruits the inhibitory kinase Csk [3], there is potential for this receptor to recruit other kinases in an ITAM-independent fashion. Examining phagocytosis using IpLITR1.1b with a truncated CYT will determine if this region of the molecule is required. If it is, then generating additional CYT mutants may help narrow down which tyrosines, or at least which regions of the tail are involved in stimulatory signaling and function.

In order to investigate IpLITR1.1b's unexpected ability to phagocytose, I examined its potential to associate with endogenous ITAM-bearing signaling adaptor molecules. Co-immunoprecipitation of IpLITR1.1b showed no association with FcεRI γ subunit even under phosphorylated conditions (i.e. sodium pervanadate treatment), despite showing the direct association of this adaptor with FcεRI α subunit. Other common stimulatory signaling adaptors, DAP10 and DAP12, are not expressed in RBL-2H3 cells. As a broader approach to confirm this receptor's ability to induce phagocytosis is independent of associating with any surface-expressed adaptor molecules, a truncated version was generated, IpLITR1.1b ΔCYT. In the absence of its CYT, IpLITR1.1b ΔCYT is still surface-expressed but failed to induce phagocytosis, indicating a requirement of this receptor's CYT for phagocytosis. To that end, I expressed IpLITR1.2a in RBL-2H3 cells and assessed its ability to phagocytose. IpLITR1.2a encodes a receptor whose CYT resembles the membrane distal region IpLITR1.1b: IpLITR1.2a contains an ITIM at tyrosine 407, an ITSM at tyrosine 433 and an ITIM-like region with a serine substituted for a tyrosine at position 429 [3]. This receptor is also surface-expressed and was shown to induce phagocytosis at levels comparable to IpLITR1.1b. Whether or not IpLITR1.1b ΔCYT or IpLITR1.2a can induce intracellular signaling was not examined in this thesis; however, it is likely that the biochemical mechanism(s) behind IpLITR1.1b's unexpected ability to phagocytose is related to the ability of its membrane-distal region to recruit an as-yet unidentified signaling molecule(s).

Taken together, the notion of an ITIM-bearing immunoregulatory receptor capable of inducing stimulatory signaling and inhibitory effector responses suggests a functional duality among certain immunoregulatory receptors that cannot simply be predicted by the presence of the canonical signaling motifs, ITAMs and ITIMs. As in the case of IpLITR1.1b, this functional plasticity may be context-dependent, resulting from differential availability of signaling molecules between RBL-2H3 cells (myeloid cells) and mouse NK cells (lymphoid cells).

In a broader context, IpLITR1.1b-mediated dual functionality raises several important questions. First, is this dual function real or an artefact of our expression system? There are limitations of using mammalian immune cell lines, which only provides potential signaling and functional information of these receptor types. However, given the lack of monoclonal antibodies and ligands against these receptors as well as an incomplete idea of IpLITR expression across different catfish immune cell lines, the use of these alternative strategies can still be useful to examine receptor signaling and function. Additionally, the Phospho-MAPK signaling and Rat Cytokine Arrays (R&D Systems) as well as phospho-specific antibodies against select signaling molecules are not available for fish signaling kinases or cytokines, thus conducting these broad approaches into IpLITR-mediated effector responses and preceding signaling events can effectively be conducted using mammalian immune cells. While the RBL-2H3 system provides us with essential clues into IpLITR function, these results remain to be confirmed using fish immune cell lines.

To that end, a second important question into IpLITR-mediated functional plasticity raised is, do catfish immune cells use dual-functional receptors to become activated or inhibited in different contexts? Lending support to this is the emergence of ITIM-bearing immunoregulatory receptors in other animals, capable of stimulating effector responses. For example, the ITIM-containing inhibitory receptor FcγRIIB recruits SHP phosphatases to inhibit immune cell responses [33,158], but this protein also stimulates phagocytosis of the parasite *Toxoplasma*

gondii [159]. Porcine FcγRIIB also appears to enhance IFNα and TNFα mRNA levels of porcine pulmonary alveolar macrophages, suggestive of an antiviral immune response, in response to porcine respiratory and reproductive syndrome virus [160]. Immune receptor expressed by myeloid cell (IREM)-1 (CD300f) encodes ITIMs in its CYT that can recruit SHP to inhibit FcεRI-mediated degranulation in RBL-2H3 cells [161]. However, mutating the ITIM tyrosines and engaging this receptor alone can also induce degranulation, which was likely mediated by binding p85α regulatory subunit of PI3K [161]. Leukocyte mono-Ig-like receptor (LMIR)-3, the mouse homolog of IREM-1, also encodes ITIMs and can inhibit FcεRI-mediated cytokine secretion in bone-marrow derived mast cells [162]. This receptor was also reported to bind PI3K p85α subunit and cross-linking of this receptor alone induced IL-6 production, mediated by its association with FcεRI γ subunit [162]. Platelet endothelial cell adhesion molecule (PECAM)-1 is another ITIM-bearing receptor that can promote or inhibit functions such as integrin activation and cell survival in immune cells as well as activation in response to fluid shear stress in endothelial cells [163]. Another ITIM-encoding receptor is the killer cell Ig-like receptor (KIR) 2DL4, that is capable of inhibiting NK cell-mediated cellular cytotoxicity or inducing it as well as interferon (IFN)-γ secretion via its association with FcRγ subunit [164–168]. Overall, these findings demonstrate stimulatory capacities among several immunoregulatory receptors, predicted to be inhibitory based on the presence of cytoplasmic ITIMs. These findings also reveal functional plasticity among some immunoregulatory receptors: the ability of a single receptor to activate or inhibit different immune effector functions may provide an additional regulatory mechanism in coordinating appropriate immune responses to infection. As IpLITR1.1b-mediated inhibition was observed presumably during allogeneic recognition; and IpLITR1.1b-mediated activation was observed during phagocytosis; then perhaps IpLITRs mediate different immune cellular events in response to different classes of immune insults (i.e. alloantigen challenge or bacterial challenge, respectively). Ultimately, however, these functional studies need to be explored using catfish immune cells and IpLITR-specific antibodies.

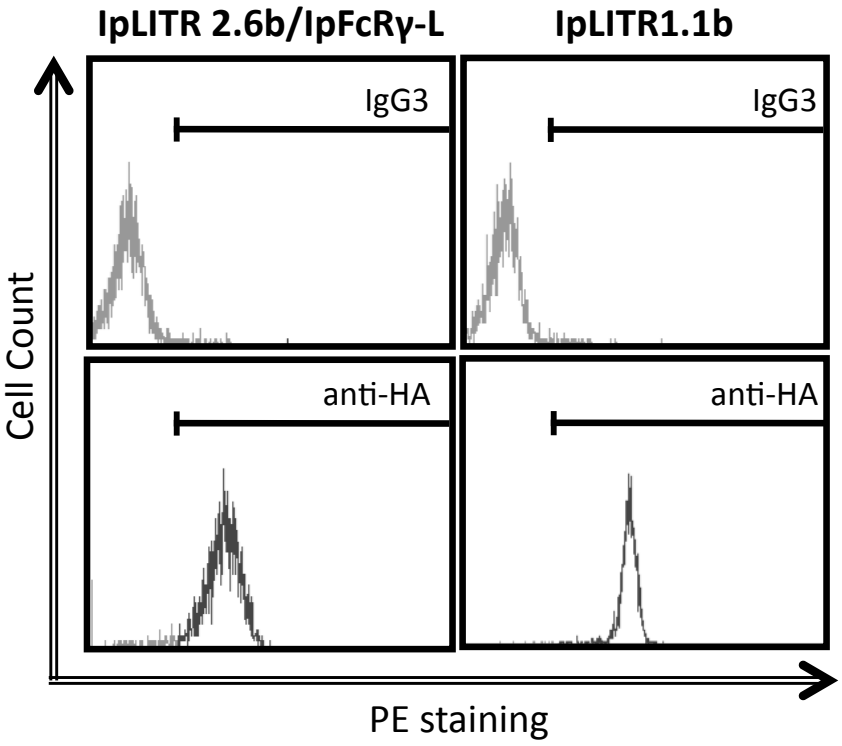

Figure 5.1. Surface expression of HA epitope-tagged IpLITR constructs in RBL-2H3 cells. Detection of the cell surface expression of IpLITR2.6b/ IpFcRγ-L (left panels) and IpLITR1.1b (right panels) in RBL-2H3 after flow cytometric staining. RBL-2H3 cells were stained with 20 μg/mL anti-HA mAb (lower panels) or 20 μg/mL IgG3 (isotype control; upper panels) followed by staining with 10 μg/mL PE-conjugated goat anti-mouse IgG (H+L). Surface expression was then detected as an increase in fluorescence (i.e. PE staining captured in the FL-2 channel) in comparison with IgG3-stained cells.

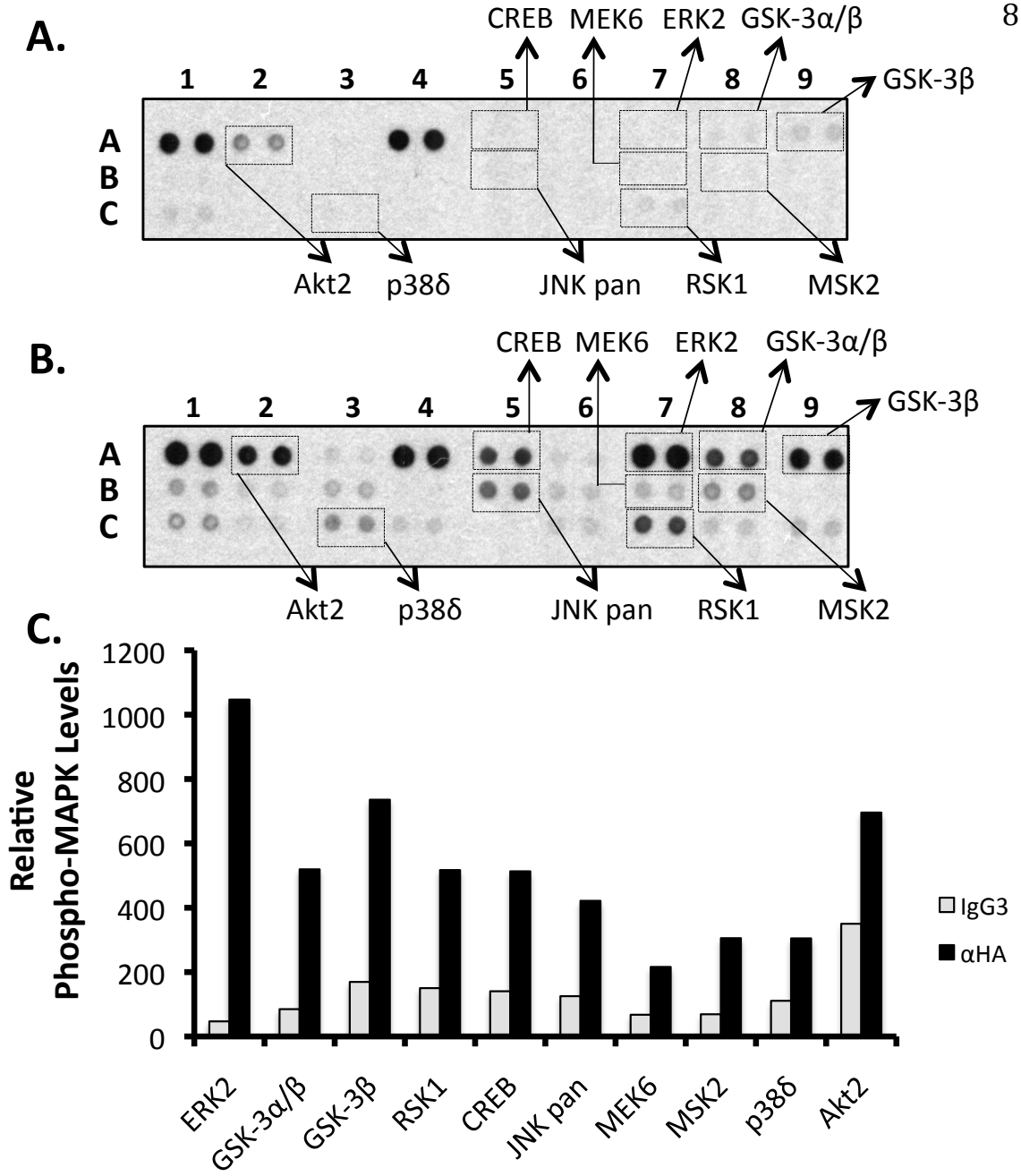

Figure 5.2. Parallel examination of the relative amounts of MAPK and other serine/threonine kinase phosphorylation levels induced by IpLITR2.6b/IpFcRγ-L cross-linking. RBL-2H3 cells ($2.5x10^6$) expressing IpLITR2.6b/IpFcRγ-L were activated by treatment with 0.625 μg/mL anti-HA mAb or 0.625 μg/mL mouse IgG3 control followed by 1.25 μg/mL goat anti-mouse IgG3 for 10 min at 37°C. Cell lysates were then examined for the presence of phosphorylated proteins as described in Section 3.16. Representative proteome profiler array result for (A) IgG3 treatment and (B) anti-HA cross-linking are shown. (C) Calculated densitometry results for (A) and (B). Duplicate spots used for calculating the relative levels of protein phosphorylation are indicated with hatched boxes, and these values were normalized for cross-array comparisons using manufacturer's negative and positive control standards. Each bar represents the experimental mean from two independent experiments.

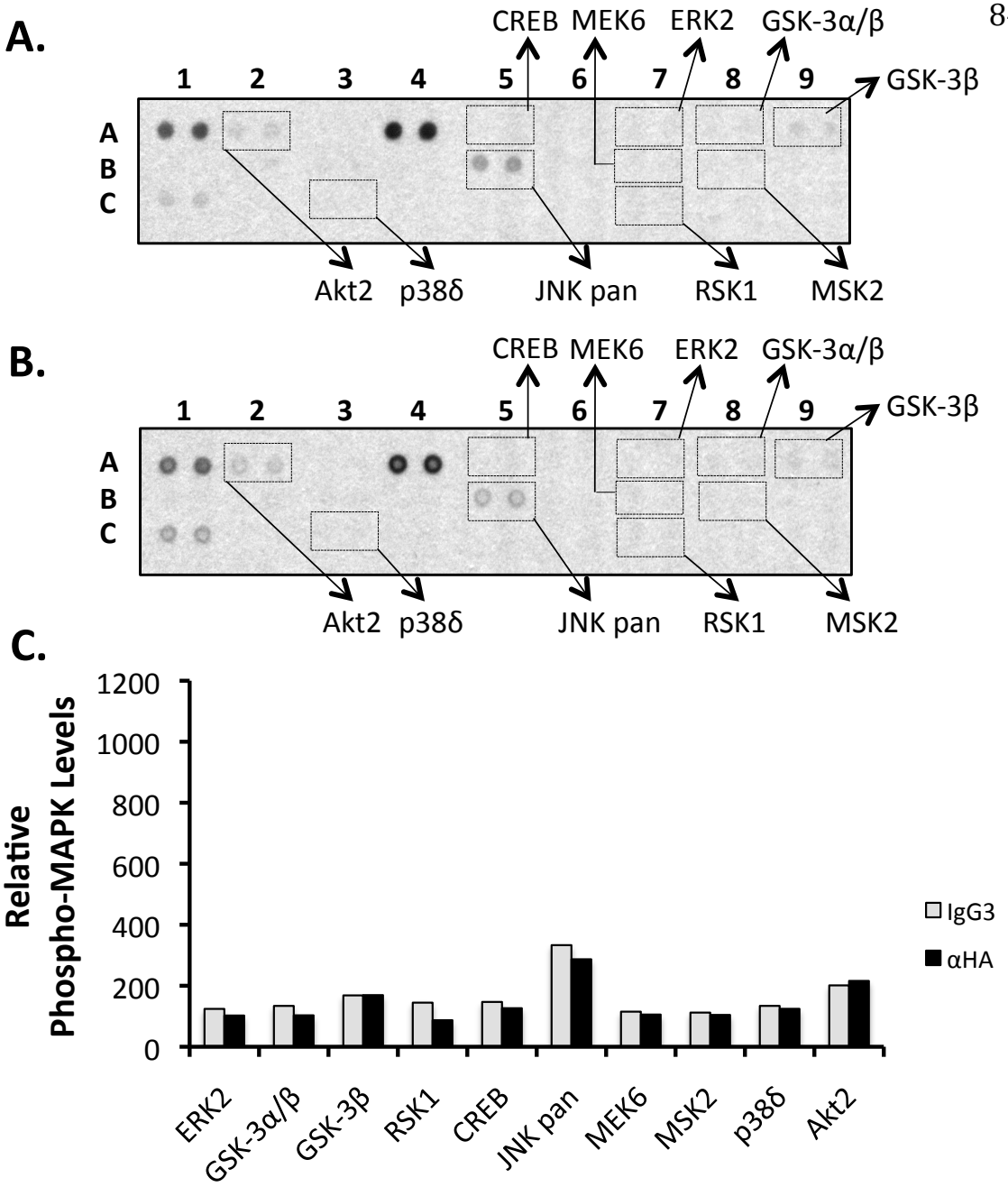

Figure 5.3. Parallel examination of the relative amounts of MAPK and other serine/threonine kinase phosphorylation levels induced by IpLITR1.1b cross-linking. RBL-2H3 cells ($2.5x10^6$) expressing IpLITR1.1b were with cross-linked with 0.625 μg/mL anti-HA mAb of 0.625 μg/mL mouse IgG3 control followed by 1.25 μg/mL anti-mouse IgG3 pAb (H+L) treatment for 10 min at 37°C. Cell lysates were then examined for the presence of phosphorylated proteins as described in Section 3.16. Representative proteome profiler array result for (A) IgG3 treatment or (B) anti-HA cross-linking are shown. (C) Calculated densitometry results are depicted, as described in Figure 5.4 (C).

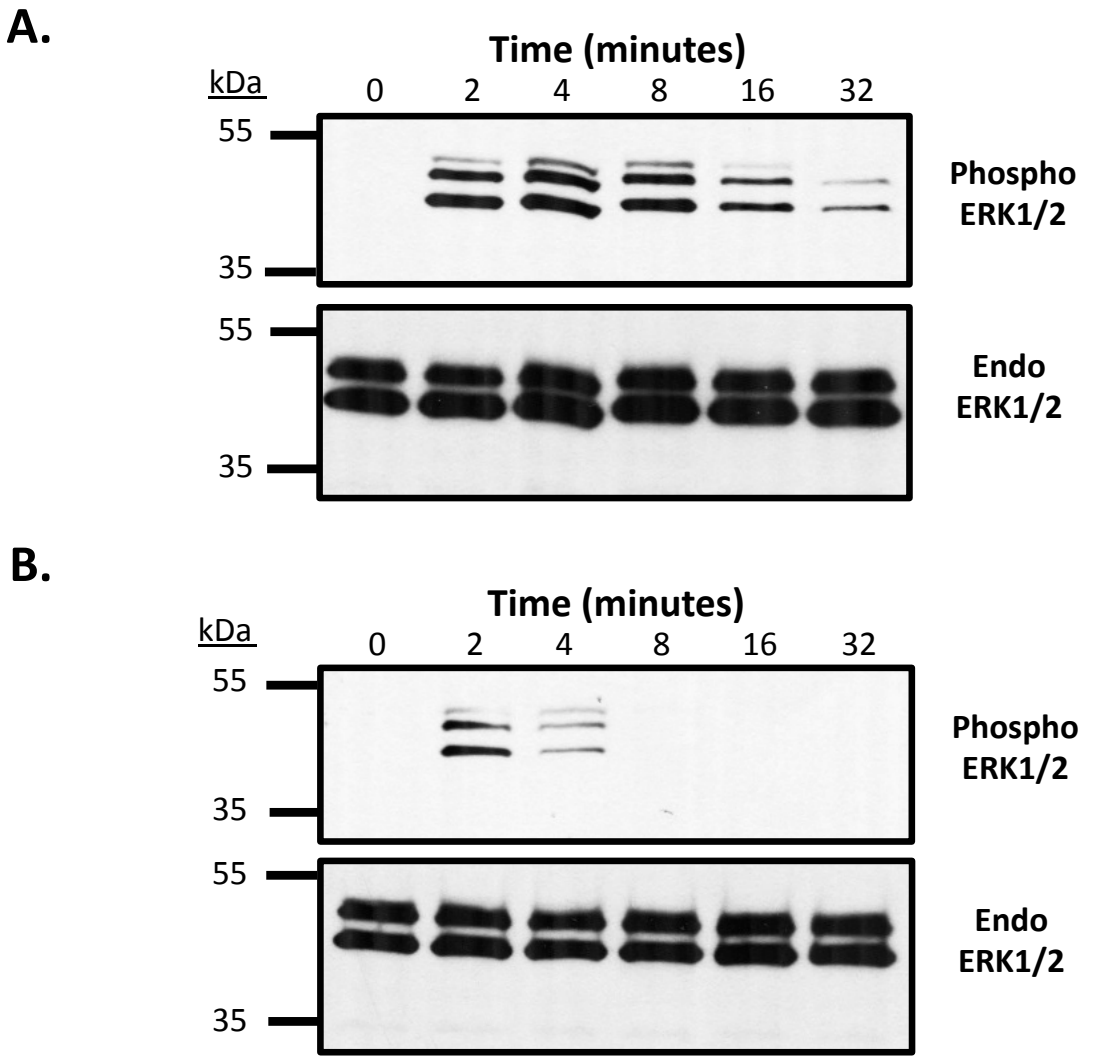

Figure 5.4. Examination of extracellular signal-related kinase (ERK) 1/2 activation by IpLITR engagement in RBL-2H3 cells. RBL-2H3 cells ($2.5x10^6$) expressing IpLITR2.6b/IpFcRγ-L (A) or IpLITR1.1b (B) were cross-linked by treatment with 0.625 μg/mL anti-HA mAb followed by 1.25 μg/mL anti-mouse IgG3 pAb (H+L) for 0, 2, 4, 8, 16, and 32 min at 37°C. Samples were separated on an 8% SDS-PAGE gel under reducing conditions, transferred to nitrocellulose and blots were probed with either the anti-phospho ERK1/2 (1:2000 v/v) mouse mAb or anti-ERK1/2 mouse mAb ("endo"; 1:2000 v/v) followed by a goat anti-mouse IgG (H+L) HRP-conjugated pAb (1:5000 v/v). Results presented are from a representative of two independent experiments that gave similar results.

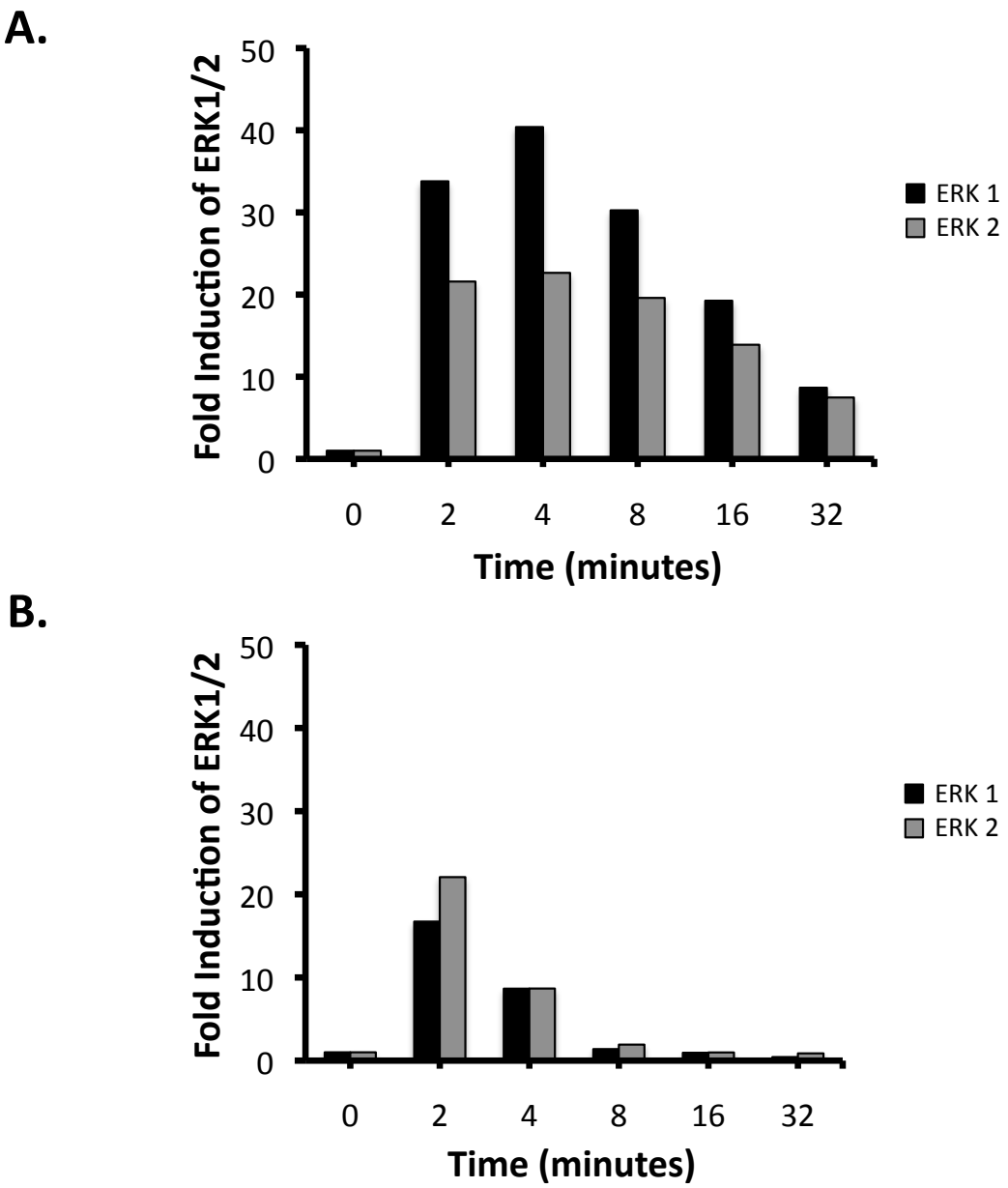

Figure 5.5. Fold induction of ERK1/2 activation by IpLITR engagement in RBL-2H3 cells. Changes in phospho-ERK1/2 levels upon IpLITR2.6b/ IpFcRγ-L (A) or IpLITR1.1b (B) engagement from the blots shown in Fig. 5.4 are reported as a fold induction value relative to the untreated RBL-2H3 cells (i.e. 0 min), which was normalized to a value of 1.0 using the equation below. All phospho ERK1/2 band intensity levels were corrected based on the endogenous expression levels of ERK1/2 (i.e. endo) as follows: [(phospho ERK1 densitometry value for # min/endo ERK1 value for # min) * 100]. This value was then divided by the calculated relative fold induction value of ERK1 expression obtained for untreated cells (0 min) and is shown as the black histogram bars. The grey histogram bars represent the relative fold induction values of phospho ERK2 expression in each lane calculated using the same equation but using the phospho and endo ERK2 values instead. Results presented are from a representative of two independent experiments that gave similar results.

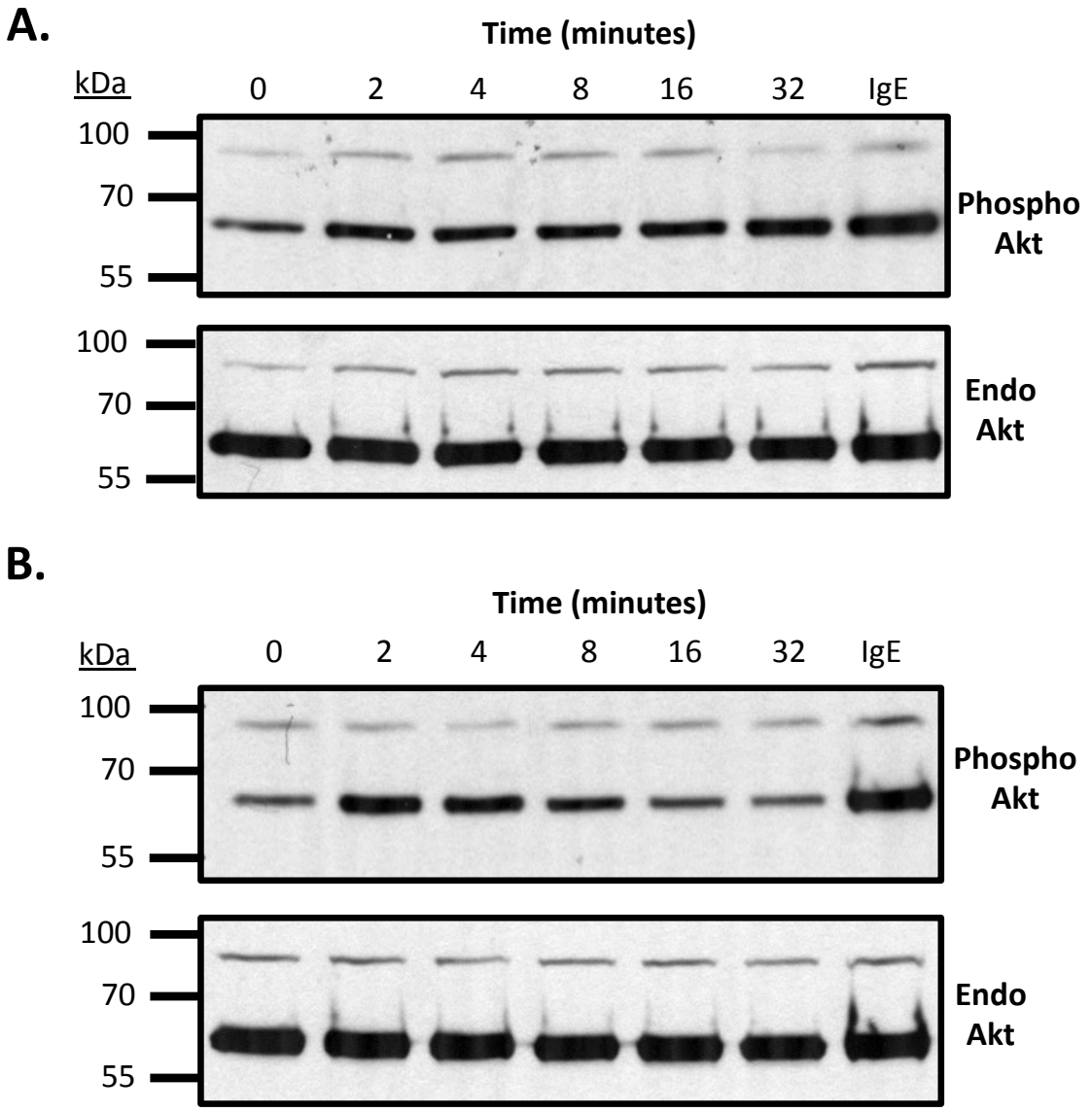

Figure 5.6. Examination of Akt activation by IpLITR engagement in RBL-2H3 cells. RBL-2H3 cells ($2.5x10^6$) expressing IpLITR2.6b/IpFcRγ-L (A) or IpLITR1.1b (B) were cross-linked by treatment with 0.625 μg/mL anti-HA mAb followed by 1.25 μg/mL anti-mouse IgG3 pAb (H+L) for 0, 2, 4, 8, 16, and 32 min at 37°C. Cells were also activated by triggering endogenous FcεRI with 200 ng/mL anti-DNP IgE sensitization and 0.1 ng/mL DNP-HSA crosslinking for 4 min. Samples were separated on an 8% SDS-PAGE gel under reducing conditions, transferred to nitrocellulose and duplicate blots were probed with either anti-phospho-Akt rabbit mAb (1:1000 v/v) or anti-Akt rabbit pAb ("endo"; 1:1000 v/v) followed by a goat anti-mouse IgG (H+L) HRP-conjugated pAb (1:5000 v/v). Results presented are from a representative of two independent experiments that gave similar results.

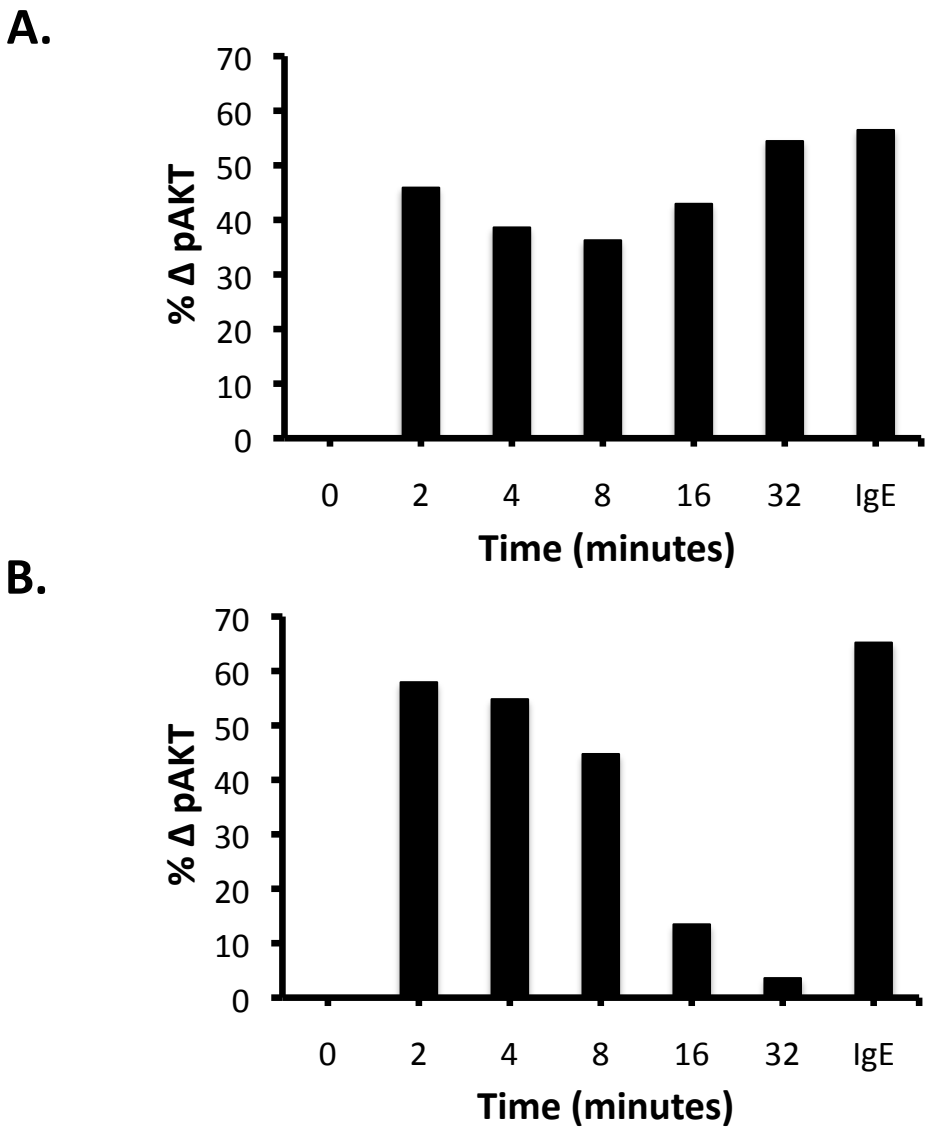

Figure 5.7. Percent change Akt activation by IpLITR engagement in RBL-2H3 cells. Phospho Akt band intensity levels after IpLITR2.6b/IpFcRγ-L (A) or IpLITR1.1b (B) engagement from the blots shown in Fig. 5.6 were corrected for endogenous Akt levels using the following equation: [(phospho Akt densitometry value for # min / endo Akt value for # min)*100]. This corrected value was then converted into a percent change in phospho Akt values or % Δ pAkt as follows: [(1-(0 min corrected phospho Akt value / corrected phospho Akt value for time point)*100]. The data displayed in the bar graphs on the right represent these calculated % Δ phospho Akt values. Results presented are from a representative of two independent experiments that gave similar results.

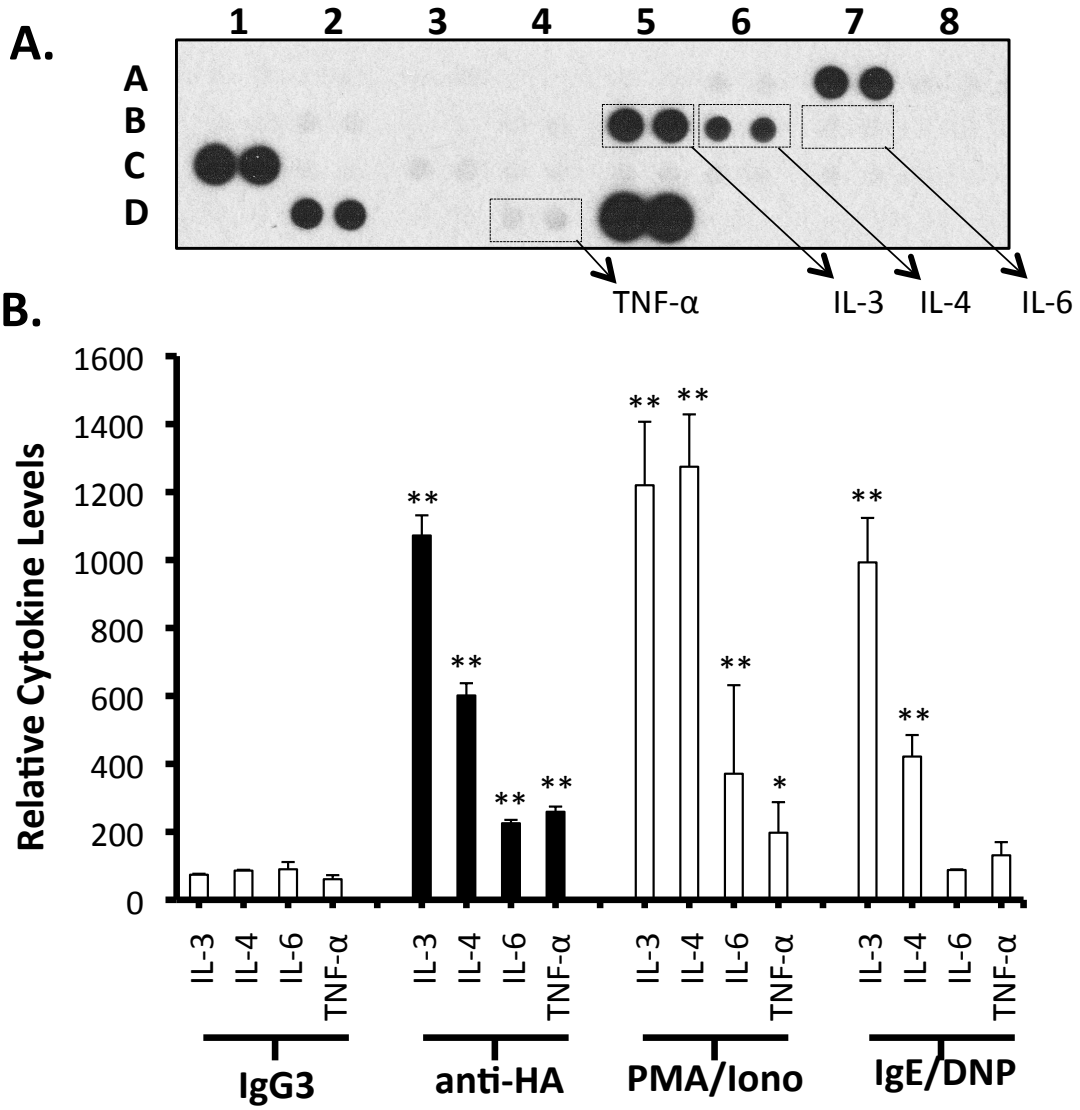

Figure 5.8. Parallel examination of the relative amounts of cytokine levels produced by IpLITR2.6b/IpFcRγ-L-activated RBL-2H3 cells. RBL-2H3 cells ($2.5x10^6$ cells) expressing IpLITR2.6b/IpFcRγ-L were sensitized with 0.625 μg/mL anti-HA mAb or 0.625 μg/mL mouse IgG3 (isotype) followed by crosslinking with 1.25 μg/mL goat anti-mouse IgG3 pAb (H+L). Cells were also treated with 50 ng/mL PMA and 0.5 μM Ca^{2+} ionophore A23187 or with 200 ng/mL anti-DNP IgE and 0.1 ng/mL DNP-HSA stimulation. Cells were incubated for 24hrs at 37°C prior to collection of the supernatants for detection of cytokine levels as described in Section 3.15. (A) A representative proteome profiler array result for anti-HA cross-linked IpLITR 2.6b/IpFcRγ-L is shown. (B) Calculated densitometry results obtained from the duplicate spots are depicted. The duplicate spots used for calculating relative cytokine levels are indicated with hatched boxes. These values were normalized for cross-array comparisons using manufacturer's negative and positive controls standards. Each bar represents the mean relative cytokine levels ± SEM of three independent experiments. **P<0.001; *P<0.05, when comparing stimulated cells to the corresponding cytokine levels of cells treated with IgG3.

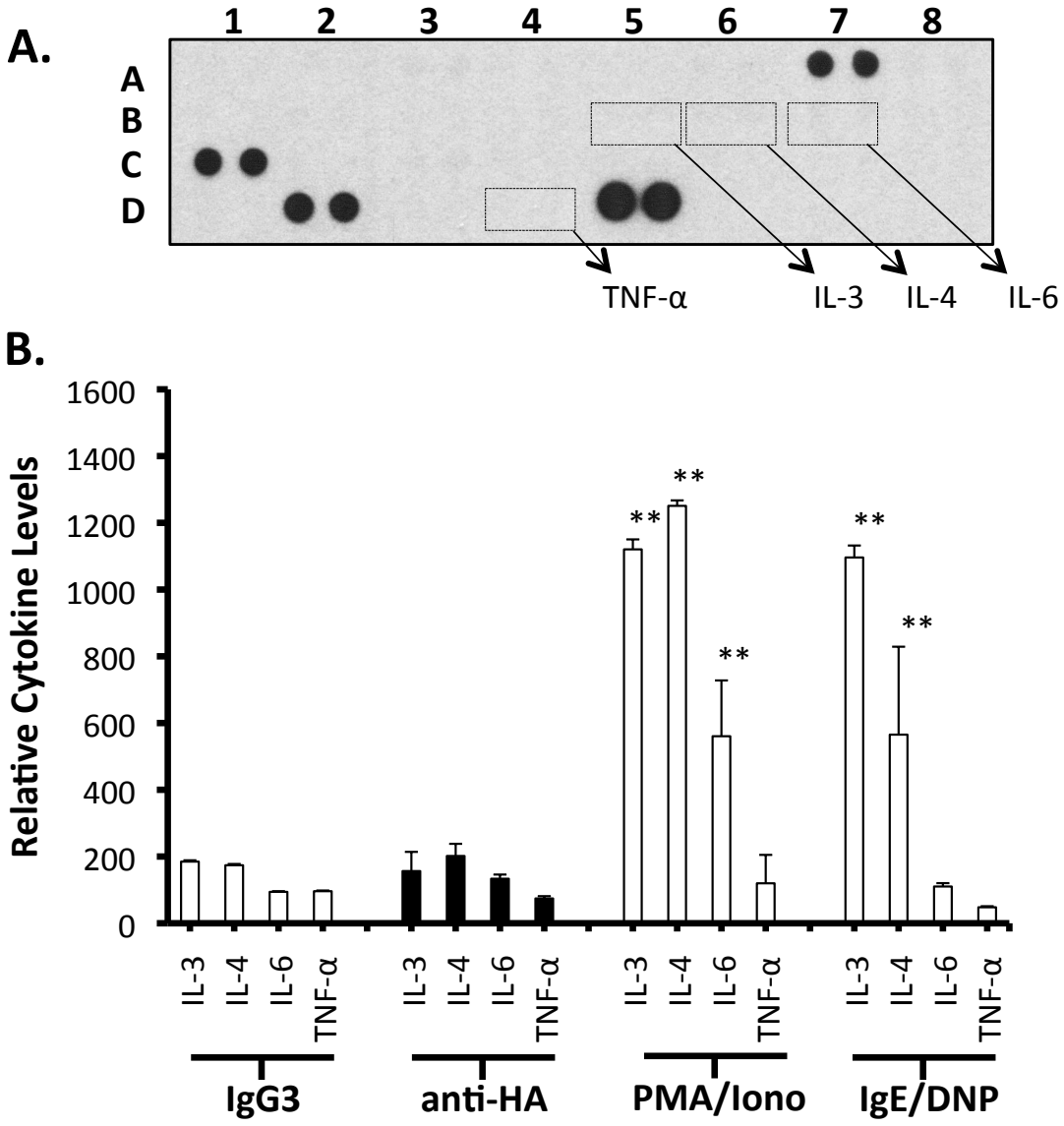

Figure 5.9. Parallel examination of the relative amounts of cytokine levels produced by IpLITR1.1b-activated RBL-2H3 cells. RBL-2H3 cells (~2.5x10^6 cells) expressing IpLITR1.1b were treated as in Figure 5.8. (A) A representative proteome profiler array result for anti-HA cross-linked IpLITR1.1b is shown. (B) Calculated densitometry results obtained from the duplicate spots are depicted, as described in Figure 5.3 (B).

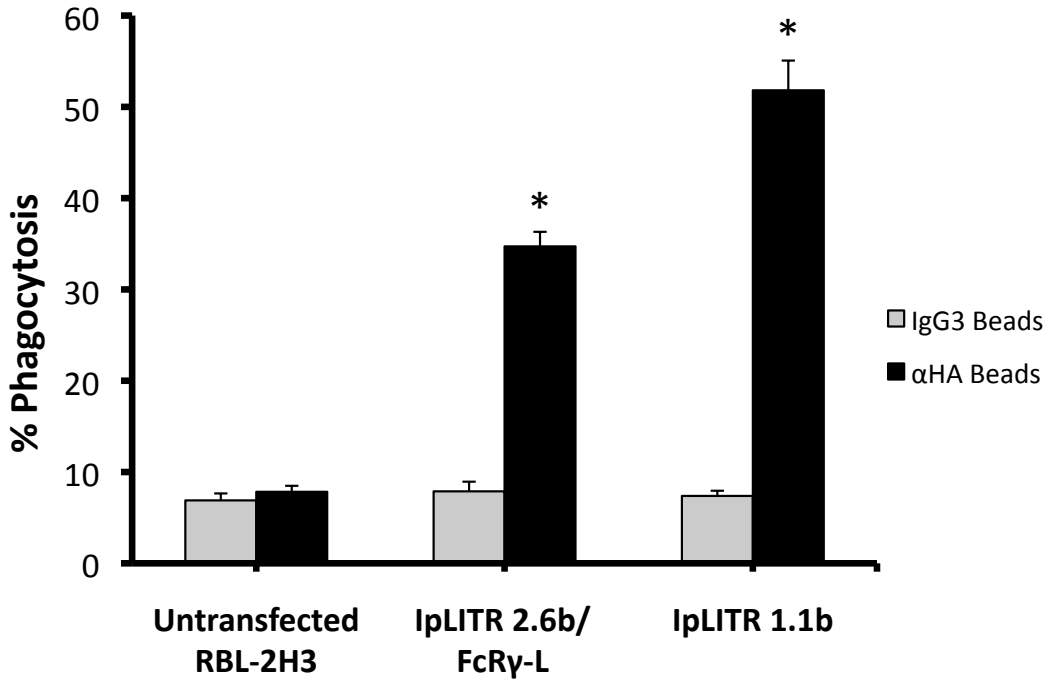

Figure 5.10. IpLITR-mediated phagocytosis of antibody-coated microspheres.
Transfected RBL-2H3 cells were incubated with IgG3 isotype- or anti-HA mAb-coated 4.5 μm YG beads for 30 mins at 37°C. Using a flow cytometric based phagocytosis assay described in Section 3.14, the % phagocytosis by untransfected RBL-2H3 cells, IpLITR2.6b/IpFcRγ-L-expressing cells, and IpLITR 1.1b-expressing cells was determined. Each bar represents the mean % phagocytosis value ± SEM for six independent experiments that were performed. *$p \leq 0.001$ when comparing the % phagocytosis of anti-HA beads vs. IgG3 beads for each group.

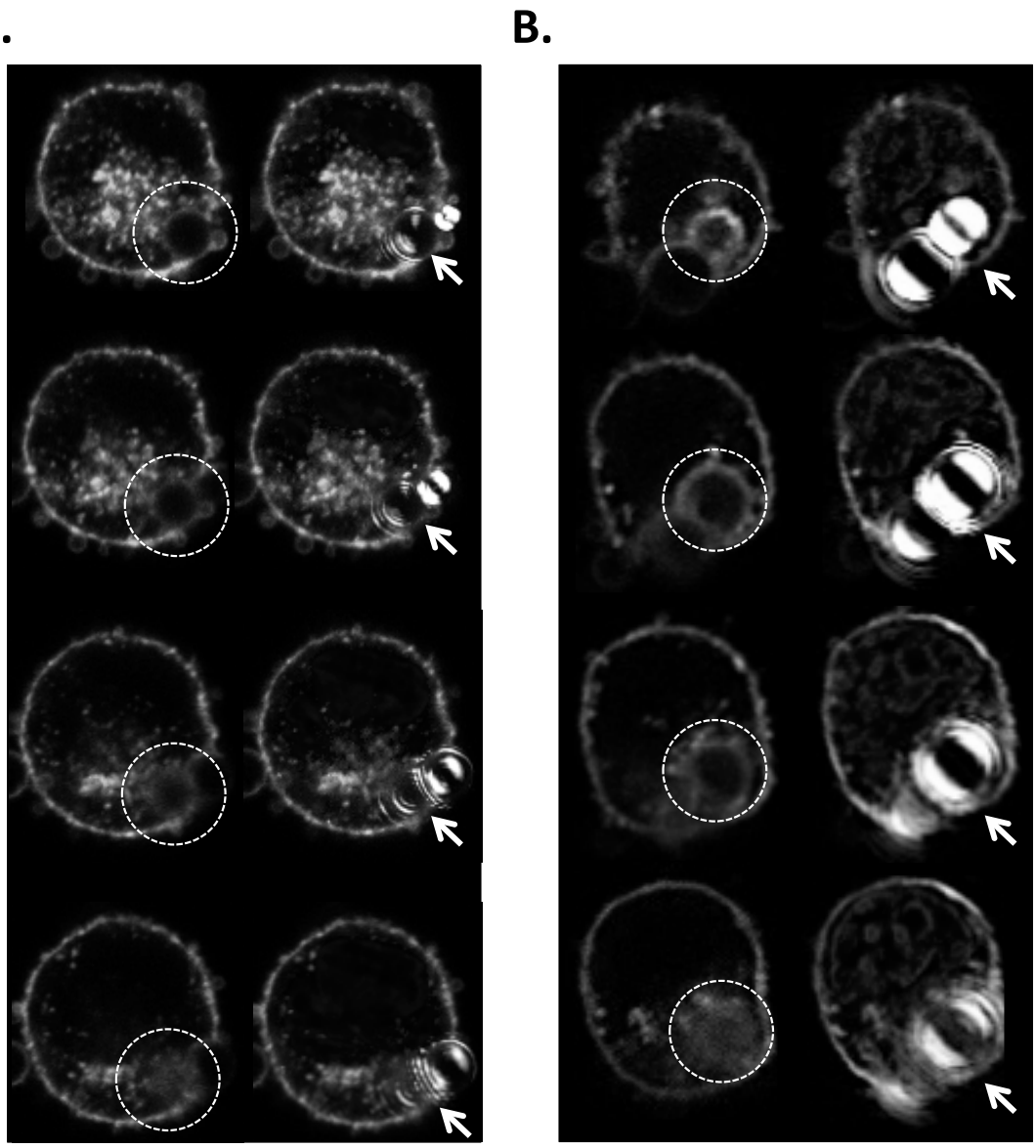

Figure 5.11. Confocal cross-section of IpLITR-expressing RBL-2H3 cells undergoing phagocytosis of an opsonized microsphere. Representative IpLITR2.6b/IpFcRγ-L (A)- or IpLITR1.1b (B)-expressing RBL-2H3 cells internalizing 4.5 μm anti-HA coated microspheres. Each consecutive image from top to bottom represents serial confocal Z-stack images of the same cell. Indicated with a hatched circle or arrow are the locations of phagocytosed beads. These fluorescence confocal images are also stained with 1.5 μg/mL DAPI and the FITC-cholera toxin B subunit.

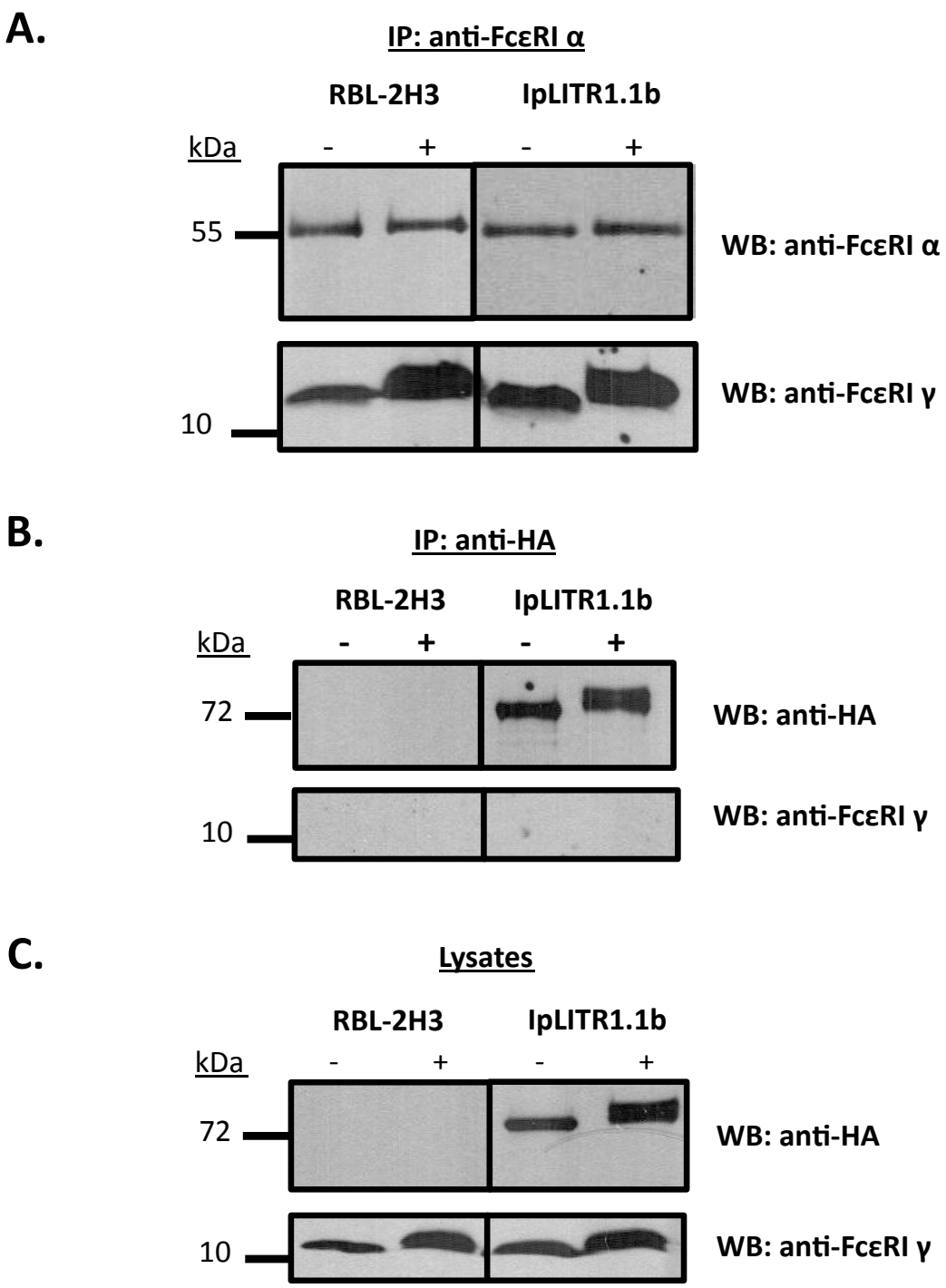

Figure 5.12. Lack of association between IpLITR1.1b and the FcεRI γ chain. Untransfected RBL-2H3 cells and cells expressing IpLITR 1.1b (~2.5x10^6) were treated with (+) or without (-) 0.1 mM Na_3VO_4 then lysed and immunoprecipitated with either 1 μg anti-FcεRI α subunit mouse mAb (A) or 1 μg anti-HA mAb (B). Immunoprecipitated samples (A, B) or cell lysates (C) were separated on an 8% or 10% SDS-PAGE gel under reducing conditions, transferred to nitrocellulose and duplicate blots were then blotted with anti-FcεRI α subunit rabbit pAb (1:1000 v/v) or anti-FcεRI γ subunit rabbit pAb (1:2000 v/v) followed by a goat anti-mouse IgG (H+L) HRP-conjugated pAb (1:5000 v/v); or an HRP-conjugated anti-HA pAb, as indicated.

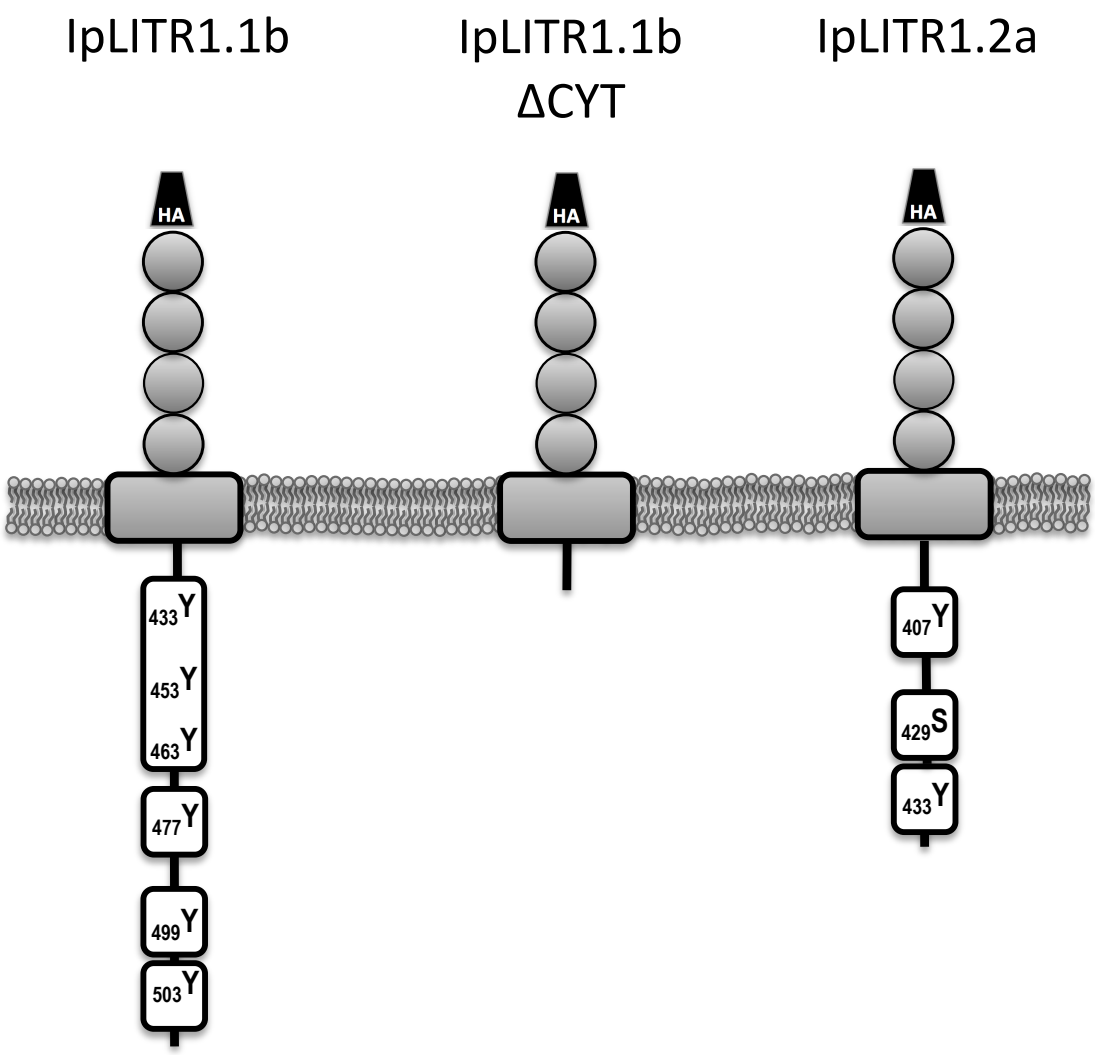

Figure 5.13. Schematic of HA-tagged IpLITR1.1b and variant constructs used in this chapter. (A) N-terminal HA epitope-tagged 'wildtype' IpLITR1.1b (GenBank Accession #ABI16050.1). Tyrosines 477 and 499 are in ITIMs. Tyrosine 503 is in an ITSM. Tyrosine 453 is required for Csk binding. (B) N-terminal HA epitope-tagged IpLITR1.1b ΔCYT, devoid of cytoplasmic tyrosines. (C) N-terminal HA epitope-tagged 'wildtype' IpLITR1.2a (#ABI16051.1). Tyrosine 407 is in an ITIM. Amino acids upstream and downstream of serine 429 match that of tyrosine 499 in IpLITR1.1b. Tyrosine 433 is in an ITSM.

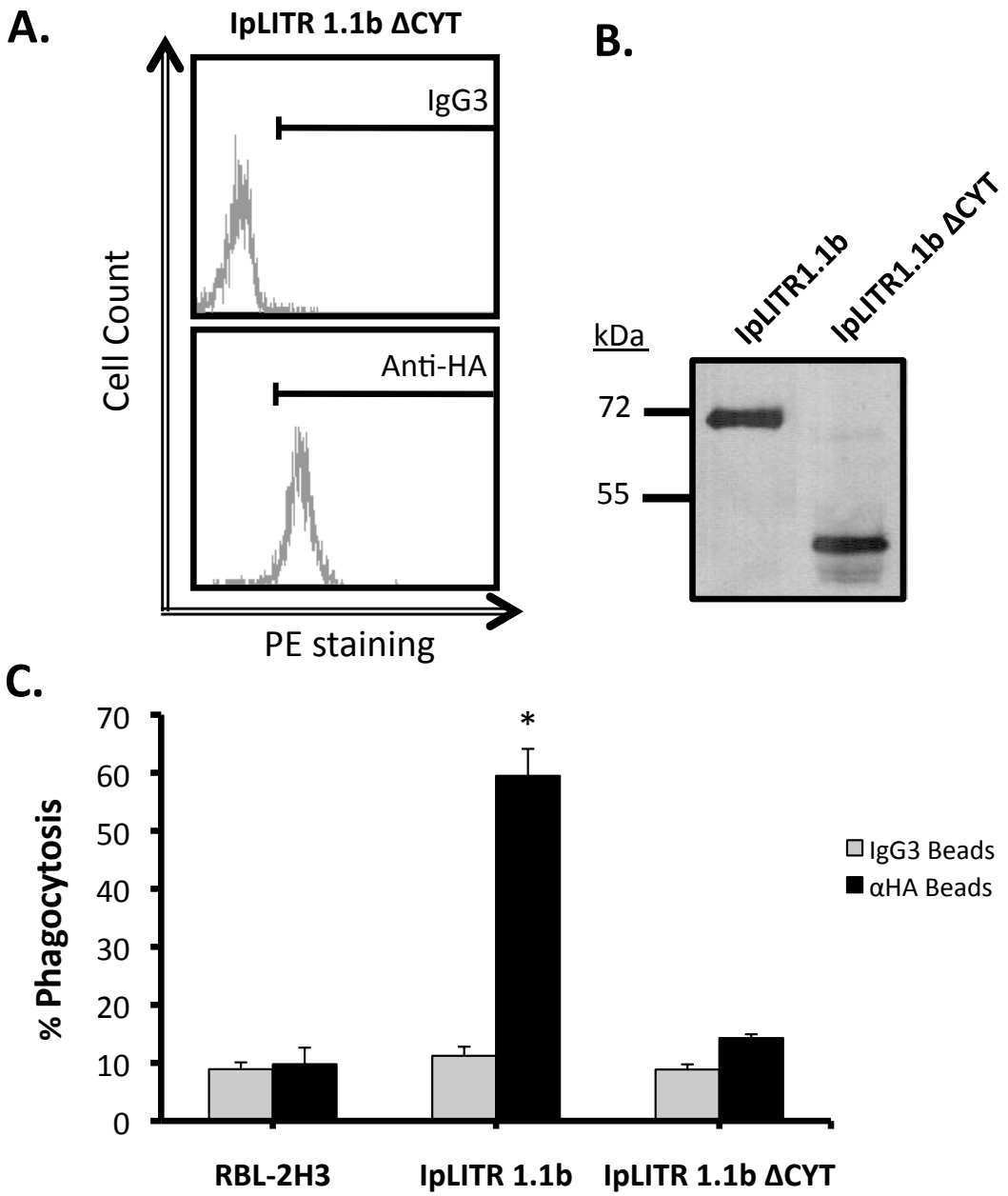

Figure 5.14. Requirement of IpLITR1.1b cytoplasmic region for phagocytosis. (A) Surface expression of IpLITR1.1bΔCYT in RBL-2H3 cells after flow cytometric staining with 20 µg/mL anti-HA mAb or 20 µg/mL IgG3 (isotype) followed by staining with 10 µg/mL PE-conjugated goat anti-mouse IgG (H+L). Surface expression was then detected as an increase in fluorescence (i.e. PE staining captured in the FL-2 channel) in comparison with IgG3-stained cells. (B) Lysates of transfected cells were separated on an 8% SDS-PAGE gel under reducing conditions, transferred to nitrocellulose and blotted with HRP-conjugated anti-HA pAb (1:1000 v/v). (C) Transfected cells were incubated with IgG3 isotype- or anti-HA mAb-coated 4.5 µm YG beads for 30 mins at 37°C. Using a flow cytometric based phagocytosis assay, the % phagocytosis was determined. Each bar represents the mean % phagocytosis value ± SEM for 3 independent experiments that were performed. *$p \leq 0.001$ when comparing the % phagocytosis of anti-HA beads vs. IgG3 beads for each group.

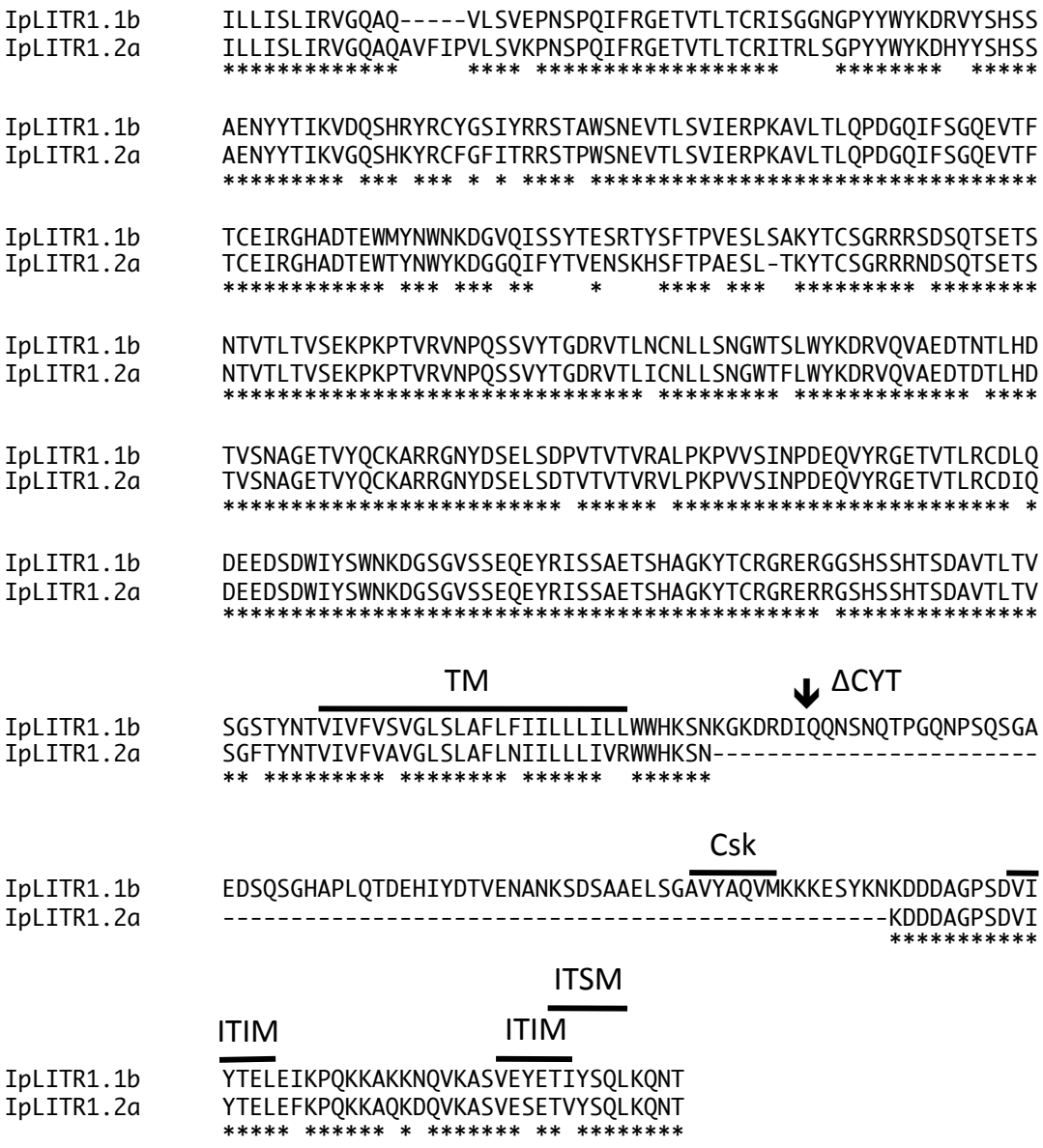

Figure 5.15. Sequence alignment of IpLITR1.1b and IpLITR1.2a. Amino acid sequences of IpLITR1.1b (#ABI16050.1) and IpLITR1.2a (#ABI16051.1) were aligned using Clustal Omega software (http://www.ebi.ac.uk/Tools/msa/clustalo/). (*) represents the same amino acid at that position in both sequences and (-) represents the absence of an amino acid, at that position. The TM overlined in black represents the transmembrane region of both protein sequences. Csk represents the tyrosine implicated in Csk-binding in NK cells. ITIM represents a tyrosine embedded in motifs that share similarities to canonical immunoreceptor tyrosine-based inhibitory motifs (ITIMs). ITSM represents an immunoreceptor tyrosine-based switch motif. '↓' indicates the location of the premature stop codon used to generate IpLITR1.1b ΔCYT.

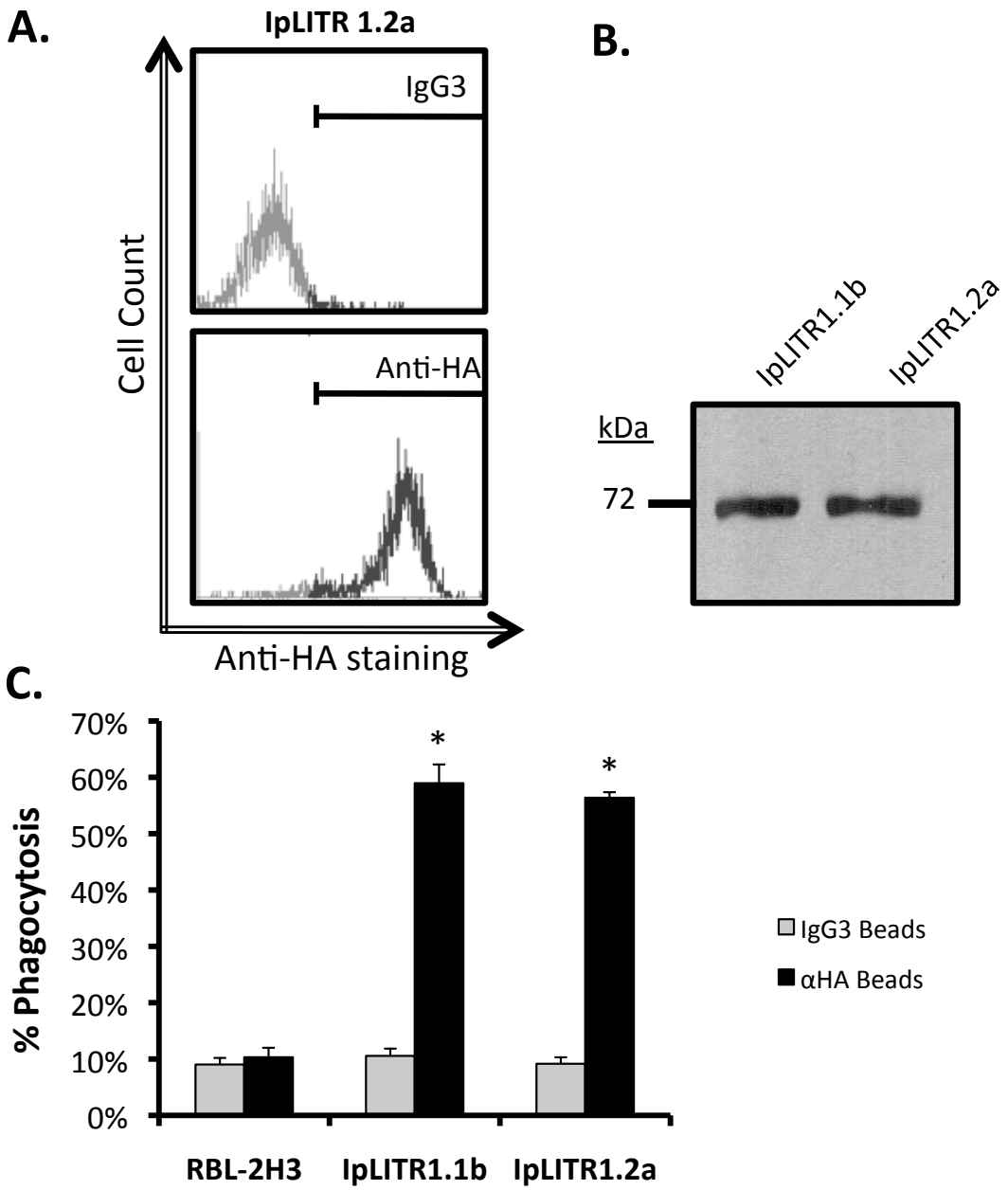

Figure 5.16. Requirement of IpLITR1.1b membrane-distal region for phagocytosis. (A) Cell surface expression of IpLITR1.1b1.2a in RBL-2H3 cells after flow cytometric staining with 20 µg/mL anti-HA mAb or 20 µg/mL IgG3 (isotype) followed by staining with 10 µg/mL PE-conjugated goat anti-mouse IgG (H+L). Surface expression was then detected as an increase in fluorescence (i.e. PE staining captured in the FL-2 channel) in comparison with IgG3-stained cells. (B) Lysates of transfected cells were separated on an 4-20% SDS-PAGE gel under reducing conditions, transferred to nitrocellulose and blotted with HRP-conjugated anti-HA pAb (1:1000 v/v). (C) Transfected cells were incubated with IgG3 isotype- or anti-HA mAb-coated 4.5 µm YG beads for 30 mins at 37°C. Using a flow cytometric based phagocytosis assay, the % phagocytosis was determined. Each bar represents the mean % phagocytosis value ± SEM for 3 independent experiments performed. *$p \leq 0.001$ when comparing the % phagocytosis of anti-HA beads vs IgG3 beads for each group.

CHAPTER 6

General Discussion and Conclusions

6.1 Summary of findings

The discovery of the IpLITR family of proteins has presented an important contribution in the characterization of immunoregulatory receptors expressed in teleost [1]. IpLITR-types share structural characteristics with mammalian receptors that activate immune effector responses and/or suppress them. Previous studies in IpLITR-types demonstrated that stimulatory IpLITR2.6b associates with the ITAM-bearing signaling adaptor IpFcRγ-L in HEK 293T cells [4]. In order to examine the signaling and functional consequences of this receptor-adaptor association, I generated a chimeric construct, IpLITR2.6b/IpFcRγ-L and expressed it in RBL-2H3 cells, a mammalian immune cell line. Engaging of this receptor-adaptor construct successfully induced signaling, degranulation and phagocytosis of opsonized microbeads in an ITAM-dependent fashion. I also expressed IpLITR1.1b, a previously characterized ITIM-bearing inhibitory receptor [2,3] in RBL-2H3 cells. Interestingly, while this receptor induced the transient phosphorylation of stimulatory signaling kinases, it did not induce cytokine secretion, whereas IpLITR2.6b/IpFcRγ-L could. Surprisingly, IpLITR1.1b induced a very potent phagocytic response. This was unlikely due to an association with endogenous FcεRI γ subunit; however an intact IpLITR1.1b CYT was required for phagocytosis. To determine which region the CYT was responsible, phagocytosis induced by IpLITR1.2a was examined, as this receptor encodes a CYT similar to the membrane-distal region of IpLITR1.1b, encoding tyrosines within an ITIM, ITIM-like and ITSM. IpLITR1.2a was also capable of phagocytosis, thus further biochemical studies focusing on this region of IpLITR1.1b's CYT will help elucidate the mechanisms behind this unexpected stimulatory function.

6.1.1 Signaling and functional characterization of a stimulatory IpLITR-type and associated adaptor

The stimulatory IpLITR-type, IpLITR2.6b, associated with channel catfish homologs to the ITAM-bearing signaling adaptors FcRγ and FcRγ-L [4]. The association of a stimulatory receptor-type and an ITAM-bearing receptor is typical of immunoregulatory receptors in mammals [42]; however, until now, the functional consequences of this stimulatory IpLITR with its ITAM-bearing adaptor were unknown. Thus to examine the signaling and functional potential of this receptor and adaptor, I generated a chimeric construct containing the two extracellular Ig domains of IpLITR2.6b fused with the TM and CYT of IpFcRγ-L. As adaptors and stimulatory receptors associate through oppositely charged TM segments [42], I introduced a D → A mutation in the TM, neutralizing it, to prevent any potential associations with other surface receptors. I also generated a construct with the ITAM tyrosines mutated to phenylalanines to 'knock out' the ITAMs. I then stably expressed these receptor-adaptor chimeric constructs in the myeloid cell line RBL-2H3. In order to examine their induction of signaling and effector functions, I engaged the chimeric constructs with epitope-specific mAb. Cross-linking this receptor/adaptor chimera with anti-HA mAb induced the phosphorylation of ERK1/2, in an ITAM-dependent manner. Typically, phosphorylation of ERK1/2 is observed in many ITAM-driven events, and is observed in the activation of immune effector responses [32]. ERK1/2 activation was also observed when stimulating RBL-2H3 cells through the endogenously expressed FcεRI.

As signaling precedes function, the role of IpLITR2.6b/IpFcRγ-L-mediated signaling events in inducing effector responses, specifically degranulation, was examined using a flow cytometry-based Annexin V-FITC staining assay [129] as well as a microplate-based β-hexosaminidase release assay [128]. Degranulation was observed in response to IpLITR-engagement using both assays. The response was

also dependent upon the presence of intact ITAMs. The ability for the stimulatory IpLITR to induce degranulation provides insights into its potential role in inducing similar effector responses in catfish leukocytes. The use of pharmacological inhibitors against specific signaling kinases also provided information as to the identity of the signaling molecules likely recruited during IpLITR2.6b/IpFcRγ-L-mediated degranulation. From this, it was determined that this receptor likely utilizes Lyn, Syk, ERK/MAPK/MEK1/2, PI3-K and PKC, as inhibitors to these molecules significantly inhibited degranulation upon anti-HA mAb cross-linking.

Database searches of potential homologs to IpLITRs found these receptors are distantly related to KIRs, LILRs as well as to FcRs, FcRLs and CEACAMs [1,17]. As these three latter receptors are involved in engaging phagocytic responses [29,30,33,131], then IpLITR-mediated phagocytosis was examined. RBL-2H3 cells expressing IpLITR2.6b/IpFcRγ-L internalized anti-HA-coated 4.5 μm fluorescent beads in an ITAM-dependent manner, as measured by flow cytometry. This response was not observed using isotype-coated beads.

Taken together, these findings provide new information in the stimulatory signaling capacity of IpLITR2.6b and its associated ITAM-encoding adaptor IpFcRγ-L with regards to their ability to recruit and activate different intracellular signaling molecules as well as their ability to trigger complex cell responses in leukocytes (i.e. degranulation and phagocytosis). As these studies were conducted in RBL-2H3 cells, it is quite interesting that a teleost receptor is capable of engaging the signaling machinery of a mammalian cell, which speaks to the conserved nature of intracellular signaling networks among vertebrates. Further examination of this receptor is still required to confirm the ability of this receptor to mediate innate protective responses in catfish immune cells. Nonetheless, in the absence of monoclonal antibodies and an incomplete picture of the expression profile of IpLITR-types in catfish leukocytes, generating epitope-tagged constructs of IpLITRs has been useful in understanding their expression and

signaling potential [2,4]. Further, the use of receptor-adaptor chimeric proteins and their expression in mammalian immune cells have been effective surrogates for examining in detail the potential effector functions of fish or other non-mammalian immunoregulatory receptors [52,141,169]. As such, using RBL-2H3 cells will continue serving as a receptor-expression system to characterize additional IpLITR-types.

6.1.2 Induction of intracellular signaling and phagocytosis by IpLITR1.1b

In addition to stimulatory IpLITR-types, putative inhibitory receptor-types, defined by the presence of one or more ITIMs within their CYT, are available for characterization. Early biochemical studies with IpLITR1.1b and IpLITR1.2a (i.e. putative inhibitory IpLITR-types) expressed in HEK 293T cells revealed that these ITIM-encoding receptors associate with SHP1 and SHP2 [2]. Subsequent expression of these receptor-types in mouse NK cells demonstrated their ability to abrogate NK-mediated cellular cytotoxicity mediated by SHP-dependent and independent mechanisms [3], reminiscent of mammalian inhibitory receptors expressed by NK cells [41,46,170]. I continued to use the RBL-2H3 cells to characterize additional IpLITR2.6b/IpFcRγ-L signaling events and functional responses, as well as expressing IpLITR1.1b, for comparison, as I hypothesized it would be incapable of inducing stimulatory signaling and functions based on this original characterization as an inhibitory immunoregulatory receptor.

As a broad approach to examine stimulatory IpLITR signaling, I utilized a signaling array to identify additional signaling molecules in IpLITR-activated lysates. As expected, multiple kinases were phosphorylated by IpLITR2.6b/IpFcRγ-L but none by IpLITR1.1b, after 10 mins cross-linking. ERK1/2 and Akt phosphorylation by both receptor-types were then examined in further as these molecules were phosphorylated by IpLITR2.6b/IpFcRγ-L, observed using the signaling array, and because of the role these molecules play in immunoregulatory signaling pathways [32]. Interestingly, time-course

phosphorylation studies of ERK1/2 and Akt revealed the ability of IpLITR1.1b cross-linking to activate both molecules, though transiently, whereas IpLITR2.6b/IpFcRγ-L induced more sustained phosphorylation of both molecules, revealing temporal differences in phosphorylation dynamics induced by both receptor-types. In addition, the unexpected phosphorylation of ERK1/2 and Akt by IpLITR1.1b may result from differential availability of signaling molecules between RBL-2H3 cells (a myeloid cell line) and mouse NK cells (lymphoid cells).

To determine if IpLITR1.1b-induced phosphorylation events lead to the activation of immune cells and subsequent induction of effector responses, I examined cytokine secretion after IpLITR cross-linking using a cytokine array. Secretion of IL-3, 4, 6 and TNF-α was observed by RBL-2H3 cells stimulated through the endogenous FcεRI and well as by PMA/calcium ionophore treatment. While IpLITR2.6b/IpFcRγ-L cross-linking also yielded the release of these same cytokines, IpLITR1.1b failed to induce any appreciable cytokine secretion. Thus, while IpLITR2.6b/IpFcRγ-L continues to function as a classical stimulatory receptor, IpLITR1.1b, despite its ability to activate certain intracellular signaling kinases, appears unable to induce this response.

As observed previously, IpLITR2.6b/IpFcRγ-L significantly internalized more anti-HA coated beads than isotype-coated beads. Most surprising, however, was IpLITR1.1b's ability to also phagocytose. This finding suggests the notion of dual functionality by IpLITR1.1b, wherein this ITIM-bearing receptor can inhibit cellular cytotoxicity in NK cells [3] and yet induce phagocytosis in RBL-2H3 cells. Phagocytosis by both receptor-types was visualized by confocal microscopy, revealing the association of internalized beads with lipid raft-containing membranes. Thus, IpLITR-mediated phagocytosis likely involves receptor aggregation at lipid rafts in RBL-2H3 cells. As lipid rafts have been reported in phagosomes of teleost macrophages, then IpLITRs potentially associate with lipid rafts in catfish leukocytes as well [157].

Several possibilities may account for IpLITR1.1b-mediated phagocytosis in RBL-2H3 cells. (1) IpLITR1.1b may associate with an endogenously expressed ITAM-bearing adaptor and signal indirectly through it to initiate signaling and phagocytosis. (2) IpLITR1.1b may signal directly through its CYT: as it encodes two membrane-proximal tyrosines embedded in uncharacterized regions, this region of IpLITR1.1b CYT can recruit a kinase in an ITAM-independent manner, akin to the previously observed recruitment of inhibitory Csk [3]. (3) As receptors bearing ITSMs are capable of inhibiting and inducing immune effector responses [171], IpLITR1.1b may initiate stimulatory signaling with its ITSM, located in the membrane-distal region of IpLITR1.1b CYT, which also encodes two ITIMs.

To examine the possible association of IpLITR1.1b with an ITAM-bearing receptor, I determined by immunoprecipitation that IpLITR1.1b did not associate with endogenous FcεRI γ subunit, despite observing the association of this adaptor protein with FcεRI α subunit. While this observation does not preclude possible interactions with other adaptors, it is important to note that RBL-2H3 cells do not express DAP12, another common stimulatory signaling adaptor.

To further reinforce that IpLITR.1b-mediated phagocytosis was independent of an association with surface-expressed signaling adaptors as well examine if IpLITR1.1b-mediated phagocytosis is due to direct signaling from its CYT, I truncated the CYT and reassessed phagocytosis. This construct, IpLITR1.1b ΔCYT, when expressed in RBL-2H3 cells, failed to induce internalization of opsonized beads. From this, it is likely that cell-surface adaptors do not facilitate IpLITR1.1b-mediated phagocytosis, but rather a cytoplasmic adaptor molecule(s) may be involved.

To determine which region of the IpLITR1.1b CYT was required for its phagocytic responses, examination of a closely related inhibitory IpLITR-type, IpLITR1.2a, was performed since it lacked the membrane-proximal region but

encoded a similar membrane-distal region. Expressed in RBL-2H3 cells, IpLITR1.2a can also significantly induce phagocytosis of opsonized beads, thus the mechanisms for signaling cascades initiated by IpLITR1.1b leading to phagocytosis likely require the membrane-distal region of its CYT. IpLITR1.2a CYT encodes an ITIM, however the ITIM tyrosine at position 499 in IpLITR1.1b is a serine in IpLITR1.2a. Finally, IpLITR1.2a also encodes an ITSM, as does IpLITR1.1b. Thus this motif may play a role in inducing phagocytosis.

Altogether, IpLITR1.1b's ability to activate as well as abrogate different effector responses suggests a functional plasticity, wherein its function, i.e., cytotoxicity or phagocytosis, may depend on the differential availability of signaling molecules of the cell type expressing this receptor. Whereas IpLITR1.1b functions as a prototypical inhibitory receptor, abrogating NK cellular cytotoxicity using ITIM-dependent (i.e. SHP recruitment) and -independent (i.e. Csk recruitment) mechanisms [3], there is still an unclear understanding of the precise mechanisms behind IpLITR1.1b's stimulatory signaling and its ability to induce phagocytosis in RBL-2H3 cells. Despite this, it is apparent that the stimulatory and/or inhibitory functions of immunoregulatory receptors cannot be predicted simply by the presence of canonical motifs, ITAMs or ITIMs, respectively.

6.1.3 IpLITRs as a multigene immunoregulatory receptor family

The IpLITR family of receptors presents a unique opportunity to conduct research into the origins of vertebrate immunoregulatory receptor families. As there are dozens of confirmed IpLITR-types and potentially hundreds more [1,119], this polymorphic and polygenic receptor family may represent a superfamily of teleost immunoregulatory receptors. The principal observations to support this notion are (1) sequence similarity to many different classes of mammalian IgSF members; and (2) multiple, paralogous LITR-like loci on the zebrafish genome. IpLITRs are similar to members of the human LRC such as KIRs and LILRs, and thus may be involved in MHC binding and thus, self/non-self recognition. Sequence

similarity to CEACAMs may indicate that some IpLITR-types function as cell adhesion molecules [1,17]. Finally, IpLITRs are similar to Siglecs, based on sequence identity and thus may function in sialic-acid recognition during cell-to-cell interactions [1,17]. IpLITRs also share sequence similarity to immunoregulatory receptors located on human chromosome 1, FcRs and FCRLs [1,17]. In particular, IpLITRs share highest sequence identity to FCRLs[17], a group of receptors located nearby FcRs on chromosome 1 that also bind Igs, specifically isotype IgA and IgG, but differently than FcRs [172,173], thus these receptors may function to bind Ig molecules. Currently, there is a limited understanding of the function of these receptor types *in vivo*, with studies in our lab focusing on their intracellular signaling capacities. However, future, long-term research may elucidate the precise role of these different receptors, confirming (or debunking) their predicted role(s) in self-recognition, Ig binding or cell adhesion. These studies may then necessitate the need to rename LITRs as a superfamily, subdivided into new receptor classes, such as IpFcRs, IpFCRLs, IpLILRs, IpSiglecs, IpCAMs, etc.

The observation of multiple independently segregating but homologous LITR-like loci on the zebrafish genome suggests that IpLITRs are products of multiple gene duplication and translocation events from a common ancestral gene. This suggests that these LITR-like loci may have evolved into genomically and functionally distinct receptors, accounting for the observed homology of IpLITRs to receptors found in the LRC and FcR-locus. Thus future functional studies into different IpLITR-types and mapping their location on the zebrafish genome will allow correlations between receptor function and chromosomal organization of teleost LITR-types. This will provide valuable insights into the origins of the gene duplication events that have given rise to the complexity of vertebrate immunoregulatory receptors and organization onto distinct clusters of related genes.

6.2 Future Directions

6.2.1 Potential mechanisms behind IpLITR1.1b-mediated signaling and phagocytosis

The mechanisms behind IpLITR1.1b-mediated activation of ERK1/2 and Akt and phagocytosis could be mitigated by the tyrosines found within the membrane-distal portion of this receptor's CYT. Tyrosine-503 is found within an ITSM, which can typically bind SHP-1 and SHP-2 to mediate cellular inhibition [174] but can also activate cellular signaling by selectively recruiting adaptor proteins such as SH2 domain protein 1A (SH2D1A) and Ewing's sarcoma (EWS)-activated transcript 2 (EAT-2) [175]. ITSMs can also induce PI3K-dependent signaling [176,177] as well as trigger downstream activation of ERK1/2 and Akt [171]. ERK1/2 activation may also be mediated by SHP-2 as recruitment to an ITSM or ITIM induces the phosphorylation of a C-terminal tyrosine on SHP-2 in turn serving as a binding site for growth factor receptor-bound 2 (Grb2), an SH2-containing adaptor molecule [178,179]. Grb2 can then promote activation of the Ras-MEK1/2-ERK1/2 pathway [180–182]. Given that IpLITR1.1b is capable of recruiting SHP2 [2], then ITIM- or ITSM-dependent SHP2 recruitment may provide a plausible mechanism behind IpLITR1.1b's stimulatory functions. Database searches have confirmed the presence of these molecules and adaptors in fish [3], thus lending support to these possible mechanisms.

In addition to its ITIMs and ITSM, other regions of IpLITR1.1b's CYT may contribute to its functional capacity. Tyrosine-463 matches the consensus Grb2-binding motif (YxN) [183], which may allow for direct binding of Grb2 to IpLITR1.1b. As IpLITR1.2a, which lacks this YxN motif, can still induce phagocytosis, perhaps direct Grb2 binding in IpLITR1.1b is redundant to SHP-2-mediated binding. Grb2 is an important intracellular scaffold that can associate with the guanine nucleotide exchange factor (GEF) Son of Sevenless (Sos) via Grb2's SH3 domain [184]. This Grb2-Sos complex can target membrane-bound

GEFs such as members of the Ras subfamily of small GTPases, subsequently leading to the activation of Raf and phosphorylation of ERK1/2 [185,186]. Grb2 can also associate with additional scaffold proteins such as Grb2-associated binder (Gab) 2 [182]: when phosphorylated, Gab2 can bind and activate PI3K, resulting in the downstream activation of Akt [187,188]. Taken together, the direct or indirect binding (via SHP-2) of Grb2 to the CYT of IpLITR1.1b may provide a mechanism for this receptor's ability to activate ERK1/2 and Akt signaling in RBL-2H3.

As signaling precedes function, then IpLITR1.1b-mediated signaling events leading to the induction of phagocytosis in RBL-2H3 cells also need to be examined. As indicated above, the direct or indirect binding of Grb2 can recruit Gab2 and PI3K which then culminates in the generation of phosphatidylinositol-(3,4,5)-tris-phosphate [PI(3,4,5)P_3]. This is required for actin cytoskeletal-dependent extension of pseudopods and internalization of large particles [189–191]. Pleckstrin-homology (PH)-domain containing adaptor molecules, such as Vav, are typically recruited to membrane regions containing PI(3,4,5)P_3 [192]. Vav is a GEF involved in activation of the Rho family of GTPases, including Cdc42, Rac1 and RhoA, which act to regulate actin polymerization and the formation of phagocytic lamellipodia [193]. As Vav activation of Rho GTPases has been implicated in FcRγ-, complement receptor- and CEACAM-mediated phagocytosis [192,194], it is worth exploring if IpLITR-mediated phagocytosis also engages Vav.

6.2.2 Biochemical and functional examinations of IpLITR1.1b-mediated cellular events

Based on the potential mechanisms behind IpLITR1.1b-mediated signaling and phagocytosis, biochemical studies into the potential associations between IpLITR1.1b and Grb2, Gab2, PI3K and SHP 2 in RBL-2H3 ought to be conducted. Preliminary co-immunoprecipitation studies have shown a direct association between IpLITR1.1b and the p85 regulatory subunit of PI3K (Zwozdesky, et al.,

unpublished results), demonstrating the recruitment of a key player in the phagocytic process to IpLITR1.1b.

Pre-treatment of IpLITR-expressing RBL-2H3 cells with pharmacological inhibitors prior to incubation with opsonized-beads will also be valuable in determining the precise signaling mediators involved in the activation of phagocytosis. Signaling molecules and their pharmacological inhibitors to be examined include Src family kinases (PP2), Syk (ER27319 and piceatannol) and PI3K (Wortmannin and LY294002) as well as to the Rho GTPases Cdc42 (ML141), Rac1/1b/2/3 (EHT1864) and Rho-associated protein kinase (Rock; GSK269962). Any decreases in phagocytosis upon inhibitor treatment will imply the likely requirement of that signaling molecule in IpLITR1.1b-mediated phagocytosis. Preliminary experiments indicate that treatment with inhibitors to Src, Syk, PI3K, Cdc42 and Rac1/2/3 do not appear to block phagocytosis in IpLITR1.1b-expressing cells (Lillico, et al., unpublished results). While the effect of the PI3K inhibitors may contradict the observed association of the p85 regulatory subunit of PI3K with IpLITR1.1b, further optimization of inhibitor treatment may be required. Alternatively, perhaps the p55 subunit associates with IpLITR1.1b as a scaffold to being other signaling molecules in close proximity to this receptor.

Finally, generating additional IpLITR1.1b variants with specific mutations in its CYT will also provide information as to the specific biochemical requirements for this receptor's stimulatory signaling and functional responses. Akin to the previously reported IpLITR2.6b/IpFcRγ-L 'FF' mutant [130], key tyrosines could be mutated to phenylalanines. 'Knocking out' the membrane-distal tyrosines in the ITSM and/or one or more ITIMs could disrupt this receptor's ability to directly recruit PI3K to the ITSM or indirectly recruit Grb2 via SHP-2 binding to an ITIM or ITSM, preventing the subsequent activations of Akt and ERK1/2. Additionally, generating a membrane-proximal YxN 'knock out' may also disrupt direct Grb2 binding to the CYT and subsequent ERK1/2 phosphorylation. These mutagenesis

experiments will complement above-mentioned biochemical and functional studies, in elucidating IpLITR1.1b-mediated events.

While relatively little is known of the function of fish immunoregulatory receptors, my work in functionally characterizing IpLITRs in RBL-2H3 cells has contributed significantly to our understanding of receptor-mediated control of immune responses. Additionally, IpLITR1.1b is the first teleost receptor reported to induce and inhibit immune effector responses. Based on my findings, it is clear that the stimulatory or inhibitory function of an immunoregulatory receptor cannot simply be predicted by the presence of ITIMs or ITAMs as other signaling motifs or even the cellular context may dictate receptor function. My findings have set the stage for elucidating the precise mechanisms behind IpLITR1.1b receptor plasticity, mentioned above. As well, using RBL-2H3 as an expression system will afford the characterization of additional IpLITR-types. Finally, IpLITR-expressing RBL-2H3 cells can be utilized to generate monoclonal antibodies reactive to the extracellular Ig domains of IpLITRs. This would be highly beneficial, as it would confirm IpLITR-induced signaling and functional responses in catfish clonal cell lines.

CHAPTER 7

References

1. Stafford, J. L. *et al.* A novel family of diversified immunoregulatory receptors in teleosts is homologous to both mammalian Fc receptors and molecules encoded within the leukocyte receptor complex. *Immunogenetics* **58,** 758–773 (2006).
2. Montgomery, B. C. S., Mewes, J., Davidson, C., Burshtyn, D. N. & Stafford, J. L. Cell surface expression of channel catfish leukocyte immune-type receptors (IpLITRs) and recruitment of both Src homology 2 domain-containing protein tyrosine phosphatase (SHP)-1 and SHP-2. *Dev. Comp. Immunol.* **33,** 570–582 (2009).
3. Montgomery, B. C., Cortes, H. D., Burshtyn, D. N. & Stafford, J. L. Channel catfish leukocyte immune-type receptor mediated inhibition of cellular cytotoxicity is facilitated by SHP-1-dependent and -independent mechanisms. *Dev. Comp. Immunol.* **37,** 151–163 (2012).
4. Mewes, J., Verheijen, K., Montgomery, B. C. S. & Stafford, J. L. Stimulatory catfish leukocyte immune-type receptors (IpLITRs) demonstrate a unique ability to associate with adaptor signaling proteins and participate in the formation of homo- and heterodimers. *Mol. Immunol.* **47,** 318–331 (2009).
5. Barclay, A. N. Membrane proteins with immunoglobulin-like domains—a master superfamily of interaction molecules. *Semin. Immunol.* **15,** 215–223 (2003).
6. Barrow, A. D. & Trowsdale, J. The extended human leukocyte receptor complex: diverse ways of modulating immune responses. *Immunol. Rev.* **224,** 98–123 (2008).
7. Carlyle, J. R. *et al.* Evolution of the Ly49 and Nkrp1 recognition systems. *Semin. Immunol.* **20,** 321–330 (2008).
8. Crocker, P. R., Paulson, J. C. & Varki, A. Siglecs and their roles in the immune system. *Nat. Rev. Immunol.* **7,** 255–266 (2007).
9. Flornes, L. M. *et al.* The complete inventory of receptors encoded by the rat natural killer cell gene complex. *Immunogenetics* **62,** 521–530 (2010).
10. Hardison, S. E. & Brown, G. D. C-type lectin receptors orchestrate antifungal immunity. *Nat. Immunol.* **13,** 817–822 (2012).
11. Kingeter, L. M. & Lin, X. C-type lectin receptor-induced NF-κB activation in innate immune and inflammatory responses. *Cell. Mol. Immunol.* **9,** 105–112 (2012).
12. Kumar, H., Kawai, T. & Akira, S. Pathogen recognition by the innate immune system. *Int. Rev. Immunol.* **30,** 16–34 (2011).
13. Sancho, D. & Reis e Sousa, C. Signaling by myeloid C-type lectin receptors in immunity and homeostasis. *Annu. Rev. Immunol.* **30,** 491–529 (2012).

14. Xie, J. The C-type lectin-like receptors of Dectin-1 cluster in natural killer gene complex. *Glycoconj. J.* **29,** 273–284 (2012).
15. Viertlboeck, B. C. & Göbel, T. W. The chicken leukocyte receptor cluster. *Vet. Immunol. Immunopathol.* **144,** 1–10 (2011).
16. Guselnikov, S. V., Ramanayake, T., Robert, J. & Taranin, A. V. Diversity of the FcR- and KIR-related genes in an amphibian Xenopus. *Front. Biosci. J. Virtual Libr.* **14,** 130–140 (2009).
17. Montgomery, B. C., Cortes, H. D., Mewes-Ares, J., Verheijen, K. & Stafford, J. L. Teleost IgSF immunoregulatory receptors. *Dev. Comp. Immunol.* **35,** 1223–1237 (2011).
18. Parham, P. Killer cell immunoglobulin-like receptor diversity: balancing signals in the natural killer cell response. *Immunol. Lett.* **92,** 11–13 (2004).
19. Stanietsky, N. & Mandelboim, O. Paired NK cell receptors controlling NK cytotoxicity. *Febs Lett.* **584,** 4895–4900 (2010).
20. Vilches, C. & Parham, P. KIR: diverse, rapidly evolving receptors of innate and adaptive immunity. *Annu. Rev. Immunol.* **20,** 217–251 (2002).
21. Brown, D., Trowsdale, J. & Allen, R. The LILR family: modulators of innate and adaptive immune pathways in health and disease. *Tissue Antigens* **64,** 215–225 (2004).
22. Katz, H. R. Inhibition of inflammatory responses by leukocyte Ig-like receptors. *Adv. Immunol.* **91,** 251–272 (2006).
23. Thomas, R., Matthias, T. & Witte, T. Leukocyte immunoglobulin-like receptors as new players in autoimmunity. *Clin. Rev. Allergy Immunol.* **38,** 159–162 (2010).
24. Arnon, T. I. *et al.* The mechanisms controlling the recognition of tumor- and virus-infected cells by NKp46. *Blood* **103,** 664–672 (2004).
25. Byrd, A., Hoffmann, S. C., Jarahian, M., Momburg, F. & Watzl, C. Expression analysis of the ligands for the Natural Killer cell receptors NKp30 and NKp44. *Plos One* **2,** e1339 (2007).
26. Joyce, M. G. *et al.* Crystal structure of human natural cytotoxicity receptor NKp30 and identification of its ligand binding site. *Proc. Natl. Acad. Sci. U. S. A.* **108,** 6223–6228 (2011).
27. Li, Y., Wang, Q. & Mariuzza, R. A. Structure of the human activating natural cytotoxicity receptor NKp30 bound to its tumor cell ligand B7-H6. *J. Exp. Med.* **208,** 703–714 (2011).
28. Varki, A. & Angata, T. Siglecs--the major subfamily of I-type lectins. *Glycobiology* **16,** 1R–27R (2006).
29. Nimmerjahn, F. & Ravetch, J. V. Fcgamma receptors: old friends and new family members. *Immunity* **24,** 19–28 (2006).
30. Nimmerjahn, F. & Ravetch, J. V. Fc-receptors as regulators of immunity. *Adv. Immunol.* **96,** 179–204 (2007).
31. Takai, T. Roles of Fc receptors in autoimmunity. *Nat. Rev. Immunol.* **2,** 580–592 (2002).
32. Gilfillan, A. M. & Tkaczyk, C. Integrated signalling pathways for mast-cell activation. *Nat. Rev. Immunol.* **6,** 218–230 (2006).

33. Takai, T. Fc receptors and their role in immune regulation and autoimmunity. *J. Clin. Immunol.* **25,** 1–18 (2005).
34. Fan, Q. R., Long, E. O. & Wiley, D. C. Crystal structure of the human natural killer cell inhibitory receptor KIR2DL1-HLA-Cw4 complex. *Nat. Immunol.* **2,** 452–460 (2001).
35. Natarajan, K., Dimasi, N., Wang, J., Mariuzza, R. A. & Margulies, D. H. Structure and function of natural killer cell receptors: multiple molecular solutions to self, nonself discrimination. *Annu. Rev. Immunol.* **20,** 853–885 (2002).
36. Chapman, T. L., Heikeman, A. P. & Bjorkman, P. J. The inhibitory receptor LIR-1 uses a common binding interaction to recognize class I MHC molecules and the viral homolog UL18. *Immunity* **11,** 603–613 (1999).
37. Chapman, T. L., Heikema, A. P., West, A. P., Jr & Bjorkman, P. J. Crystal structure and ligand binding properties of the D1D2 region of the inhibitory receptor LIR-1 (ILT2). *Immunity* **13,** 727–736 (2000).
38. Biassoni, R. *et al.* Human natural killer cell receptors and co-receptors. *Immunol. Rev.* **181,** 203–214 (2001).
39. Takai, T. Paired immunoglobulin-like receptors and their MHC class I recognition. *Immunology* **115,** 433–440 (2005).
40. Djeu, J. Y., Jiang, K. & Wei, S. A view to a kill: signals triggering cytotoxicity. *Clin. Cancer Res. Off. J. Am. Assoc. Cancer Res.* **8,** 636–640 (2002).
41. Yokoyama, W. M. & Plougastel, B. F. M. Immune functions encoded by the natural killer gene complex. *Nat. Rev. Immunol.* **3,** 304–316 (2003).
42. Feng, J., Call, M. E. & Wucherpfennig, K. W. The assembly of diverse immune receptors is focused on a polar membrane-embedded interaction site. *Plos Biol.* **4,** e142 (2006).
43. Gilfillan, A. M. & Rivera, J. The tyrosine kinase network regulating mast cell activation. *Immunol. Rev.* **228,** 149–169 (2009).
44. Mulrooney, T. J., Posch, P. E. & Hurley, C. K. DAP12 impacts trafficking and surface stability of killer immunoglobulin-like receptors on natural killer cells. *J. Leukoc. Biol.* (2013). doi:10.1189/jlb.0213093
45. Nakajima, H., Samaridis, J., Angman, L. & Colonna, M. Human myeloid cells express an activating ILT receptor (ILT1) that associates with Fc receptor gamma-chain. *J. Immunol. Baltim. Md 1950* **162,** 5–8 (1999).
46. Bakker, A. B., Wu, J., Phillips, J. H. & Lanier, L. L. NK cell activation: distinct stimulatory pathways counterbalancing inhibitory signals. *Hum. Immunol.* **61,** 18–27 (2000).
47. Bezbradica, J. S. & Medzhitov, R. Role of ITAM signaling module in signal integration. *Curr. Opin. Immunol.* **24,** 58–66 (2012).
48. Li, X. *et al.* The unique cytoplasmic domain of human FcγRIIIA regulates receptor-mediated function. *J. Immunol. Baltim. Md 1950* **189,** 4284–4294 (2012).
49. Ravetch, J. V. & Lanier, L. L. Immune inhibitory receptors. *Science* **290,** 84–89 (2000).

50. Vivier, E. & Daëron, M. Immunoreceptor tyrosine-based inhibition motifs. *Immunol. Today* **18,** 286–291 (1997).
51. Göbel, T. W. *et al.* Characterization of avian natural killer cells and their intracellular CD3 protein complex. *Eur. J. Immunol.* **24,** 1685–1691 (1994).
52. Viertlboeck, B. C. *et al.* The chicken leukocyte receptor complex: a highly diverse multigene family encoding at least six structurally distinct receptor types. *J. Immunol. Baltim. Md 1950* **175,** 385–393 (2005).
53. Viertlboeck, B. C., Crooijmans, R. P. M. A., Groenen, M. A. M. & Göbel, T. W. F. Chicken Ig-like receptor B2, a member of a multigene family, is mainly expressed on B lymphocytes, recruits both Src homology 2 domain containing protein tyrosine phosphatase (SHP)-1 and SHP-2, and inhibits proliferation. *J. Immunol. Baltim. Md 1950* **173,** 7385–7393 (2004).
54. Göbel, T. W., Meier, E. L. & Du Pasquier, L. Biochemical analysis of the Xenopus laevis TCR/CD3 complex supports the 'stepwise evolution' model. *Eur. J. Immunol.* **30,** 2775–2781 (2000).
55. Guselnikov, S. V., Bell, A., Najakshin, A. M., Robert, J. & Taranin, A. V. Signaling FcRgamma and TCRzeta subunit homologs in the amphibian Xenopus laevis. *Dev. Comp. Immunol.* **27,** 727–733 (2003).
56. Guselnikov, S. V. *et al.* The Xenopus FcR family demonstrates continually high diversification of paired receptors in vertebrate evolution. *Bmc Evol. Biol.* **8,** 148 (2008).
57. Dennis, G., Jr, Kubagawa, H. & Cooper, M. D. Paired Ig-like receptor homologs in birds and mammals share a common ancestor with mammalian Fc receptors. *Proc. Natl. Acad. Sci. U. S. A.* **97,** 13245–13250 (2000).
58. Viertlboeck, B. C. *et al.* The chicken leukocyte receptor complex encodes a primordial, activating, high-affinity IgY Fc receptor. *Proc. Natl. Acad. Sci. U. S. A.* **104,** 11718–11723 (2007).
59. Viertlboeck, B. C., Schweinsberg, S., Schmitt, R., Herberg, F. W. & Göbel, T. W. The chicken leukocyte receptor complex encodes a family of different affinity FcY receptors. *J. Immunol. Baltim. Md 1950* **182,** 6985–6992 (2009).
60. Laun, K. *et al.* The leukocyte receptor complex in chicken is characterized by massive expansion and diversification of immunoglobulin-like Loci. *Plos Genet.* **2,** e73 (2006).
61. Rajalingam, R., Parham, P. & Abi-Rached, L. Domain Shuffling Has Been the Main Mechanism Forming New Hominoid Killer Cell Ig-Like Receptors. *J. Immunol.* **172,** 356–369 (2004).
62. Khakoo, S. I. *et al.* Rapid evolution of NK cell receptor systems demonstrated by comparison of chimpanzees and humans. *Immunity* **12,** 687–698 (2000).
63. Crocker, P. R., Paulson, J. C. & Varki, A. Siglecs and their roles in the immune system. *Nat. Rev. Immunol.* **7,** 255–266 (2007).
64. Lanier, L. L. Evolutionary struggles between NK cells and viruses. *Nat. Rev. Immunol.* **8,** 259–268 (2008).
65. Wagner, C. S., Ljunggren, H.-G. & Achour, A. Immune Modulation by the Human Cytomegalovirus-Encoded Molecule UL18, a Mystery Yet to Be Solved. *J. Immunol.* **180,** 19–24 (2008).

66. Prod'homme, V. *et al.* The Human Cytomegalovirus MHC Class I Homolog UL18 Inhibits LIR-1+ but Activates LIR-1− NK Cells. *J. Immunol.* **178,** 4473–4481 (2007).
67. Abi-Rached, L. & Parham, P. Natural selection drives recurrent formation of activating killer cell immunoglobulin-like receptor and Ly49 from inhibitory homologues. *J. Exp. Med.* **201,** 1319–1332 (2005).
68. Angata, T., Margulies, E. H., Green, E. D. & Varki, A. Large-scale sequencing of the CD33-related Siglec gene cluster in five mammalian species reveals rapid evolution by multiple mechanisms. *Proc. Natl. Acad. Sci. U. S. A.* **101,** 13251–13256 (2004).
69. Santini, F., Harmon, L. J., Carnevale, G. & Alfaro, M. E. Did genome duplication drive the origin of teleosts? A comparative study of diversification in ray-finned fishes. *Bmc Evol. Biol.* **9,** 194 (2009).
70. Miller, N. *et al.* Functional and molecular characterization of teleost leukocytes. *Immunol. Rev.* **166,** 187–197 (1998).
71. Miller, N. W., Chinchar, V. G. & Clem, L. W. Development of leukocyte cell lines from the channel catfish (Ictalurus punctatus). *J. Tissue Cult. Methods* **16,** 117–123 (1994).
72. Miller, N. W. *et al.* Development and characterization of channel catfish long term B cell lines. *J. Immunol. Baltim. Md 1950* **152,** 2180–2189 (1994).
73. Stuge, T. B. *et al.* Development and analysis of various clonal alloantigen-dependent cytotoxic cell lines from channel catfish. *J. Immunol. Baltim. Md 1950* **164,** 2971–2977 (2000).
74. Majji, S. *et al.* Expression profiles of cloned channel catfish (Ictalurus punctatus) lymphoid cell lines and mixed lymphocyte cultures. *Dev. Comp. Immunol.* **33,** 224–234 (2009).
75. Vallejo, A. N., Ellsaesser, C. F., Miller, N. W. & Clem, L. W. Spontaneous development of functionally active long-term monocytelike cell lines from channel catfish. *Vitro Cell. Dev. Biol. J. Tissue Cult. Assoc.* **27A,** 279–286 (1991).
76. Shen, L. *et al.* Channel catfish NK-like cells are armed with IgM via a putative FcmicroR. *Dev. Comp. Immunol.* **27,** 699–714 (2003).
77. Stuge, T. B., Yoshida, S. H., Chinchar, V. G., Miller, N. W. & Clem, L. W. Cytotoxic activity generated from channel catfish peripheral blood leukocytes in mixed leukocyte cultures. *Cell. Immunol.* **177,** 154–161 (1997).
78. Alderson, K. L. & Sondel, P. M. Clinical cancer therapy by NK cells via antibody-dependent cell-mediated cytotoxicity. *J. Biomed. Biotechnol.* **2011,** 379123 (2011).
79. Amin, K. The role of mast cells in allergic inflammation. *Respir. Med.* **106,** 9–14 (2012).
80. Fieren, M. W. J. A. The local inflammatory responses to infection of the peritoneal cavity in humans: their regulation by cytokines, macrophages, and other leukocytes. *Mediators Inflamm.* **2012,** 976241 (2012).
81. Schmitt, C., Ghazi, B. & Bensussan, A. NK cells and surveillance in humans. *Reprod. Biomed. Online* **16,** 192–201 (2008).

82. Underhill, D. M. & Goodridge, H. S. Information processing during phagocytosis. *Nat. Rev. Immunol.* **12,** 492–502 (2012).
83. Esteban, M. A. & Meseguer, J. Factors influencing phagocytic response of macrophages from the sea bass (Dicentrarchus labrax L.): an ultrastructural and quantitative study. *Anat. Rec.* **248,** 533–541 (1997).
84. Engstad, R. E. & Robertsen, B. Recognition of yeast cell wall glucan by Atlantic salmon (Salmo salar L.) macrophages. *Dev. Comp. Immunol.* **17,** 319–330 (1993).
85. Wang, R., Neumann, N. ., Shen, Q. & Belosevic, M. Establishment and characterization of a macrophage cell line from the goldfish. *Fish Shellfish Immunol.* **5,** 329–346 (1995).
86. Neumann, N. F., Barreda, D. & Belosevic, M. Production of a macrophage growth factor(s) by a goldfish macrophage cell line and macrophages derived from goldfish kidney leukocytes. *Dev. Comp. Immunol.* **22,** 417–432 (1998).
87. Ganassin, R. C. & Bols, N. C. Development of a monocyte/macrophage-like cell line, RTS11, from rainbow trout spleen. *Fish Shellfish Immunol.* **8,** 457–476 (1998).
88. Frøystad, M. K., Rode, M., Berg, T. & Gjøen, T. A role for scavenger receptors in phagocytosis of protein-coated particles in rainbow trout head kidney macrophages. *Dev. Comp. Immunol.* **22,** 533–549 (1998).
89. Li, J. *et al.* B lymphocytes from early vertebrates have potent phagocytic and microbicidal abilities. *Nat. Immunol.* **7,** 1116–1124 (2006).
90. Dezfuli, B. S. & Giari, L. Mast cells in the gills and intestines of naturally infected fish: evidence of migration and degranulation. *J. Fish Dis.* **31,** 845–852 (2008).
91. Katzenback, B. A. & Belosevic, M. Isolation and functional characterization of neutrophil-like cells, from goldfish (Carassius auratus L.) kidney. *Dev. Comp. Immunol.* **33,** 601–611 (2009).
92. Palić, D., Andreasen, C. B., Menzel, B. W. & Roth, J. A. A rapid, direct assay to measure degranulation of primary granules in neutrophils from kidney of fathead minnow (Pimephales promelas Rafinesque, 1820). *Fish Shellfish Immunol.* **19,** 217–227 (2005).
93. Forlenza, M. *et al.* Differential contribution of neutrophilic granulocytes and macrophages to nitrosative stress in a host–parasite animal model. *Mol. Immunol.* **45,** 3178–3189 (2008).
94. Fischer, U. *et al.* Cytotoxic activities of fish leucocytes. *Fish Shellfish Immunol.* **20,** 209–226 (2006).
95. Øvergård, A.-C., Nepstad, I., Nerland, A. H. & Patel, S. Characterisation and expression analysis of the Atlantic halibut (Hippoglossus hippoglossus L.) cytokines: IL-1β, IL-6, IL-11, IL-12β and IFNγ. *Mol. Biol. Rep.* **39,** 2201–2213 (2012).
96. De Bruijn, I. *et al.* Immune gene expression in trout cell lines infected with the fish pathogenic oomycete Saprolegnia parasitica. *Dev. Comp. Immunol.* **38,** 44–54 (2012).

97. Neumann, N. F., Fagan, D. & Belosevic, M. Macrophage activating factor(s) secreted by mitogen stimulated goldfish kidney leukocytes synergize with bacterial lipopolysaccharide to induce nitric oxide production in teleost macrophages. *Dev. Comp. Immunol.* **19,** 473–482 (1995).
98. Stafford, J. L., Neumann, N. F. & Belosevic, M. Products of proteolytic cleavage of transferrin induce nitric oxide response of goldfish macrophages. *Dev. Comp. Immunol.* **25,** 101–115 (2001).
99. Yoshida, S. H., Stuge, T. B., Miller, N. W. & Clem, L. W. Phylogeny of lymphocyte heterogeneity: cytotoxic activity of channel catfish peripheral blood leukocytes directed against allogeneic targets. *Dev. Comp. Immunol.* **19,** 71–77 (1995).
100. Shen, L. *et al.* Identification and characterization of clonal NK-like cells from channel catfish (Ictalurus punctatus). *Dev. Comp. Immunol.* **28,** 139–152 (2004).
101. Fischer, U., Ototake, M. & Nakanishi, T. In vitro cell-mediated cytotoxicity against allogeneic erythrocytes in ginbuna crucian carp and goldfish using a non-radioactive assay. *Dev. Comp. Immunol.* **22,** 195–206 (1998).
102. Pardo, J. *et al.* The biology of cytotoxic cell granule exocytosis pathway: granzymes have evolved to induce cell death and inflammation. *Microbes Infect. Inst. Pasteur* **11,** 452–459 (2009).
103. Vujanovic, N. L., Nagashima, S., Herberman, R. B. & Whiteside, T. L. Nonsecretory apoptotic killing by human NK cells. *J. Immunol. Baltim. Md 1950* **157,** 1117–1126 (1996).
104. Panagos, P. G. *et al.* Immune-related, lectin-like receptors are differentially expressed in the myeloid and lymphoid lineages of zebrafish. *Immunogenetics* **58,** 31–40 (2006).
105. Ribeiro, C. M. S. *et al.* A novel soluble immune-type receptor (SITR) in teleost fish: carp SITR is involved in the nitric oxide-mediated response to a protozoan parasite. *Plos One* **6,** e15986 (2011).
106. Stafford, J. L. *et al.* Identification and characterization of a FcR homolog in an ectothermic vertebrate, the channel catfish (Ictalurus punctatus). *J. Immunol. Baltim. Md 1950* **177,** 2505–2517 (2006).
107. Rast, J. P., Haire, R. N., Litman, R. T., Pross, S. & Litman, G. W. Identification and characterization of T-cell antigen receptor-related genes in phylogenetically diverse vertebrate species. *Immunogenetics* **42,** 204–212 (1995).
108. Evenhuis, J. *et al.* Characterization of additional novel immune type receptors in channel catfish, Ictalurus punctatus. *Immunogenetics* **59,** 661–671 (2007).
109. Hawke, N. A. *et al.* Extraordinary variation in a diversified family of immune-type receptor genes. *Proc. Natl. Acad. Sci. U. S. A.* **98,** 13832–13837 (2001).
110. Piyaviriyakul, P., Kondo, H., Hirono, I. & Aoki, T. A novel immune-type receptor of Japanese flounder (Paralichthys olivaceus) is expressed in both T and B lymphocytes. *Fish Shellfish Immunol.* **22,** 467–476 (2007).

111. Yoder, J. A. *et al.* Cloning novel immune-type inhibitory receptors from the rainbow trout, Oncorhynchus mykiss. *Immunogenetics* **54,** 662–670 (2002).
112. Yoder, J. A. *et al.* Evidence for a transposition event in a second NITR gene cluster in zebrafish. *Immunogenetics* **60,** 257–265 (2008).
113. Desai, S., Heffelfinger, A. K., Orcutt, T. M., Litman, G. W. & Yoder, J. A. The medaka novel immune-type receptor (NITR) gene clusters reveal an extraordinary degree of divergence in variable domains. *Bmc Evol. Biol.* **8,** 177 (2008).
114. Yoder, J. A. *et al.* Immune-type receptor genes in zebrafish share genetic and functional properties with genes encoded by the mammalian leukocyte receptor cluster. *Proc. Natl. Acad. Sci. U. S. A.* **98,** 6771–6776 (2001).
115. Yoder, J. A. *et al.* Resolution of the novel immune-type receptor gene cluster in zebrafish. *Proc. Natl. Acad. Sci. U. S. A.* **101,** 15706–15711 (2004).
116. Strong, S. J. *et al.* A novel multigene family encodes diversified variable regions. *Proc. Natl. Acad. Sci. U. S. A.* **96,** 15080–15085 (1999).
117. Litman, G. W., Hawke, N. A. & Yoder, J. A. Novel immune-type receptor genes. *Immunol. Rev.* **181,** 250–259 (2001).
118. Yoder, J. A. Form, function and phylogenetics of NITRs in bony fish. *Dev. Comp. Immunol.* **33,** 135–144 (2009).
119. Stafford, J. L., Bengtén, E., Du Pasquier, L., Miller, N. W. & Wilson, M. Channel catfish leukocyte immune-type receptors contain a putative MHC class I binding site. *Immunogenetics* **59,** 77–91 (2007).
120. Nayak, D. K., Tang, A., Wilson, M., Miller, N. W. & Bengtén, E. Channel catfish soluble FcmuR binds conserved linear epitopes present on Cmu3 and Cmu4. *Mol. Immunol.* **47,** 1306–1316 (2010).
121. Wei, S. *et al.* The zebrafish activating immune receptor Nitr9 signals via Dap12. *Immunogenetics* **59,** 813–821 (2007).
122. Yoder, J. A., Orcutt, T. M., Traver, D. & Litman, G. W. Structural characteristics of zebrafish orthologs of adaptor molecules that associate with transmembrane immune receptors. *Gene* **401,** 154–164 (2007).
123. Hyka-Nouspikel, N. & Phillips, J. H. Physiological roles of murine DAP10 adapter protein in tumor immunity and autoimmunity. *Immunol. Rev.* **214,** 106–117 (2006).
124. Cannon, J. P. *et al.* A bony fish immunological receptor of the NITR multigene family mediates allogeneic recognition. *Immunity* **29,** 228–237 (2008).
125. Eccleston, E., Leonard, B. J., Lowe, J. S. & Welford, H. J. Basophilic leukaemia in the albino rat and a demonstration of the basopoietin. *Nature. New Biol.* **244,** 73–76 (1973).
126. Demo, S. D. *et al.* Quantitative measurement of mast cell degranulation using a novel flow cytometric annexin-V binding assay. *Cytometry* **36,** 340–348 (1999).
127. Nanamori, M., Chen, J., Du, X. & Ye, R. D. Regulation of leukocyte degranulation by cGMP-dependent protein kinase and phosphoinositide 3-kinase: potential roles in phosphorylation of target membrane SNARE

complex proteins in rat mast cells. *J. Immunol. Baltim. Md 1950* **178,** 416–427 (2007).
128. Naal, R. M. Z. G., Tabb, J., Holowka, D. & Baird, B. In situ measurement of degranulation as a biosensor based on RBL-2H3 mast cells. *Biosens. Bioelectron.* **20,** 791–796 (2004).
129. García-García, E., Brown, E. J. & Rosales, C. Transmembrane mutations to FcgammaRIIA alter its association with lipid rafts: implications for receptor signaling. *J. Immunol. Baltim. Md 1950* **178,** 3048–3058 (2007).
130. Cortes, H. D., Montgomery, B. C., Verheijen, K., García-García, E. & Stafford, J. L. Examination of the stimulatory signaling potential of a channel catfish leukocyte immune-type receptor and associated adaptor. *Dev. Comp. Immunol.* **36,** 62–73 (2012).
131. Nimmerjahn, F. & Ravetch, J. V. FcγRs in health and disease. *Curr. Top. Microbiol. Immunol.* **350,** 105–125 (2011).
132. Ford, J. W. & McVicar, D. W. TREM and TREM-like receptors in inflammation and disease. *Curr. Opin. Immunol.* **21,** 38–46 (2009).
133. Bouchon, A., Facchetti, F., Weigand, M. A. & Colonna, M. TREM-1 amplifies inflammation and is a crucial mediator of septic shock. *Nature* **410,** 1103–1107 (2001).
134. Meyaard, L. *et al.* LAIR-1, a novel inhibitory receptor expressed on human mononuclear leukocytes. *Immunity* **7,** 283–290 (1997).
135. Kuespert, K., Pils, S. & Hauck, C. R. CEACAMs: their role in physiology and pathophysiology. *Curr. Opin. Cell Biol.* **18,** 565–571 (2006).
136. Lebbink, R. J. *et al.* Collagens are functional, high affinity ligands for the inhibitory immune receptor LAIR-1. *J. Exp. Med.* **203,** 1419–1425 (2006).
137. McCaw, S. E., Schneider, J., Liao, E. H., Zimmermann, W. & Gray-Owen, S. D. Immunoreceptor tyrosine-based activation motif phosphorylation during engulfment of Neisseria gonorrhoeae by the neutrophil-restricted CEACAM3 (CD66d) receptor. *Mol. Microbiol.* **49,** 623–637 (2003).
138. Ostergaard, A. E. *et al.* Genomic organisation analysis of novel immunoglobulin-like transcripts in Atlantic salmon (Salmo salar) reveals a tightly clustered and multigene family. *Bmc Genomics* **11,** 697 (2010).
139. Stet, R. J. M. *et al.* Novel immunoglobulin-like transcripts in teleost fish encode polymorphic receptors with cytoplasmic ITAM or ITIM and a new structural Ig domain similar to the natural cytotoxicity receptor NKp44. *Immunogenetics* **57,** 77–89 (2005).
140. Yoder, J. A. & Litman, G. W. The phylogenetic origins of natural killer receptors and recognition: relationships, possibilities, and realities. *Immunogenetics* **63,** 123–141 (2011).
141. Tsujita, T. *et al.* Sensing bacterial flagellin by membrane and soluble orthologs of Toll-like receptor 5 in rainbow trout (Onchorhynchus mikiss). *J. Biol. Chem.* **279,** 48588–48597 (2004).
142. Barsumian, E. L., Isersky, C., Petrino, M. G. & Siraganian, R. P. IgE-induced histamine release from rat basophilic leukemia cell lines: isolation of releasing and nonreleasing clones. *Eur. J. Immunol.* **11,** 317–323 (1981).

143. Amoui, M., Dráberová, L., Tolar, P. & Dráber, P. Direct interaction of Syk and Lyn protein tyrosine kinases in rat basophilic leukemia cells activated via type I Fc epsilon receptors. *Eur. J. Immunol.* **27,** 321–328 (1997).
144. Holowka, D., Sil, D., Torigoe, C. & Baird, B. Insights into immunoglobulin E receptor signaling from structurally defined ligands. *Immunol. Rev.* **217,** 269–279 (2007).
145. Mócsai, A., Ruland, J. & Tybulewicz, V. L. J. The SYK tyrosine kinase: a crucial player in diverse biological functions. *Nat. Rev. Immunol.* **10,** 387–402 (2010).
146. Xu, R., Seger, R. & Pecht, I. Cutting edge: extracellular signal-regulated kinase activates syk: a new potential feedback regulation of Fc epsilon receptor signaling. *J. Immunol. Baltim. Md 1950* **163,** 1110–1114 (1999).
147. Ishizuka, T. *et al.* Stem cell factor augments Fc epsilon RI-mediated TNF-alpha production and stimulates MAP kinases via a different pathway in MC/9 mast cells. *J. Immunol. Baltim. Md 1950* **161,** 3624–3630 (1998).
148. Ishizuka, T. *et al.* Mitogen-activated protein kinase activation through Fc epsilon receptor I and stem cell factor receptor is differentially regulated by phosphatidylinositol 3-kinase and calcineurin in mouse bone marrow-derived mast cells. *J. Immunol. Baltim. Md 1950* **162,** 2087–2094 (1999).
149. Kawakami, Y., Hartman, S. E., Holland, P. M., Cooper, J. A. & Kawakami, T. Multiple signaling pathways for the activation of JNK in mast cells: involvement of Bruton's tyrosine kinase, protein kinase C, and JNK kinases, SEK1 and MKK7. *J. Immunol. Baltim. Md 1950* **161,** 1795–1802 (1998).
150. Daws, M. R. *et al.* Pattern recognition by TREM-2: binding of anionic ligands. *J. Immunol. Baltim. Md 1950* **171,** 594–599 (2003).
151. N'Diaye, E.-N. *et al.* TREM-2 (triggering receptor expressed on myeloid cells 2) is a phagocytic receptor for bacteria. *J. Cell Biol.* **184,** 215–223 (2009).
152. Takahashi, K., Rochford, C. D. P. & Neumann, H. Clearance of apoptotic neurons without inflammation by microglial triggering receptor expressed on myeloid cells-2. *J. Exp. Med.* **201,** 647–657 (2005).
153. Rajalingam, R. Overview of the killer cell immunoglobulin-like receptor system. *Methods Mol. Biol. Clifton Nj* **882,** 391–414 (2012).
154. Tsuchiya, N., Kyogoku, C., Miyashita, R. & Kuroki, K. Diversity of human immune system multigene families and its implication in the genetic background of rheumatic diseases. *Curr. Med. Chem.* **14,** 431–439 (2007).
155. Baumruker, T. & Prieschl, E. E. Sphingolipids and the regulation of the immune response. *Semin. Immunol.* **14,** 57–63 (2002).
156. Yoshizaki, F. *et al.* Role of glycosphingolipid-enriched microdomains in innate immunity: microdomain-dependent phagocytic cell functions. *Biochim. Biophys. Acta* **1780,** 383–392 (2008).
157. Garcia-Garcia, E., Grayfer, L., Stafford, J. L. & Belosevic, M. Evidence for the presence of functional lipid rafts in immune cells of ectothermic organisms. *Dev. Comp. Immunol.* **37,** 257–269 (2012).

158. Koncz, G., Pecht, I., Gergely, J. & Sármay, G. Fcgamma receptor-mediated inhibition of human B cell activation: the role of SHP-2 phosphatase. *Eur. J. Immunol.* **29,** 1980–1989 (1999).
159. Joiner, K. A., Fuhrman, S. A., Miettinen, H. M., Kasper, L. H. & Mellman, I. Toxoplasma gondii: fusion competence of parasitophorous vacuoles in Fc receptor-transfected fibroblasts. *Science* **249,** 641–646 (1990).
160. Zhang, Y. *et al.* Ligation of Fc gamma receptor IIB enhances levels of antiviral cytokine in response to PRRSV infection in vitro. *Vet. Microbiol.* **160,** 473–480 (2012).
161. Alvarez-Errico, D., Sayós, J. & López-Botet, M. The IREM-1 (CD300f) inhibitory receptor associates with the p85alpha subunit of phosphoinositide 3-kinase. *J. Immunol. Baltim. Md 1950* **178,** 808–816 (2007).
162. Izawa, K. *et al.* An activating and inhibitory signal from an inhibitory receptor LMIR3/CLM-1: LMIR3 augments lipopolysaccharide response through association with FcRgamma in mast cells. *J. Immunol. Baltim. Md 1950* **183,** 925–936 (2009).
163. Newman, P. J. & Newman, D. K. Signal transduction pathways mediated by PECAM-1: new roles for an old molecule in platelet and vascular cell biology. *Arterioscler. Thromb. Vasc. Biol.* **23,** 953–964 (2003).
164. Faure, M. & Long, E. O. KIR2DL4 (CD158d), an NK cell-activating receptor with inhibitory potential. *J. Immunol. Baltim. Md 1950* **168,** 6208–6214 (2002).
165. Rajagopalan, S., Fu, J. & Long, E. O. Cutting edge: induction of IFN-gamma production but not cytotoxicity by the killer cell Ig-like receptor KIR2DL4 (CD158d) in resting NK cells. *J. Immunol. Baltim. Md 1950* **167,** 1877–1881 (2001).
166. Yusa, S., Catina, T. L. & Campbell, K. S. SHP-1- and phosphotyrosine-independent inhibitory signaling by a killer cell Ig-like receptor cytoplasmic domain in human NK cells. *J. Immunol. Baltim. Md 1950* **168,** 5047–5057 (2002).
167. Kikuchi-Maki, A., Yusa, S., Catina, T. L. & Campbell, K. S. KIR2DL4 is an IL-2-regulated NK cell receptor that exhibits limited expression in humans but triggers strong IFN-gamma production. *J. Immunol. Baltim. Md 1950* **171,** 3415–3425 (2003).
168. Kikuchi-Maki, A., Catina, T. L. & Campbell, K. S. Cutting edge: KIR2DL4 transduces signals into human NK cells through association with the Fc receptor gamma protein. *J. Immunol. Baltim. Md 1950* **174,** 3859–3863 (2005).
169. Carlyle, J. R. *et al.* Missing self-recognition of Ocil/Clr-b by inhibitory NKR-P1 natural killer cell receptors. *Proc. Natl. Acad. Sci. U. S. A.* **101,** 3527–3532 (2004).
170. Vivier, E., Nunès, J. A. & Vély, F. Natural killer cell signaling pathways. *Science* **306,** 1517–1519 (2004).
171. Sidorenko, S. P. & Clark, E. A. The dual-function CD150 receptor subfamily: the viral attraction. *Nat. Immunol.* **4,** 19–24 (2003).

172. Franco, A. *et al.* Human Fc receptor-like 5 binds intact IgG via mechanisms distinct from those of Fc receptors. *J. Immunol. Baltim. Md 1950* **190,** 5739–5746 (2013).
173. Wilson, T. J., Fuchs, A. & Colonna, M. Cutting edge: human FcRL4 and FcRL5 are receptors for IgA and IgG. *J. Immunol. Baltim. Md 1950* **188,** 4741–4745 (2012).
174. Chemnitz, J. M., Parry, R. V., Nichols, K. E., June, C. H. & Riley, J. L. SHP-1 and SHP-2 associate with immunoreceptor tyrosine-based switch motif of programmed death 1 upon primary human T cell stimulation, but only receptor ligation prevents T cell activation. *J. Immunol. Baltim. Md 1950* **173,** 945–954 (2004).
175. Shlapatska, L. M. *et al.* CD150 association with either the SH2-containing inositol phosphatase or the SH2-containing protein tyrosine phosphatase is regulated by the adaptor protein SH2D1A. *J. Immunol. Baltim. Md 1950* **166,** 5480–5487 (2001).
176. Mikhalap, S. V. *et al.* CDw150 associates with src-homology 2-containing inositol phosphatase and modulates CD95-mediated apoptosis. *J. Immunol. Baltim. Md 1950* **162,** 5719–5727 (1999).
177. Aoukaty, A. & Tan, R. Association of the X-linked lymphoproliferative disease gene product SAP/SH2D1A with 2B4, a natural killer cell-activating molecule, is dependent on phosphoinositide 3-kinase. *J. Biol. Chem.* **277,** 13331–13337 (2002).
178. Li, C., Iosef, C., Jia, C. Y. H., Han, V. K. M. & Li, S. S.-C. Dual functional roles for the X-linked lymphoproliferative syndrome gene product SAP/SH2D1A in signaling through the signaling lymphocyte activation molecule (SLAM) family of immune receptors. *J. Biol. Chem.* **278,** 3852–3859 (2003).
179. Brummer, T., Schmitz-Peiffer, C. & Daly, R. J. Docking proteins. *Febs J.* **277,** 4356–4369 (2010).
180. Li, W. *et al.* A new function for a phosphotyrosine phosphatase: linking GRB2-Sos to a receptor tyrosine kinase. *Mol. Cell. Biol.* **14,** 509–517 (1994).
181. Bennett, A. M., Tang, T. L., Sugimoto, S., Walsh, C. T. & Neel, B. G. Protein-tyrosine-phosphatase SHPTP2 couples platelet-derived growth factor receptor beta to Ras. *Proc. Natl. Acad. Sci. U. S. A.* **91,** 7335–7339 (1994).
182. Belov, A. A. & Mohammadi, M. Grb2, a double-edged sword of receptor tyrosine kinase signaling. *Sci. Signal.* **5,** pe49 (2012).
183. Songyang, Z. *et al.* Specific motifs recognized by the SH2 domains of Csk, 3BP2, fps/fes, GRB-2, HCP, SHC, Syk, and Vav. *Mol. Cell. Biol.* **14,** 2777–2785 (1994).
184. Lowenstein, E. J. *et al.* The SH2 and SH3 domain-containing protein GRB2 links receptor tyrosine kinases to ras signaling. *Cell* **70,** 431–442 (1992).
185. Simon, M. A., Bowtell, D. D., Dodson, G. S., Laverty, T. R. & Rubin, G. M. Ras1 and a putative guanine nucleotide exchange factor perform crucial steps in signaling by the sevenless protein tyrosine kinase. *Cell* **67,** 701–716 (1991).

186. Li, N. *et al.* Guanine-nucleotide-releasing factor hSos1 binds to Grb2 and links receptor tyrosine kinases to Ras signalling. *Nature* **363,** 85–88 (1993).
187. Gotoh, N. Regulation of growth factor signaling by FRS2 family docking/scaffold adaptor proteins. *Cancer Sci.* **99,** 1319–1325 (2008).
188. Gu, H. *et al.* Essential role for Gab2 in the allergic response. *Nature* **412,** 186–190 (2001).
189. Bohdanowicz, M., Cosío, G., Backer, J. M. & Grinstein, S. Class I and class III phosphoinositide 3-kinases are required for actin polymerization that propels phagosomes. *J. Cell Biol.* **191,** 999–1012 (2010).
190. Araki, N., Johnson, M. T. & Swanson, J. A. A role for phosphoinositide 3-kinase in the completion of macropinocytosis and phagocytosis by macrophages. *J. Cell Biol.* **135,** 1249–1260 (1996).
191. Cox, D., Tseng, C. C., Bjekic, G. & Greenberg, S. A requirement for phosphatidylinositol 3-kinase in pseudopod extension. *J. Biol. Chem.* **274,** 1240–1247 (1999).
192. Katzav, S. Vav1: a hematopoietic signal transduction molecule involved in human malignancies. *Int. J. Biochem. Cell Biol.* **41,** 1245–1248 (2009).
193. Hall, A. B. *et al.* Requirements for Vav guanine nucleotide exchange factors and Rho GTPases in FcgammaR- and complement-mediated phagocytosis. *Immunity* **24,** 305–316 (2006).
194. Schmitter, T. *et al.* The granulocyte receptor carcinoembryonic antigen-related cell adhesion molecule 3 (CEACAM3) directly associates with Vav to promote phagocytosis of human pathogens. *J. Immunol. Baltim. Md 1950* **178,** 3797–3805 (2007).

APPENDIX

	1	2	3	4	5	6	7	8
A	CINC-1	CINC-2α/β	CINC-3	CNTF	CX3CL1	GM-CSF	sICAM-1	IFN-γ
B	IL-1α	IL-1β	IL-1ra	IL-2	IL-3	IL-4	IL-6	IL-10
C	IL-13	IL-17	CXCL10	CD62L	CXCL9	CCL3	CCL20	*Blank*
D	CCL5	CXCL7	TIMP-1	TNF-α	VEGF	*Blank*	*Blank*	*Blank*

Table A1.
Profiler coordinates for the Rat Cytokine Array Panel A Array Kit (R&D Systems) used in this thesis.

	1	2	3	4	5	6	7	8	9
A	Akt1	Akt2	Akt3	Akt pan	CREB	ERK1	ERK2	GSK-3α/β	GSK-3β
B	HSP27	JNK1	JNK2	JNK3	JNK pan	MEK3	MEK6	MSK2	*Blank*
C	p38α	p38β	p38δ	p38γ	P53	S6K1	RSK1	RSK2	TOR

Table A2.
Profiler coordinates for the Human Phospho-MAPK Array Kit (R&D Systems) used in this thesis.

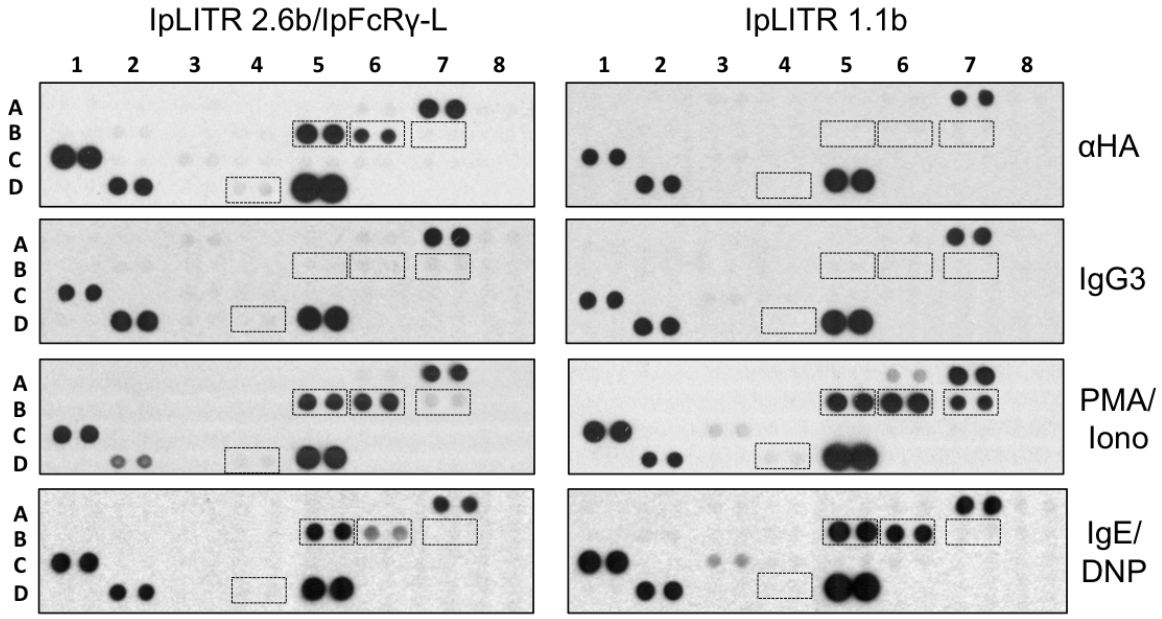

Figure A1. Parallel examination of the relative amounts of cytokine levels produced by IpLITR-activated RBL-2H3 cells. RBL-2H3 cells ($2.5x10^6$) expressing the N-terminal HA-epitope tagged IpLITR2.6b/IpFcRγ-L (left panels) or IpLITR 1.1b (right panels) were crosslinked by treatment with 0.625 µg/mL anti-HA mAb or mouse IgG3 (isotype control) followed by 1.25 µg/mL anti-mouse IgG3 pAb (H+L) for 24 h at 37°C. Cells were also activated with 50 ng/mL PMA/0.5 µM Ca^{2+} ionophore A23187 (i.e. PMA/Iono) or after triggering them via their endogenous FcεRI with anti-DNP-IgE and DNP-HSA (i.e. IgE/DNP). Cell supernatants were examined for the presence of various rat cytokines using the antibody capture chemiluminescent-based Rat Cytokine Array Panel Array Kit (R&D Systems). Representative proteome profiler array results are shown. The duplicate spots used for calculating the relative cytokine levels are indicated with hatched boxes, and the array coordinates are presented in Table A1.

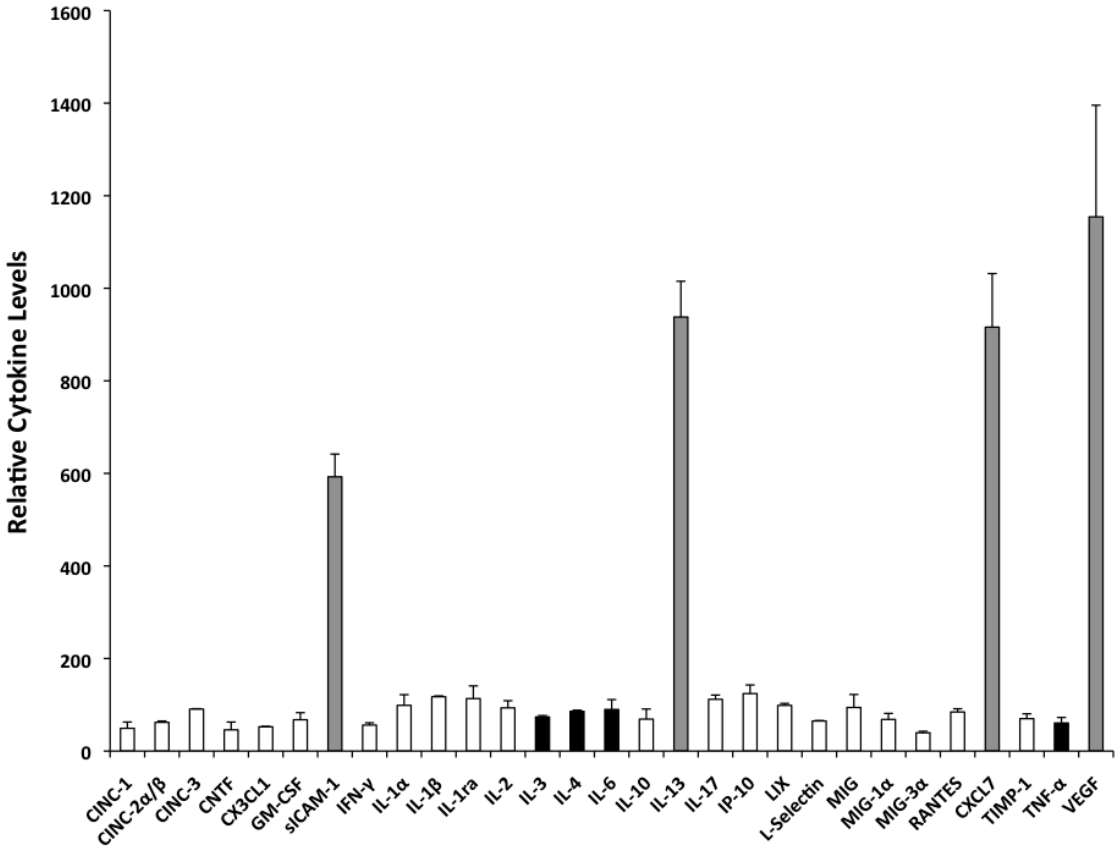

Figure A2. Cytokine production <u>by IpLITR 2.6b/IpFcRγ-L</u>-expressing RBL-2H3 following crosslinking with <u>mouse IgG3</u>: complete array data. RBL-2H3 cells ($2.5x10^6$) expressing the N-terminal HA-epitope tagged IpLITR2.6b/IpFcRγ-L were crosslinked by treatment with 0.625 µg/ml of mouse IgG3 (isotype control) followed by 1.25 µg/ml of anti-mouse IgG3 pAb (H+L) for 24 h at 37°C. Cell supernatants were examined for the presence of various rat cytokines using the antibody capture chemiluminescent-based Rat Cytokine Array Panel Array Kit (R&D Systems) using manufacturer's protocol. Relative cytokine levels were calculated using densitometry values obtained from the array spots as described. Each bar represents the mean relative cytokine levels ± SEM of three independent experiments. Cytokine levels reported in Chapter 5 are indicated with black bars and cytokines constitutively generated by RBL-2H3 cells are indicated with grey bars.

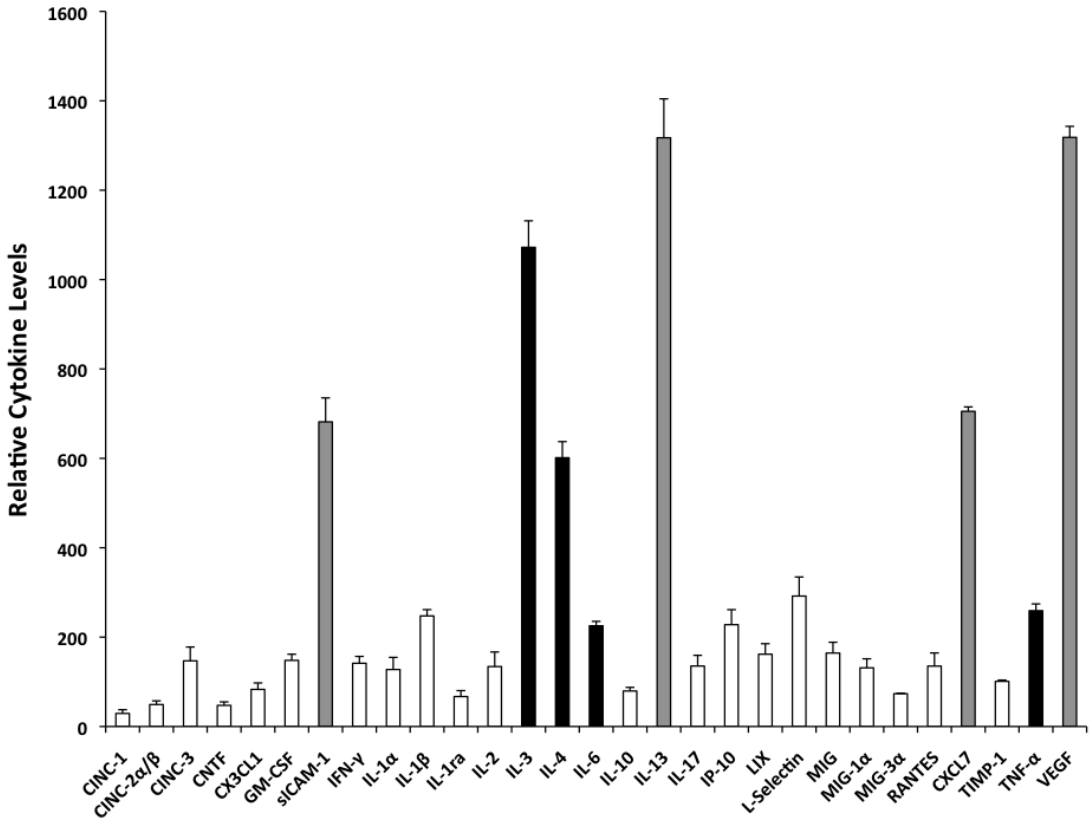

Figure A3. Cytokine production by <u>IpLITR 2.6b/IpFcRγ-L</u>-expressing RBL-2H3 following crosslinking with <u>anti-HA mAb</u>: complete array data. RBL-2H3 cells ($2.5x10^6$) expressing the N-terminal HA-epitope tagged IpLITR2.6b/IpFcRγ-L were crosslinked by treatment with 0.625 μg/ml of anti-HA mAb followed by 1.25 μg/ml of anti-mouse IgG3 pAb (H+L) for 24 h at 37^oC. Cell supernatants were examined for the presence of various rat cytokines using the antibody capture chemiluminescent-based Rat Cytokine Array Panel Array Kit (R&D Systems) using manufacturer's protocol. Relative cytokine levels were calculated using densitometry values obtained from the array spots as described. Each bar represents the mean relative cytokine levels ± SEM of three independent experiments. Cytokine levels reported in Chapter 5 are indicated with black bars and cytokines constitutively generated by RBL-2H3 cells are indicated with grey bars.

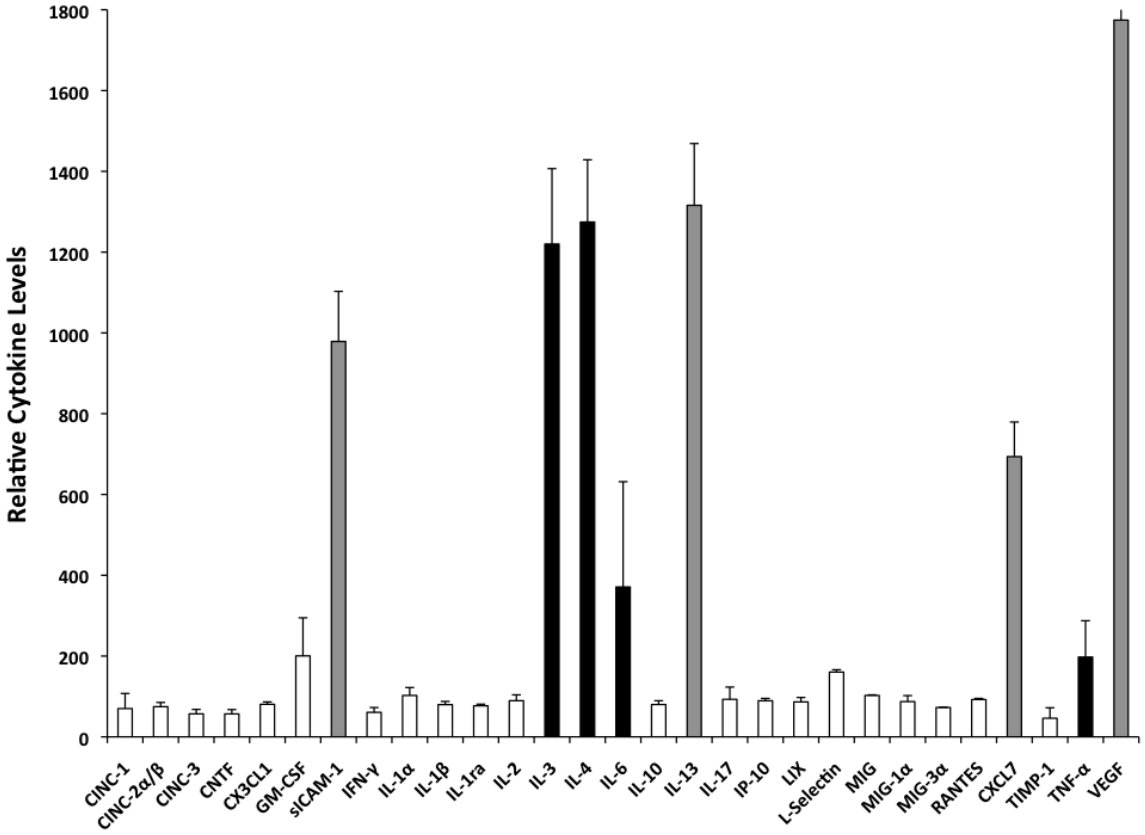

Figure A4. Cytokine production by IpLITR 2.6b/IpFcRγ-L-expressing RBL-2H3 following stimulation with PMA/A23187: complete array data. RBL-2H3 cells ($2.5x10^6$) expressing the N-terminal HA-epitope tagged IpLITR2.6b/IpFcRγ-L were activated with 50 ng/ml PMA/0.5 μM Ca^{2+} ionophore A23187 for 24 h at 37°C. Cell supernatants were examined for the presence of various rat cytokines using the antibody capture chemiluminescent-based Rat Cytokine Array Panel Array Kit (R&D Systems) using manufacturer's protocol. Relative cytokine levels were calculated using densitometry values obtained from the array spots as described. Each bar represents the mean relative cytokine levels ± SEM of three independent experiments. Cytokine levels reported in Chapter 5 are indicated with black bars and cytokines constitutively generated by RBL-2H3 cells are indicated with grey bars.

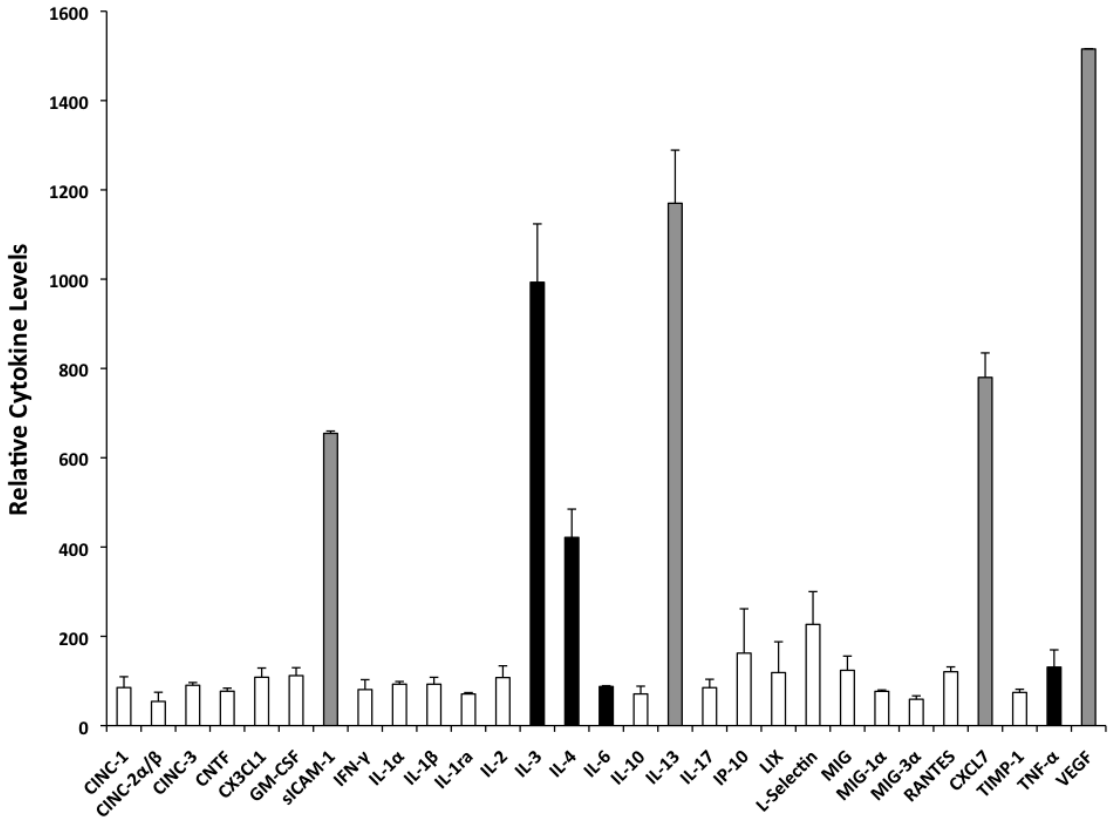

Figure A5. Cytokine production by IpLITR 2.6b/IpFcRγ-L-expressing RBL-2H3 following FcεRI triggering: complete array data.
RBL-2H3 cells ($2.5x10^6$) expressing the N-terminal HA-epitope tagged IpLITR2.6b/IpFcRγ-L were activated via the endogenous FcεRI after sensitization with 200 ng/ml anti-DNP-IgE and triggering with 0.1 ng/ml DNP-HSA for 24 h at 37°C. Cell supernatants were examined for the presence of various rat cytokines using the antibody capture chemiluminescent-based Rat Cytokine Array Panel Array Kit (R&D Systems) using manufacturer's protocol. Relative cytokine levels were calculated using densitometry values obtained from the array spots as described. Each bar represents the mean relative cytokine levels ± SEM of three independent experiments. Cytokine levels reported in the manuscript are indicated with black bars and cytokines constitutively generated by RBL-2H3 cells are indicated with grey bars.

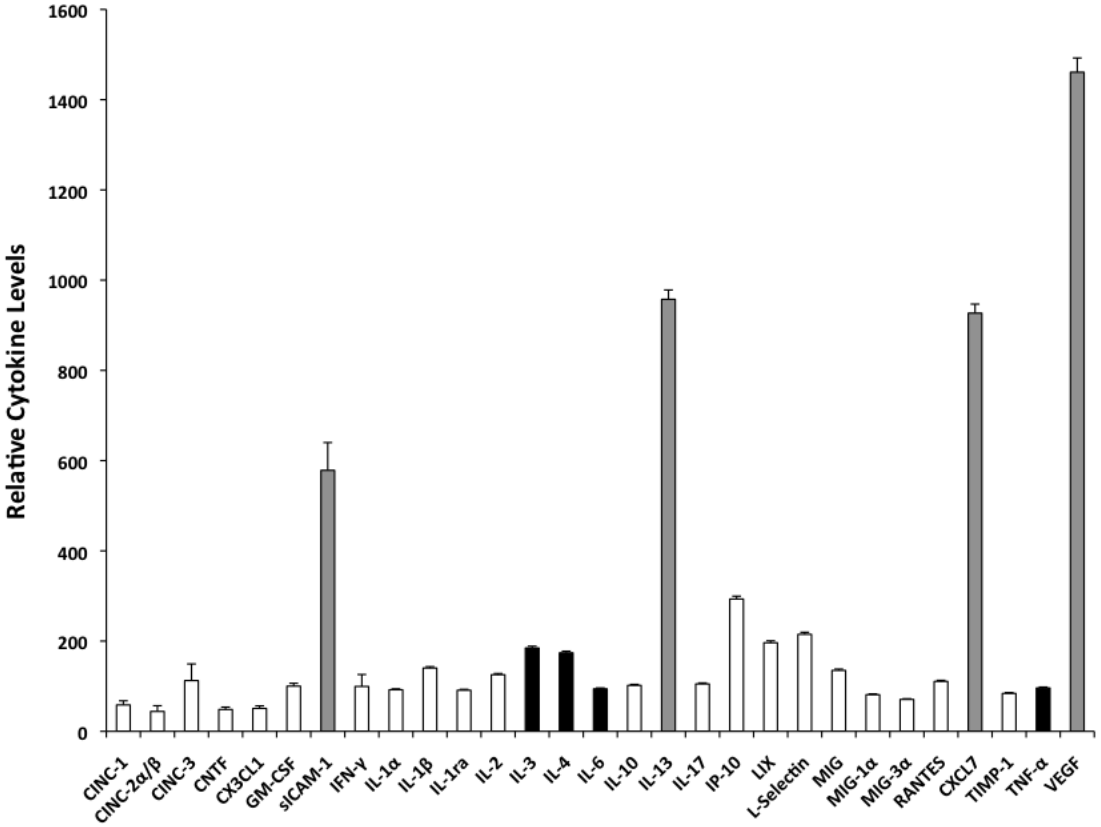

Figure A6. Cytokine production by IpLITR 1.1b-expressing RBL-2H3 following crosslinking with mouse IgG3: complete array data.
RBL-2H3 cells ($2.5x10^6$) expressing the N-terminal HA-epitope tagged IpLITR 1.1b crosslinked by treatment with 0.625 μg/ml of mouse IgG3 (isotype control) followed by 1.25 μg/ml of anti-mouse IgG3 pAb (H+L) for 24 h at 37°C. Cell supernatants were examined for the presence of various rat cytokines using the antibody capture chemiluminescent-based Rat Cytokine Array Panel Array Kit (R&D Systems) using manufacturer's protocol. Relative cytokine levels were calculated using densitometry values obtained from the array spots as described. Each bar represents the mean relative cytokine levels ± SEM of three independent experiments. Cytokine levels reported in Chapter 5 are indicated with black bars and cytokines constitutively generated by RBL-2H3 cells are indicated with grey bars.

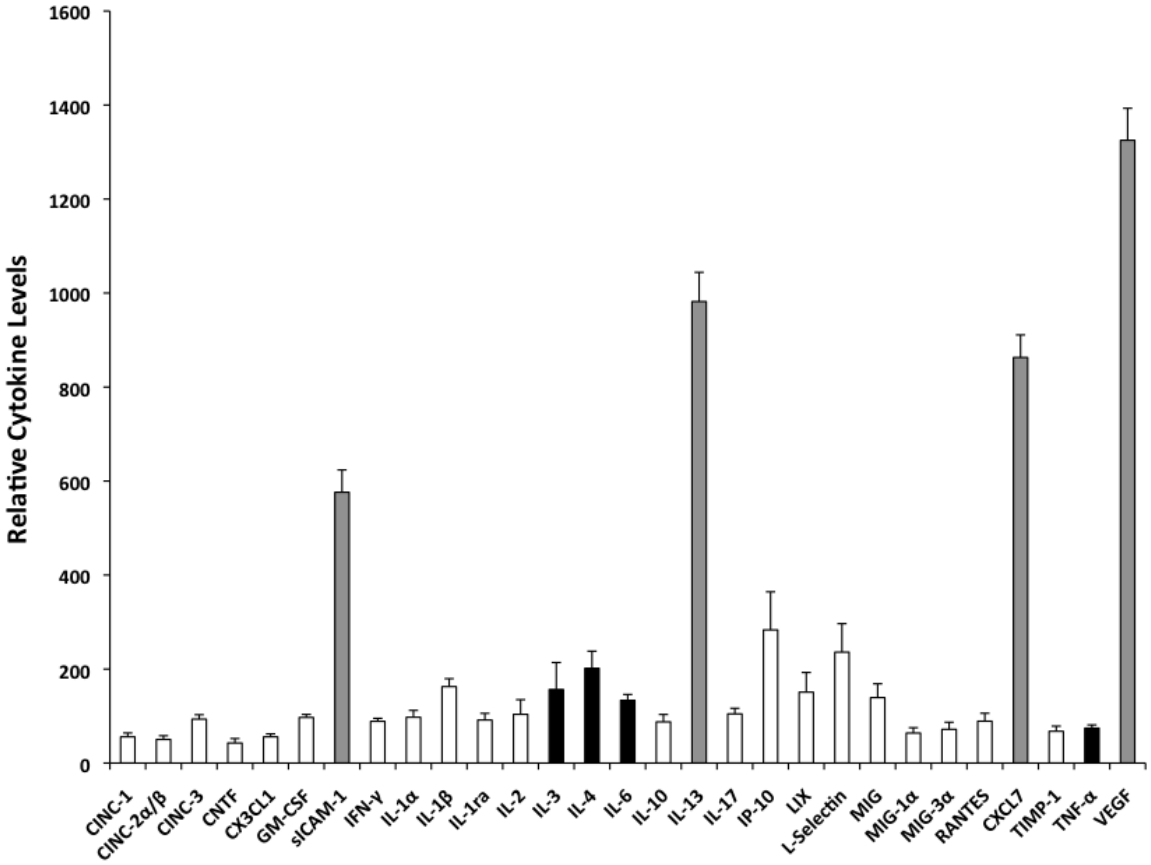

Figure A7. Cytokine production by IpLITR 1.1b-expressing RBL-2H3 following crosslinking with anti-HA mAb: complete array data.
RBL-2H3 cells ($2.5x10^6$) expressing the N-terminal HA-epitope tagged IpLITR 1.1b were crosslinked by treatment with 0.625 µg/ml of anti-HA mAb followed by 1.25 µg/ml of anti-mouse IgG3 pAb (H+L) for 24 h at 37°C. Cell supernatants were examined for the presence of various rat cytokines using the antibody capture chemiluminescent-based Rat Cytokine Array Panel Array Kit (R&D Systems) using manufacturer's protocol. Relative cytokine levels were calculated using densitometry values obtained from the array spots as described. Each bar represents the mean relative cytokine levels ± SEM of three independent experiments. Cytokine levels reported in Chapter 5 are indicated with black bars and cytokines constitutively generated by RBL-2H3 cells are indicated with grey bars.

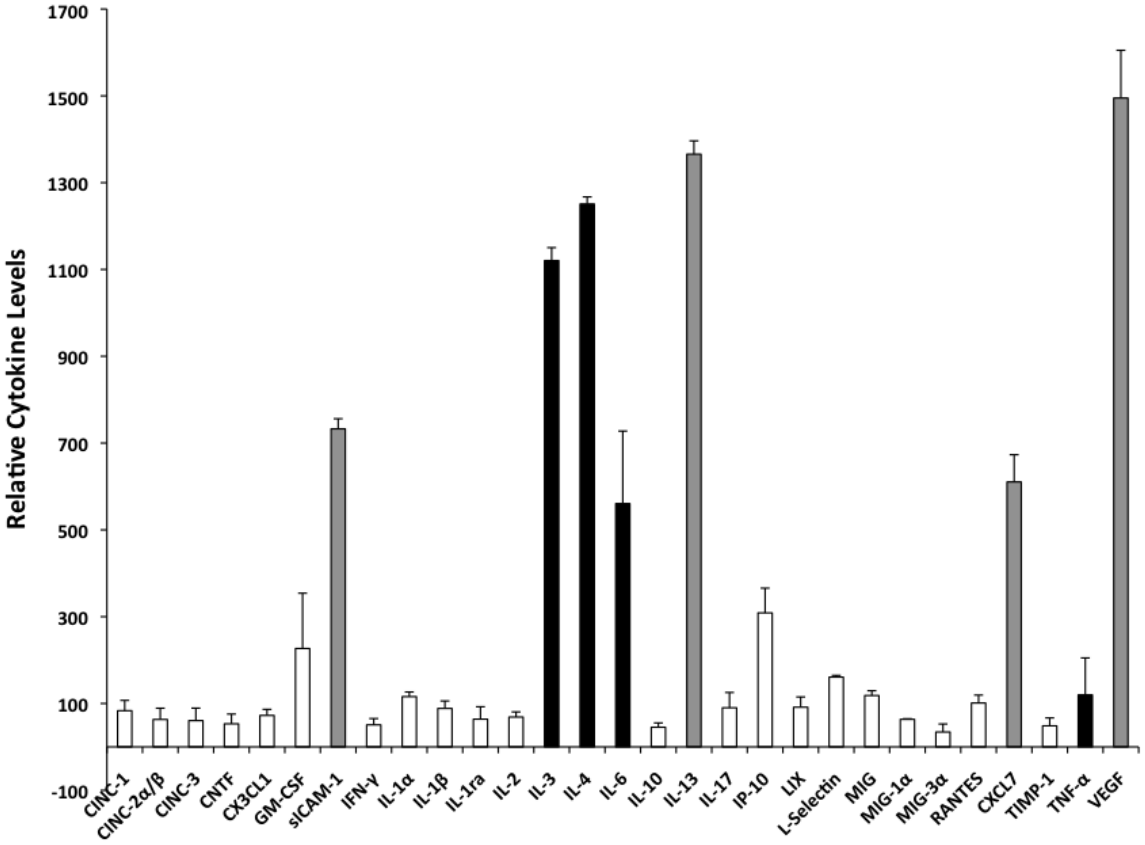

Figure A8. Cytokine production by IpLITR 1.1b-expressing RBL-2H3 following stimulation with PMA/A23187: complete array data.
RBL-2H3 cells ($2.5x10^6$) expressing the N-terminal HA-epitope tagged IpLITR 1.1b were activated with 50 ng/ml PMA/0.5 μM Ca^{2+} ionophore A23187 for 24 h at 37°C. Cell supernatants were examined for the presence of various rat cytokines using the antibody capture chemiluminescent-based Rat Cytokine Array Panel Array Kit (R&D Systems) using manufacturer's protocol. Relative cytokine levels were calculated using densitometry values obtained from the array spots as described. Each bar represents the mean relative cytokine levels ± SEM of three independent experiments. Cytokine levels reported in Chapter 5 are indicated with black bars and cytokines constitutively generated by RBL-2H3 cells are indicated with grey bars.

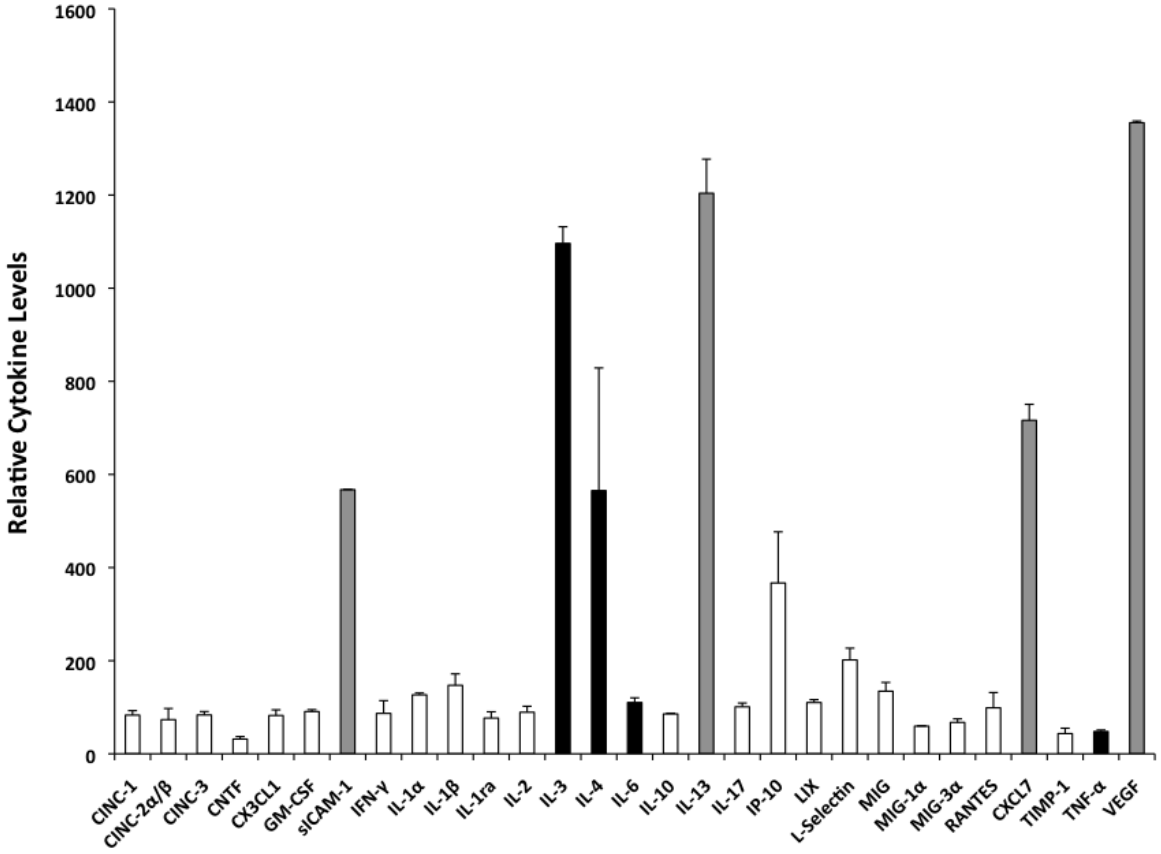

Figure A9. Cytokine production by IpLITR 1.1b-expressing RBL-2H3 following FcεRI triggering: complete array data.
RBL-2H3 cells ($2.5x10^6$) expressing the N-terminal HA-epitope tagged IpLITR 1.1b were activated via the endogenous FcεRI after sensitization with 200 ng/ml anti-DNP-IgE and triggering with 0.1 ng/ml DNP-HSA for 24 h at 37°C. Cell supernatants were examined for the presence of various rat cytokines using the antibody capture chemiluminescent-based Rat Cytokine Array Panel Array Kit (R&D Systems) using manufacturer's protocol. Relative cytokine levels were calculated using densitometry values obtained from the array spots as described. Each bar represents the mean relative cytokine levels ± SEM of three independent experiments. Cytokine levels reported in Chapter 5 are indicated with black bars and cytokines constitutively generated by RBL-2H3 cells are indicated with grey bars.

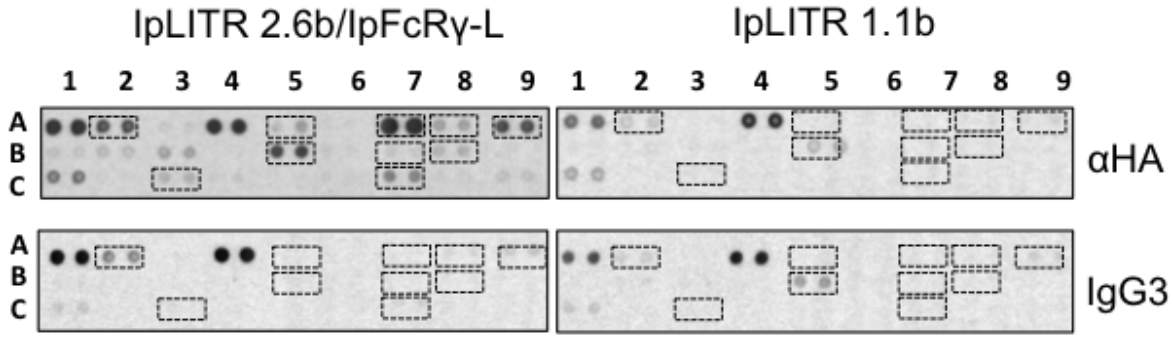

Figure A10. Parallel examination of the relative amounts of phosphorylated kinases activated by IpLITR-activated RBL-2H3 cells. RBL-2H3 cells ($2.5x10^6$) expressing the N-terminal HA-epitope tagged IpLITR2.6b/IpFcRγ-L (left panels) or IpLITR 1.1b (right panels) were crosslinked by treatment with 0.625 μg/mL anti-HA mAb or mouse IgG3 (isotype control) followed by 1.25 μg/mL anti-mouse IgG3 pAb (H+L) for 10 min at 37°C. Cells were also activated with 50 ng/mL PMA/0.5 μM Ca^{2+} ionophore A23187 (i.e. PMA/Iono) or after triggering them via their endogenous FcεRI with anti-DNP-IgE and DNP-HSA (i.e. IgE/DNP). Cell lysates were examined for the presence of phosphorylated kinases using the antibody capture chemiluminescent-based Human Phospho MAPK Array Kit (R&D Systems). Representative proteome profiler array results are shown. The duplicate spots used for calculating the relative phospho-protein levels are indicated with hatched boxes, and the array coordinates are presented in Table A2.

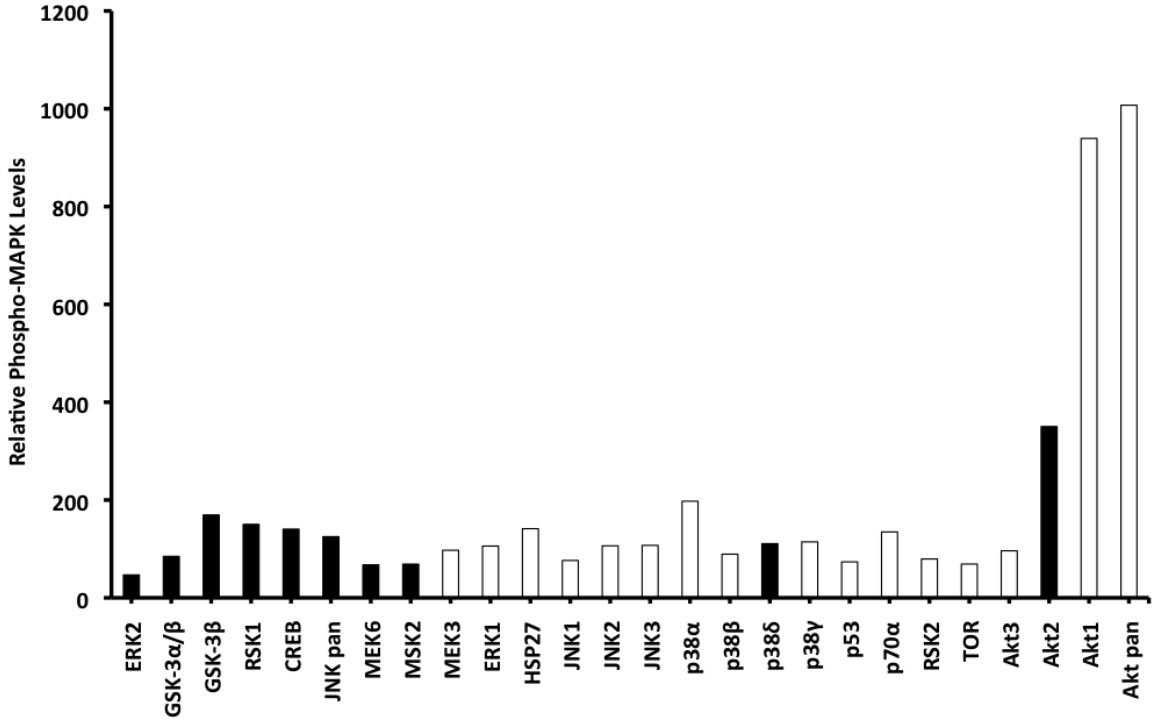

Figure A11. Phosphorylated kinase activation by <u>IpLITR 2.6b/IpFcRγ-L</u>-expressing RBL-2H3 following crosslinking with <u>mouse IgG3</u>: complete array data. RBL-2H3 cells ($2.5x10^6$) expressing the N-terminal HA-epitope tagged IpLITR2.6b/IpFcRγ-L were crosslinked by treatment with 0.625 μg/ml of mouse IgG3 (isotype control) followed by 1.25 μg/ml of anti-mouse IgG3 pAb (H+L) for 10 min at 37°C. Cell lysates were then examined for the presence of phosphorylated proteins using the antibody capture chemiluminescent-based Human Phospho MAPK Array Kit (R&D Systems) using manufacturer's protocol. Relative phospho-MAPK levels were calculated using densitometry values obtained from the array spots as described. Each bar represents the mean relative phospho-MAPK from an independent experiment of two that were performed giving similar results. Phospho-MAPK levels reported in Chapter 5 are indicated with black bars.

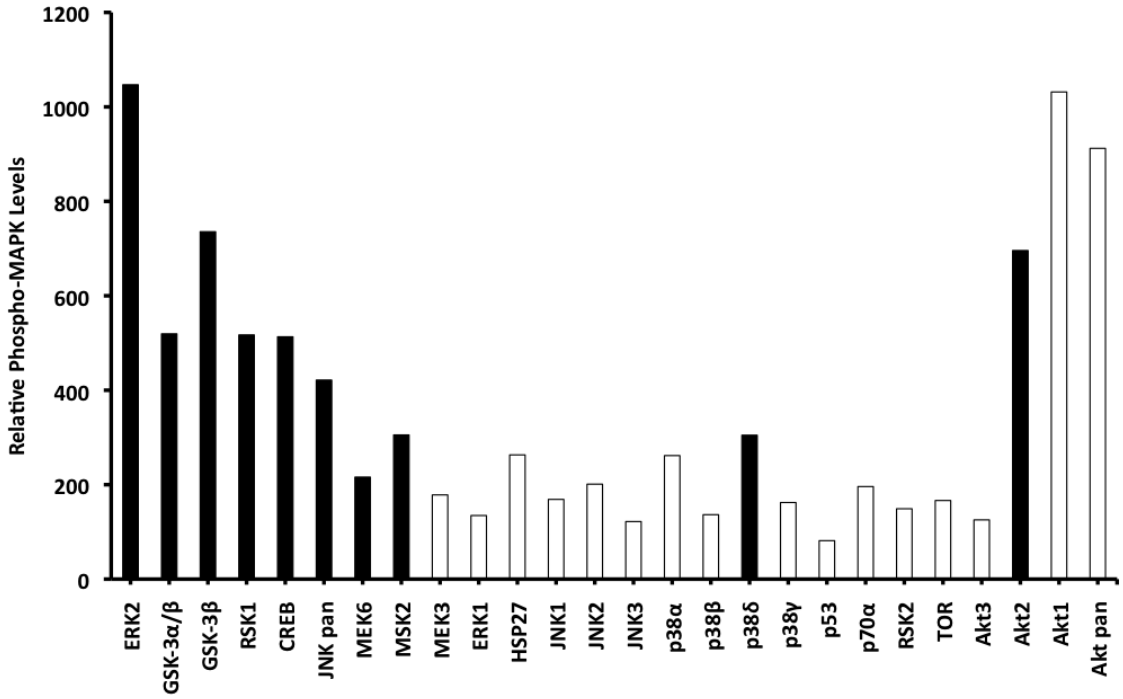

Figure A12. Phosphorylated kinase activation by <u>IpLITR 2.6b/IpFcRγ-L</u>-expressing RBL-2H3 following crosslinking with <u>anti-HA mAb</u>: complete array data. RBL-2H3 cells ($2.5x10^6$) expressing the N-terminal HA-epitope tagged IpLITR2.6b/IpFcRγ-L were crosslinked by treatment with 0.625 μg/ml of anti-HA mAb followed by 1.25 μg/ml of anti-mouse IgG3 pAb (H+L) for 10 min at 37°C. Cell lysates were then examined for the presence of phosphorylated proteins using the antibody capture chemiluminescent-based Human Phospho MAPK Array Kit (R&D Systems) using manufacturer's protocol. Relative phospho-MAPK levels were calculated using densitometry values obtained from the array spots as described. Each bar represents the mean relative phospho-MAPK from an independent experiment of two that were performed giving similar results. Phospho-MAPK levels reported in Chapter 5 are indicated with black bars.

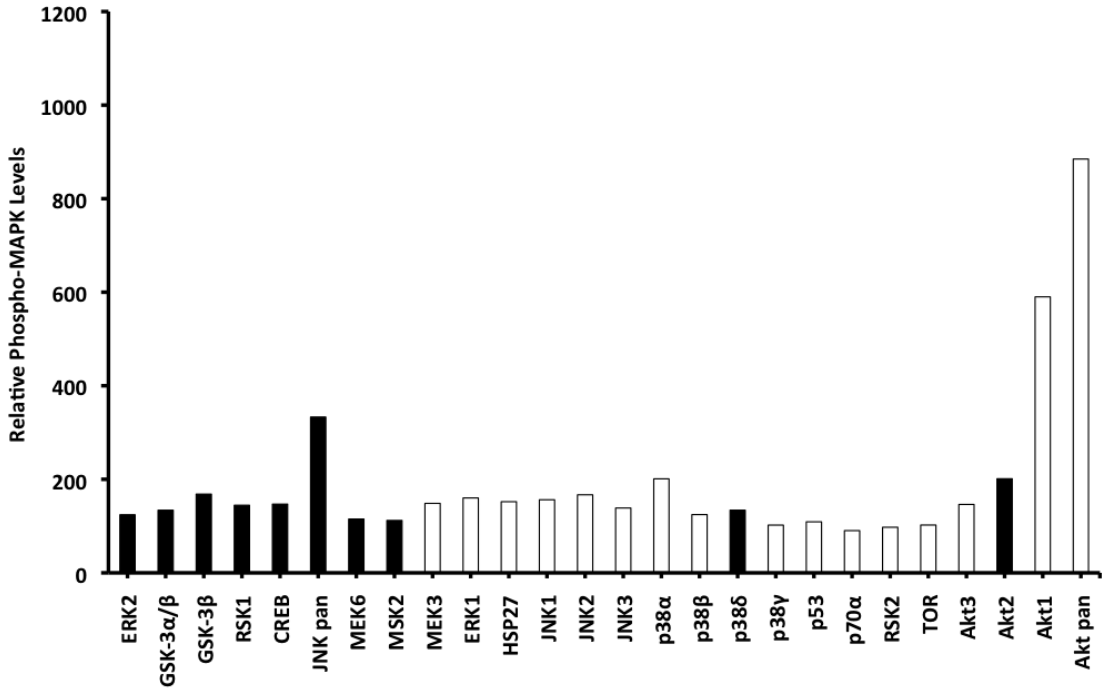

Figure A13. Phosphorylated kinase activation by <u>IpLITR 1.1b</u>-expressing RBL-2H3 following crosslinking with <u>mouse IgG3</u>: complete array data. RBL-2H3 cells ($2.5x10^6$) expressing the N-terminal HA-epitope tagged IpLITR 1.1b were crosslinked by treatment with 0.625 µg/ml of mouse IgG3 (isotype control) followed by 1.25 µg/ml of anti-mouse IgG3 pAb (H+L) for 10 min at 37°C. Cell lysates were then examined for the presence of phosphorylated proteins using the antibody capture chemiluminescent-based Human Phospho MAPK Array Kit (R&D Systems) using manufacturer's protocol. Relative phospho-MAPK levels were calculated using densitometry values obtained from the array spots as described. Each bar represents the mean relative phospho-MAPK from an independent experiment of two that were performed giving similar results. Phospho-MAPK levels reported in Chapter 5 are indicated with black bars.

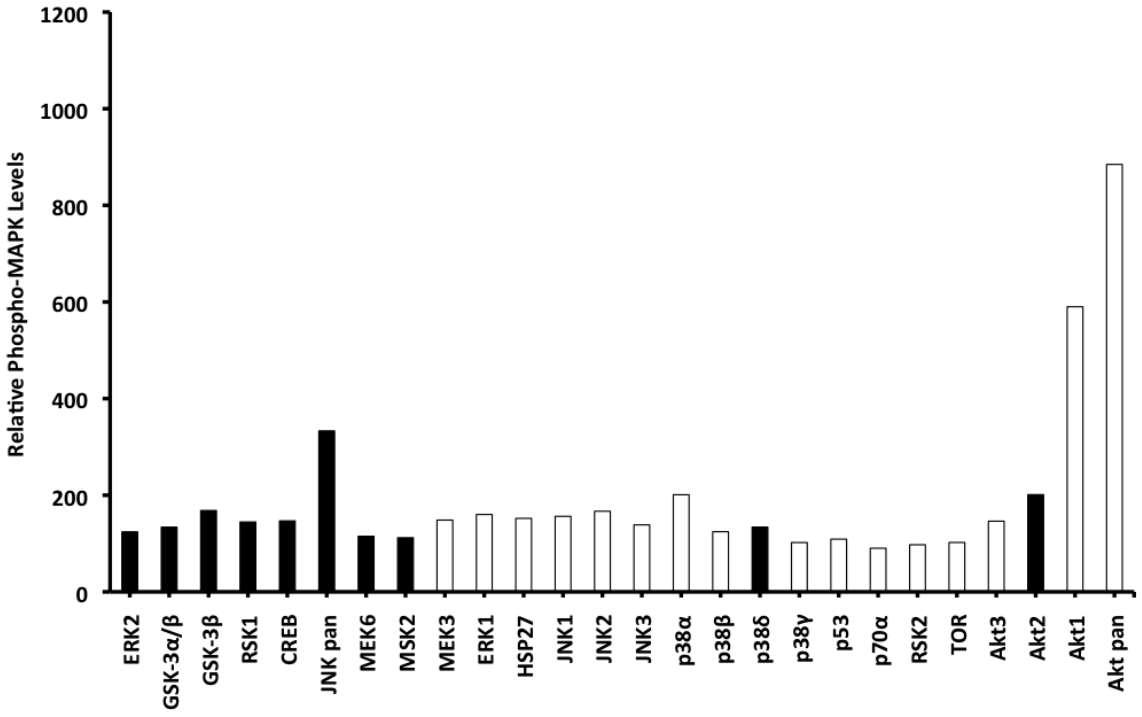

Figure A14. Phosphorylated kinase activation by <u>IpLITR 1.1b</u>-expressing RBL-2H3 following crosslinking with <u>anti-HA mAb</u>: complete array data. RBL-2H3 cells ($2.5x10^6$) expressing the N-terminal HA-epitope tagged IpLITR 1.1b were crosslinked by treatment with 0.625 µg/ml of anti-HA mAb followed by 1.25 µg/ml of anti-mouse IgG3 pAb (H+L) for 10 min at 37°C. Cell lysates were then examined for the presence of phosphorylated proteins using the antibody capture chemiluminescent-based Human Phospho MAPK Array Kit (R&D Systems) using manufacturer's protocol. Relative phospho-MAPK levels were calculated using densitometry values obtained from the array spots as described. Each bar represents the mean relative phospho-MAPK from an independent experiment of two that were performed giving similar results. Phospho-MAPK levels reported in Chapter 5 are indicated with black bars.